

https://dspace.org/

The Merensky Reef and UG2 layers at de Wildt, western limb of the Bushveld Complex

Dube, Zamani Addmore

2011-03-31
http://hdl.handle.net/10539/9292

Downloaded from a DSpace repository. https://dspace.org/

The Merensky Reef and UG2 layers at De Wildt, western limb of the Bushveld Complex

by

Zamani Addmore DUBE
(0303958G)

Thesis submitted to the Faculty of Science, University of the Witwatersrand Johannesburg in partial fulfilment of the requirements for the degree of Master of Science.

02 September 2010

DECLARATION

I declare that this thesis is my own unaided work. It is being submitted for the Degree of Master of Science in the University of the Witwatersrand, Johannesburg. It has not been submitted before for any degree or examination in any other University.

Zamani A. Dube – 02/09/ 2010



TABLE OF CONTENTS

Acknowledgments **5**
List of Figures **6**
List of Tables **11**
Abstract **12**

CHAPTER 1: INTRODUCTION

1.1. Preamble **13**
1.2. Location and physiography **13**
1.3. Aims of the research **15**
1.4. Exploration Background **15**
1.5. Acronyms and Abbreviations **16**

CHAPTER 2: REGIONAL GEOLOGY

2.1. Preamble **20**
2.2. Stratigraphy of the Bushveld Complex **20**
2.3. Metallogenesis of the Bushveld Complex **23**
2.4. Intrusive and discordant bodies **26**
2.4.1. Iron Rich Ultramafic Pegmatoids (IRUPs) **27**
2.4.2. Potholes **27**
2.5. Structure and Metamorphism **28**
2.5.1. Structure of the Bushveld Igneous Complex **28**
2.5.2. Contact metamorphism **29**
2.6. Regional Geophysics **30**
2.7. Floor Rocks to the Bushveld Complex **31**
2.8. Local Geology – the Brits area **32**

CHAPTER 3: METHODOLOGY

3.1. Research approach **35**
3.2. Photogrammetry **35**
3.3. Aeromagnetic data **37**
3.4. Mapping and logging **38**
3.5. Petrography and mineralogy **39**

CHAPTER 4: REMOTE SENSING & FIELD INVESTIGATION RESULTS

4.1. Surface Mapping **43**
4.2. Photogrammetry **43**
4.3. Aeromagnetic Interpretation **46**
4.4. Radiometric Survey **48**

CHAPTER 5: STRATIGRAPHY OF DE WILDT AREA

5.1. Character of the Main Zone **50**
5.2. Character of the Critical Zone **50**
5.3. Character of the Marginal Zone **52**
5.4. Merensky Reef at De Wildt **56**
5.5. UG2 Chromitite layer at De Wildt **61**
5.6. UG2 Chromitite facies **61**
5.7. UG2 chromitite isopach **70**
5.8. UG2 hangingwall units **74**
5.9. UG2 footwall units **74**
5.10. Dykes, sills and replacement rocks at De Wildt **74**
5.11. Summary **76**

CHAPTER 6: PETROGRAPHY

6.1. Quartzite xenoliths **77**
6.2. Hornfels **77**
6.3. Chromite-rich feldspathic pyroxenite **78**
6.4. Replacement pegmatites **78**
6.5. Summary **78**

CHAPTER 7: MINERALIZATION

7.1. Merensky Reef PGE content **81**
7.2. UG2 chromitite Isochon **81**
7.3. PGM value distribution along the UG2 chromitite **82**
7.4. Mineralized UG2 footwall at De Wildt **86**
7.4.1. UG2 footwall isopach **89**
7.4.2. UG2 footwall isochon **90**
7.4.3. Combined UG2 and UG2 footwall isopach **91**

CHAPTER 8: DISCUSSION

8.1. Merensky Reef **92**
8.2. UG2 Chromitite layer **94**
8.3. Meta-sedimentary xenoliths **100**
8.4. Metamorphism **102**
8.5. Structure and deformation pattern **103**

CHAPTER 9: CONCLUSIONS

REFERENCES **105**
APPENDIX **112**

ACKNOWLEDGMENTS

I would like to extend my gratitude to Prof. Kim A.A. Ncube-Hein for her mentorship skills, unwavering patience and time (especially during the field visits) in supervising this work. Also I would like to express my sincere thanks to Nkwe Platinum as they provided funding and data for this work. This thesis was improved by the careful review of Prof. Grant Cawthorn

LIST OF FIGURES

Figure 1: General geological map of the Bushveld Complex (adapted from Van der Merwe and Cawthorn 2005). The main limbs of the complex are shown; Western Limb, Eastern Limb and Northern Limb. The location of the De Wildt project, east of the Brits Graben is shown.

Figure 2: Mineral permits of farm portions making the De Wildt prospect are shaded in blue (as at January 2005).

Figure 3: Diamond drill holes in and adjacent to the de Wildt prospect.

Figure 4: Stratigraphy of the Rustenburg Layered Suite of the Bushveld Complex (after Schürmann et al., 1988).

Figure 5: Regional geological variations in the nature of Merensky Reef (after Viljoen, 1994). The Swartklip facies is located due south of the Pilanesberg Complex while the Rustenburg facies is centred on the town of Rustenburg. The De Wildt project area lies due east of the town of Brits.

Figure 6: Floor folds in the Magaliesberg Quartzite Formation in the south-western Bushveld Complex, west of the De Wildt project area (modified after Davey, 1992). Floor folds include the Kookfontein and Spruitfontein upfolds.

Figure 7: Major gravity anomalies in the western BC (modified after Viljoen, 1999). Gravity highs occur north of Pilanesburg, north of the town of Rustenburg and due west of the De Wildt project area. The gravity highs correspond with thickened mafic units that may represent feeder sites.

Figure 8: The second vertical magnetic derivative map across the De Wildt project (Antonie, 2004). Structures such as dykes and faults, which disrupt the mafic layers of the BC, where delineated from this image.

Figure 9: Schematic representations of borehole logs drilled in the De Wildt project area by Nkwe Platinum. The boreholes were used in the study to characterize the distribution and continuance of the MR and UG2 layers.

Figure 10: Stratigraphic logs drawn from historical diamond boreholes that were re-logged and used in the study (MR=Merensky Reef, UG2=Upper Group 2 chromitite and UG1=Upper Group 1 chromitite layer).

Figure 11: Schematic representation of logs of boreholes drilled by Nkwe Platinum in the western portion of the De Wildt project area (MR=Merensky Reef, UG2=Upper Group 2 chromitite layer).

Figure 12: Schematic map that combines interpretations of black and white aerial photographs and Google Earth images of the De Wildt project area (blue) with those of topography and 1st and 2nd vertical derivative aeromagnetic data. West-trending lineaments are evident in the BC mafic units and these are crosscut by an array of NE and NW-trending faults and two dyke sets. Displacement on the Schietfontein, Zilkaatsnek and Lindiwe fault is sinistral (apparent) but the faults are most likely scissor faults with normal displacement and west block down. The BC mafic units dip north.

Figure 13: Photographic mosaic of De Wildt project area (orange box). NE trending lineaments (faint blue) are apparent across the prospect. Quartzite hills occur to the east and south of the project area and are crosscut and displaced by NW and NE-trending fractures. Small streams are marked in green.

Figure 14: Geological interpretation of the magnetic signatures from the 1st and 2nd vertical aeromagnetic data. The Central Zone shaded in grey is highly disturbed and characterized by faults and fractures. NW-trending dykes traverse the prospect (interpreted from aeromagnetic data from Antoine, 2004).

Figure 15: Interpretation map of Potassium and Thorium radiometrics across the project area. Zones of high Th-K radiation occur in the central and western parts of the De Wildt Project area (interpreted from aeromagnetic data from Antoine, 2004).

Figure 16: Provisional local stratigraphy of De Wildt prospect. The base of the GMA is interpreted as the boundary between the Main Zone and the Critical Zone. The vertical separation between the Merensky Reef and UG2 chromitite layer ranged from 115 m to 170 m.

Figure 17: Schematic borehole cross section depicting of the separation between Merensky Reef and UG2 across the De Wildt project area. In the intersections in which the UG2 reef was multi-layered, the top reef contact of the first UG2 chromitite unit was used for correlation. Pothole interpretations were based on transgressed/missing footwall layers, thickened hangingwall layers of MR, steep dips and overall stratigraphic attenuation of the MR-UG2 interval without any discernable evidence of faults.

Figure 18: A calc-silicate xenolith that is rich in epidote (shown in red line) within a BC norite sequence in borehole PWD4. Part of the disturbed UG2 footwall with flow structures as defined by chromitite and magnetite stringers is delineated by the dashed green lines.

Figure 19: Diamond drill core of sedimentary xenoliths (in yellow) in core of the BC within Marginal Zone of the BC at De Wildt project. Below the xenoliths is part of Transvaal Supergroup quartzite intersected in borehole DWD11.

Figure 20: Poorly developed UG2 chromitite layer intersected in borehole DWD10. The UG2 is underlain by meta-sedimentary xenoliths (borehole DWD10 intersection).

Figure 21: Typical Merensky Reef intersection of greater than 20 m thickness at De Wildt together with schematic of the borehole (PDW01). The MR is altered with chlorite and serpentinite filled joints.

Figure 22: Merensky Reef pyroxenite and the different footwall units intersected in borehole. Image **a** is of a medium crystalline feldspathic pyroxenite layer making up the MR. Image **b**, is of a poorly defined basal chromitite stringer that defines the bottom contact of MR. The MR pyroxenite is weathered and chloritized. Image **c**, shows a well developed basal chromitite stringer of MR, the undulating contact between the chromitite stringer and the footwall anorthosite is defined. Image **d**, shows a half NQ core section of an irregular basal chromitite stringer of MR in contact with mottled anorthosite footwall.

Figure 23: A schematic of the different Merensky Reef facies intersected at De Wildt. In (a) the MR is characterized by a medium crystalline feldspathic pyroxenite that has a basal chromitite stringer. In (b) the MR is wide but devoid of a basal chromitite stringer. In the potholed facies (c), the MR pyroxenite is significantly thinned (in this case down to ~5.0 m).

Figure 24: (**a**) UG2 seam intersected in DWD07, the seam is cut by quartz-biotite veins and marked by a generally high content of interstitial plagioclase. (**b**) Altered UG2 seam intersected at a depth of > 604 m, the top reef contact is poorly developed, marked by vague plagioclase lenses and anorthosite patches. The footwall pyroxenite has been heavily altered to chlorite giving the rock a dark green appearance.

Figure 25: Schematic depiction boreholes in the De Wildt project area showing the UG2 facies types in each borehole. Normal and split-reef facies occur in the area but the split-reef facies can be further subdivided into B, C, D, and E types.

Figure 26: UG2 facies distribution in the De Wildt project area.

Figure 27: (a) UG2 normal facies. **(b)** The narrow B type sub-facies of UG2 split-reef facies.

Figure 28: Upper chromitite layer of the UG2 package, and the chromite-rich feldspathic pyroxenite that separates the two chromitite layers.

Figure 29: Part of the UG2 package showing the chromite bearing norite unit. The chromite occurs in the form of blebs and irregular stringers. The lower chromitite layer in is poorly packed (intersected in borehole DWD12).

Figure 30: Stratigraphic logs showing the different UG2 split-reef. Figure (a) presents the C type sub-facies intersected in borehole DWD07. Figure (b) presents the thick B type sub-facies intersected in borehole PDW01.

Figure 31: Borehole log showing the UG2 Split reef D-type sub-facies.

Figure 32: Narrow UG2 chromitite layer (a) and the upper UG2 chromitite layer with feldspar inclusions giving it a spotted texture (b).

Figure 33: Chromite-rich feldspathic pyroxenite with chromite blebs immediately above the pencil (borehole DWD13).

Figure 34: UG2 chromitite isopach map for De Wildt. Areas in which the footwall mineralization is not developed have thicknesses are less than 1.0 m.

Figure 35: Photomicrographs of polished thin sections of selected core samples from various boreholes at De Wildt. All images are under crossed polars. Images **A** and **B** are quartzite characterized by veins composed of secondary oxide minerals. Sericite defines a zone around an (unidentified) opaque in image **B**. Image **C** shows a highly altered rock in which saussuritized plagioclase gives the rock a dusty appearance. Image **D** characterize contacts between recrystallized quartzite and dolerite: secondary mineral such biotite have formed between the contact and define contact metamorphism to hornblende-hornfels facies. Image **E** was derived from a metasedimentary xenolith that underwent low-grade metamorphism (borehole PDW04).

Figure 35: Photomicrographs of polished thin sections of selected core samples from various boreholes at De Wildt. All images are under crossed polars. Images **F** and **G** are hornfelsed rocks marked by the presence of fractured quartz, plagioclase, biotite and vague pyroxene crystals. The deformation in image F is interpreted to be localized and a result of magmatic fluids associated with intrusion of the dolerite dykes prominent within the De Wildt project area. Images **H** and **I** are of feldspathic pyroxenite hosting disseminated chromite, intersected where the UG2 seam was anticipated. The chromitite grains do not exhibit a preferred orientation but are scattered throughout the crystal mass. Image **J** is of pegmatite consisting of plagioclase, clino and othopyroxene and biotite crystals with oxides minerals in interstitices.

Figure 36: Average PGE values for Merensky Reef. In most of the boreholes drilled by Nkwe Platinum the grades were less than 0.1 g/t over widths of less than one metre near the top and bottom contacts.

Figure 37: UG2 chromitite isochon map over the De Wildt project area.

Figure 38a: PGM value distribution within the UG2 chromitite layer (normal facies type) in borehole SK02.

Figure 38b: Plots of Pt, Pd, Rh, Ru and Pt/Pd ratios of UG2 chromitite layer (from borehole PDW01). The Pt/Pd ratio value display an overall upward increase within the chromitite layer.

Figure 39: UG2 chromitite isochon map showing the plot of centimetre grams per tonne across the De Wildt project area.

Figure 40: Schematic depiction of the mineralized zone below the UG2 layer. The mineralized footwall units (feldspathic pyroxenite/norite) host disseminated chromite, chromite blebs and chromite slivers extending up to 4 m below the UG2 chromitite layer.

Figure 41: (**a**) UG2 feldspathic pyroxenite footwall characterized by irregular zones with disseminated chromite, intersected in borehole DWD07. (**b**) UG2 feldspathic pyroxenite footwall with irregular and vague chromite stringers, intersected in borehole DWD06.

Figure 42: Chromitite slivers and chromite blebs in a coarse crystalline-pegmatoidal meosonorite underlying the UG2 chromitite layer in one borehole DWD08 intersection. Chromite patches/blebs and slivers are shown by yellow lines.

Figure 43: UG2 footwall isopach across the De Wildt project area. The term ‘footwall’ in this case refers to the chromitiferous UG2 footwall units consisting of feldspathic pyroxenite/norite hosting disseminated chromite, chromite stringers and chromite blebs

Figure 44: UG2 footwall isochon showing the variation of grades within the mineralized footwall units across the De Wildt project area. The term ‘footwall’ in this case refers to the chromitiferous UG2 footwall units consisting of feldspathic pyroxenite/norite hosting disseminated chromite, chromite stringers and chromite blebs

Figure 45: PGE value distribution along the mineralized UG2 footwall unit as represented in borehole 2098. The footwall unit is made up of a feldspathic pyroxenite with disseminated chromite (~30%) and chromite slivers.

Figure 46: UG2 footwall isochon plot of centimetre grams per ton within the mineralized units across the De Wildt project area.

Figure 47: Combined UG2 layer and mineralized footwall isopach. This plot gives total length variation of the mineralized horizon (UG2 seam and footwall) across the De Wildt project area.

Figure 48: Schematic representation (not to scale) of the UG2 chromitite seam across the De Wildt project area showing the relationship between the UG2 normal reef facies, UG2 split-reef facies and feldspathic pyroxenite (fpx). The normal UG2 facies is confined to the west of the prospect while the split-facies occurs predominantly in the eastern zone on Schietfontein and Krelingspost farms.

Figure 49: Schematic representation of the stratigraphic succession on the eastern zone of the project area (at Krelingspost Farm and eastward) toward the margin of the BC. In (**A**) the UG2 chromitite layer is interpreted to abut the floor rocks of the Transvaal Supergroup at depth. In (**B)** the wedging out of the Upper Critical Zone occurs i.e. the lower stratigraphic units are cut out against the floor rocks towards the east. This also explains why there was no intersection of the UG1 layer in the eastern portions of the prospect and the absence of UG2 layer out-crop in the vicinity of the quartzite hills.

Figure 50: Potassic quartzite hornfels intersected in borehole at Krelingspost Farm. It is not known whether this unit is connected to the floor or comprises a Transvaal Supergroup outlier.

LIST OF TABLES

Table 1: The location and collar position of diamond boreholes drilled by different companies in De Wildt project area. Coordinates in WGS 84, Cape datum.

Table 2: Simplified stratigraphy of Transvaal Supergroup and age data, modified after Eriksson et al. (1993) and Dankert and Hein (2010).
(1) Burger and Coertze (1973-1974; Rb-Sr whole rocks age);
(2) Martin et al. (1998; single zircon U-Pb SHRIMP);
(3) Walveren and Martini (1995; single zircon Pb-evaporation);
(4) Unpublished; vvvvv = volcanic or pyroclastic unit.

Table 3: Specifications of airborne magnetic survey conducted over the De Wildt project area (after Antoine, 2004).

Table 4: The UG2-Merensky Reef interval in the De Wildt project area. The data records the disturbed Merensky ReefUG2 interval from the boreholes where layers were disrupted by potholing. Faults were omitted.

Table 5: Thickness of the Marginal Zone intersected in several boreholes. The boundary between the Critical Zone and Marginal Zone is tentatively taken at the level of the first appearance of the fine-grained 'chill-margin' contact-type norite.

Table 6: Merensky Reef intersections within the prospect.

Table 7: UG2 chromitite reef intersections within the De Wildt project area.

Table 8: Immediate hanging and footwall lithologies to the UG2 chromitite layer.

Table 9: Prill Splits for the UG2 chromitite and UG2 footwall at De Wildt are shown on the left while prill splits of the UG2 and MR reefs from other BC localities are given on the right.

Table 10: A summary table of the different mineralized UG2 footwall lithologies intersected in various boreholes within the project area.

ABSTRACT

Geological and geophysical investigations involving drill-core studies, aeromagnetic data and surface mapping at the De Wildt property in the south-eastern part of the western limb of the Bushveld Complex have revealed a highly variable UG2 chromitite layer and a wide Merensky Reef (Merensky Reef) layer. A full stratigraphic succession of the Rustenburg Layered Suite of the Bushveld Complex is not developed at De Wildt. Instead, the Lower Zone and Lower Critical Zone are not developed and the Upper Critical Zone is developed in close proximity to the Transvaal floor rocks. Numerous deformed metasedimentary xenoliths and hornfels were intersected that are interpreted to be the result of contact metamorphism during cooling Bushveld magmas. The rock succession at De Wildt has been disturbed by post-Bushveld faulting and dolerite dykes whose emplacement is interpreted to have been influenced by the adjacent Brits graben to the west.

The Merensky Reef intersected at De Wildt prospect, while exhibiting its regional characteristics of a non-pegmatoidal feldspathic pyroxenite and thick distal facies, has undergone further thickening up to about 20 m, and is marked by sub-economic PGE values. The UG2 chromitite layer exhibited lateral variation from east to west, exhibiting variation in being a single massive chromitite seam (averaging 1.10 m in thickness) into a multi-layered unit and/or consisting of only disseminated chromite and chromitite stringers within a feldspathic pyroxenite. Also, the UG2 layer is characterized by a PGE-enriched immediate footwall feldspathic pyroxenite and norite that is 4 metres in thickness. Such a thick UG2 footwall (consisting of chromitite lenses and blebs) may indicate the presence of higher than usual amounts of late-stage fluids during the fluidization processes. Prill splits of the UG2 chromitite show that the reef has a high Pt:Pd ratio of 3:1 in contrast to the common western Bushveld UG2 Pt:Pd ratio of 2:1. It is interpreted that the UG2 chromitite layer was exposed to late stage magmatic and/or meteoric fluid metasomatism with the subsequent remobilization of Pd as evidenced by the presence of replacement magnetite and quartz-biotite veins within the UG2 layer.

CHAPTER 1
INTRODUCTION

1.1. Preamble

The Bushveld Complex of South Africa is one of the most intensively studied layered igneous intrusions on Earth. Historically, most research has been conducted on open-pits and under-ground mine workings, but the geology away from these mines is not well documented, in particular, the setting of the platinum-rich Upper Group 2 (UG2) chromitite and Merensky Reef layers. Maier and Bowen (1996) reported that in most parts of the western Bushveld Complex, the UG2-Merensky Reef interval is situated about 100 m below the Critical Zone-Main Zone boundary. However, as a result of poor exposures and a relatively high degree of faulting, the field relationships (of UG2-Merensky Reef interval) to the east of Brits are unclear.

The De Wildt area (including the farms, Zilkaatsnek 439 JQ, Schietfontein 437 JQ and Krelingspost 425 JQ), lies on the western limb of the Bushveld Complex, northwest of Pretoria, about 15 km to the east of Brits. An exploration program carried out by Nkwe Platinum (SA) (Pty) Limited (hereafter referred to as Nkwe Platinum), which commenced in November 2003, provided the opportunity to investigate the nature of the UG2-Merensky Reef interval in that region. The program included surface mapping, aeromagnetic survey and diamond drilling (20 boreholes), and was supplemented by geochemical sampling of core and a GIS investigation of the De Wildt prospect region.

The strato-structural setting of UG2 chromitite and Merensky Reef in the De Wildt area was correlated and compared with the strato-structural setting of the UG2 chromitite and Merensky Reef in the adjacent Rustenburg facies to the west of the De Wildt project area in order to establish similarities and differences in the nature of the reefs, and to develop an overall model for reef variation.

1.2. Location and physiography

The De Wildt project is located on the topographic-cadastral Sheet 2527DB Brits (Chief Directorate: Survey and Mapping, 1996). The co-ordinates central to the De Wildt prospect are 25° 37’S and 027° 56’N. The property is located approximately 15 km east of the town of Brits, and approximately 40 km north of Pretoria (Tshwane) in the western limb of the BC (Fig. 1). The operating Maroelabult section of Barplats’s (BPL) Crocodile River mine and the Elandsfontein platinum project for Elands Platinum are situated west of the De Wildt project. The ferrochrome operation of Hernic Ferrochrome is situated to the southwest.

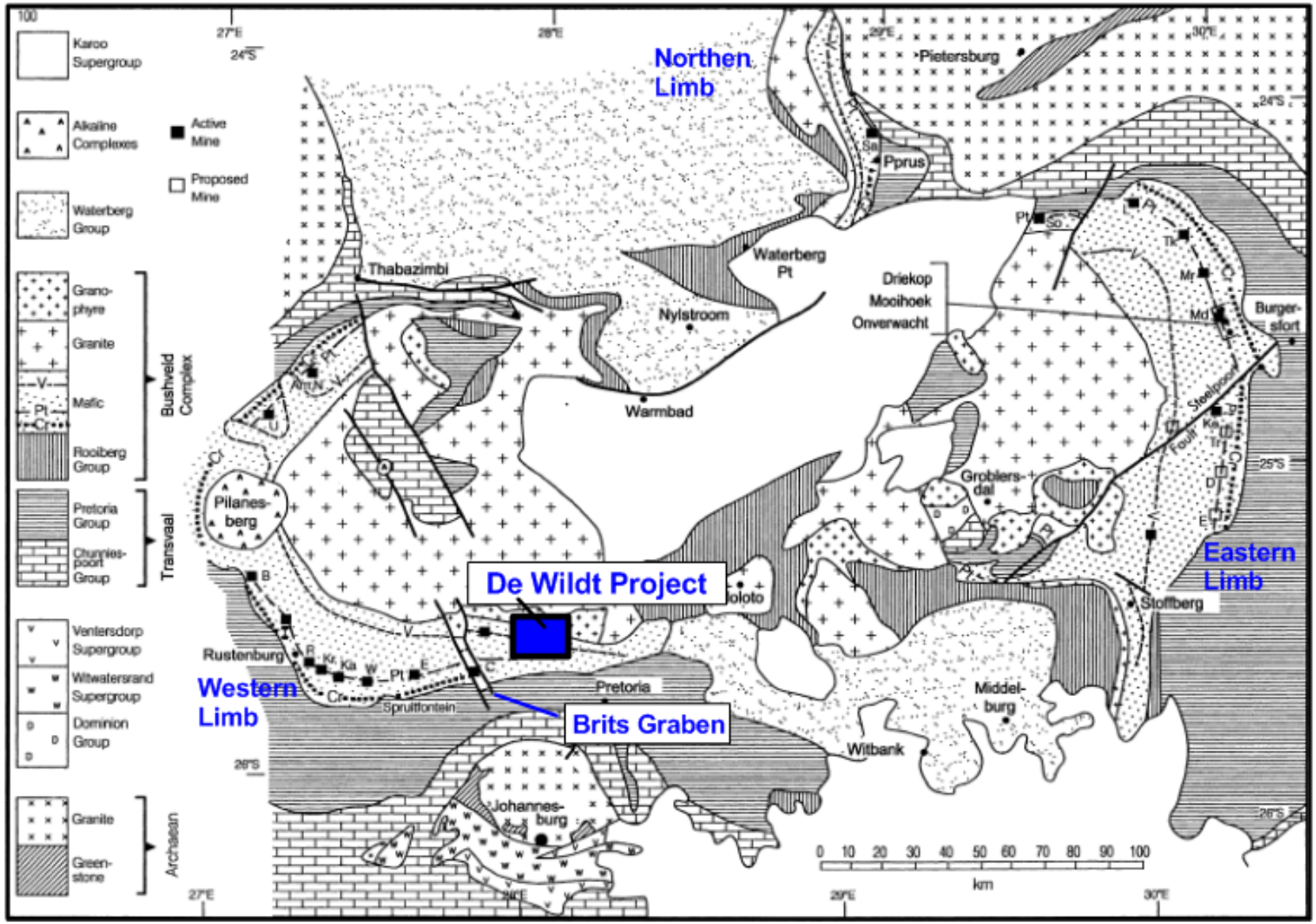


Figure 1. General geological map of the Bushveld Complex (adapted from Van der Merwe and Cawthorn 2005). The main limbs of the complex are shown; Western Limb, Eastern Limb and Northern Limb. The location of the De Wildt project, east of the Brits Graben is shown.

The De Wildt project area covers three farms namely, Zilkaatsnek 439 JQ, Schietfontein 437 JQ and Krelingspost 425 JQ, and covers a total area of ~1200 ha for which Nkwe Platinum has the mineral prospecting rights (Fig. 2). A railway line from Pretoria to Brits is situated along the northern boundary of the property while the N4 toll road is situated on the southern property boundary. The townships of Makhau and Ga-Rankuwa are located to the north of the De Wildt area: R556 road crosses the De Wildt and provides access to the two townships and the town of Brits. The area has relatively low summer rainfall of approximately 600-650 mm per annum and an average annual temperature of approximately 19°C. The area is situated within a savannah biome, comprising scattered trees and shrubs (Acocks, 1988). The topography of the area attains 1200 m with prominent hills of the Magaliesberg Quartzite and the Bushveld Complex Main Zone norite on the southern and northern boundary, respectively. The area is marked by generally warm to hot summers and mild to cold winters.

1.3. Aims of the research

- To investigate and document a comprehensive structural and geological setting of the Merensky Reef and UG2 Chromitite layer in the De Wildt area, based on geophysical and geological datasets.
- To attempt a revision of the stratigraphy of the project area.
- To evaluate the variable nature of the UG2 Chromitite layer in the De Wildt project area in relationship to surrounding operating mines.
- To establish a model for variations in the UG2 Chromitite layer in the De Wildt project area that will aid in evaluating the platinum potential.

1.4. Exploration Background

An exploration program by Nkwe Platinum was initiated in November 2003. The initial stages of the program involved surface mapping, aeromagnetic survey and diamond drilling. A total of 20 boreholes were drilled in 2005/6. Additional borehole data became available to Nkwe Platinum after its acquisition of the Impala Platinum old order mining rights in 2004. These boreholes are shown in Fig. 3.

Historically, five companies have conducted exploration studies in the project area and some on farm portions adjacent to the project area (Table 1). They included Phelps Dodge and Gencor-Impala during the late 1980's, Century Minerals (Pty) Ltd, the African Development Trust (SADT) and Meteorex in the 1990s. Phelps Dodge drilled 18 vertical-diamond-drill holes (SK1-18) on Schietfontein Farm (Figs. 2 and 3). A total of 11 holes intersected the UG2 at depth of 49-50m (SK2-10, 13 and 14) while the percussion hole ZK05 intersected the UG2 at 15 m. Gencor-Impala drilled more than seven diamond-drill holes (boreholes 1960, 1977, 1990, 2055, 2092 and 2098) which

intersected the UG2 at depths of 190-1170m. The boreholes were drilled on Zilkaatsnek and Schietfontein Farms (Figs. 2 and 3). The African Development Trust (SADT) drilled two holes on Hoekfontin 432JQ Farm, which is situated north of the De Wildt project area, and SADT drilled two diamond-drill holes (HFK1and HFK2), which intersected the UG2 at depths of 800-1100 m. In 2000/2001 Century Minerals (Pty) Limited drilled three diamond boreholes (W1, R1 and R2) and excavated three trenches on Zilkaatsnek Farm. The boreholes did not intersect the UG2 reef as they were collared in the UG2 footwall; trenches were excavated in an attempt to expose the UG2. Lastly, Metorex drilled one borehole on Zilkaatsnek (ZK1) which intersected the UG2 Chromitite layer at about 160 m.

1.5. Acronyms and Abbreviations

The stratigraphic nomenclature of the Bushveld Complex used in this research accords with the South African Committee for Stratigraphy (SACS) of 1980. The following abbreviations are used herein:-

BC - Bushveld Complex
MR - Merensky Reef
UG2 - Upper Group 2
GMA - Giant Mottled Anorthosite
RLS - Rustenburg Layered Suite/Sequence
PGEs/PGMs - Platinum Group Elements/ Platinum Group Metals
MZ-Main Zone
CZ – Critical Zone
MgZ-Marginal Zone

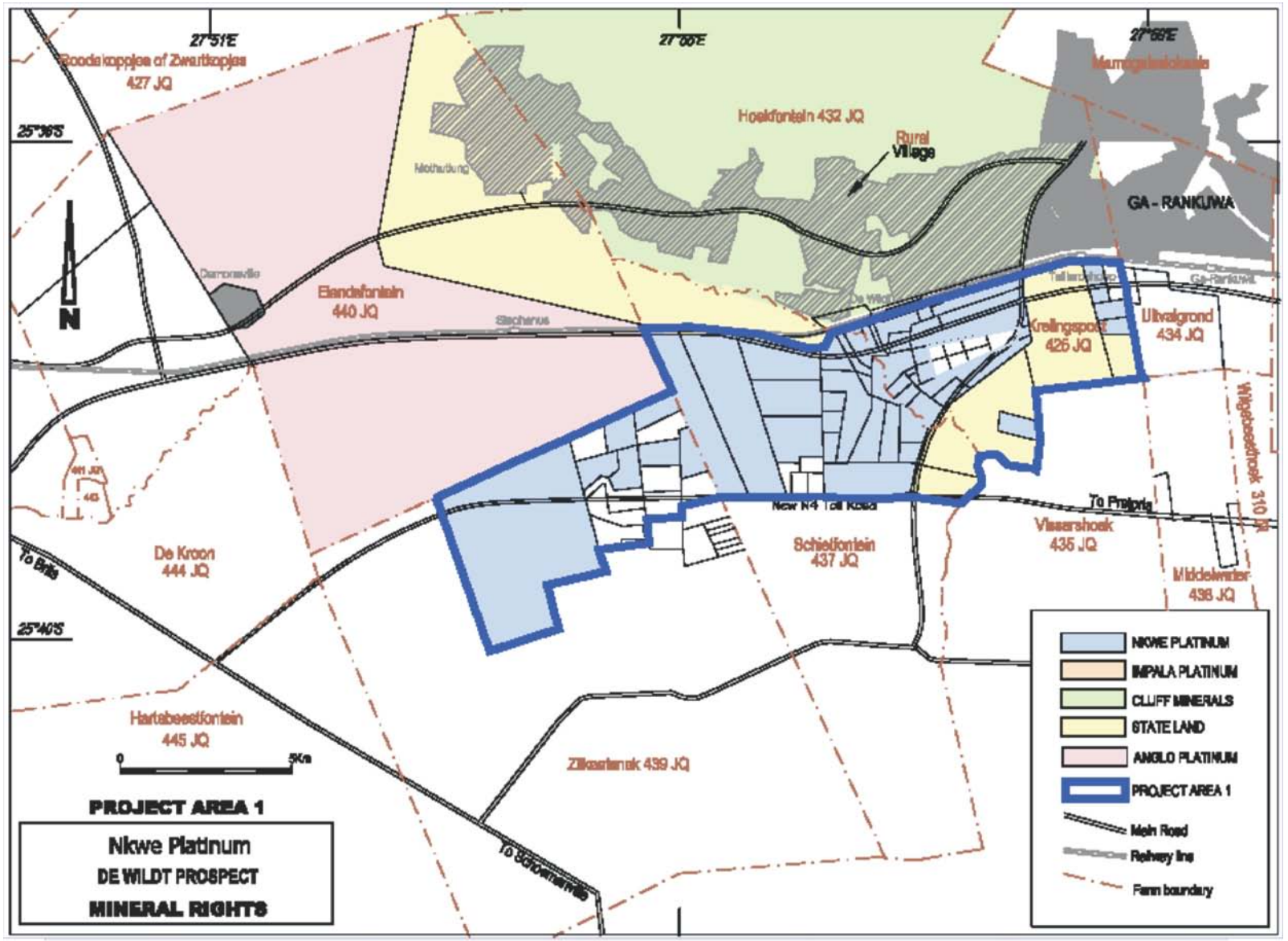


Figure 2. Mineral permits of farm portions making the De Wildt prospect are shaded in blue (as at January 2005).

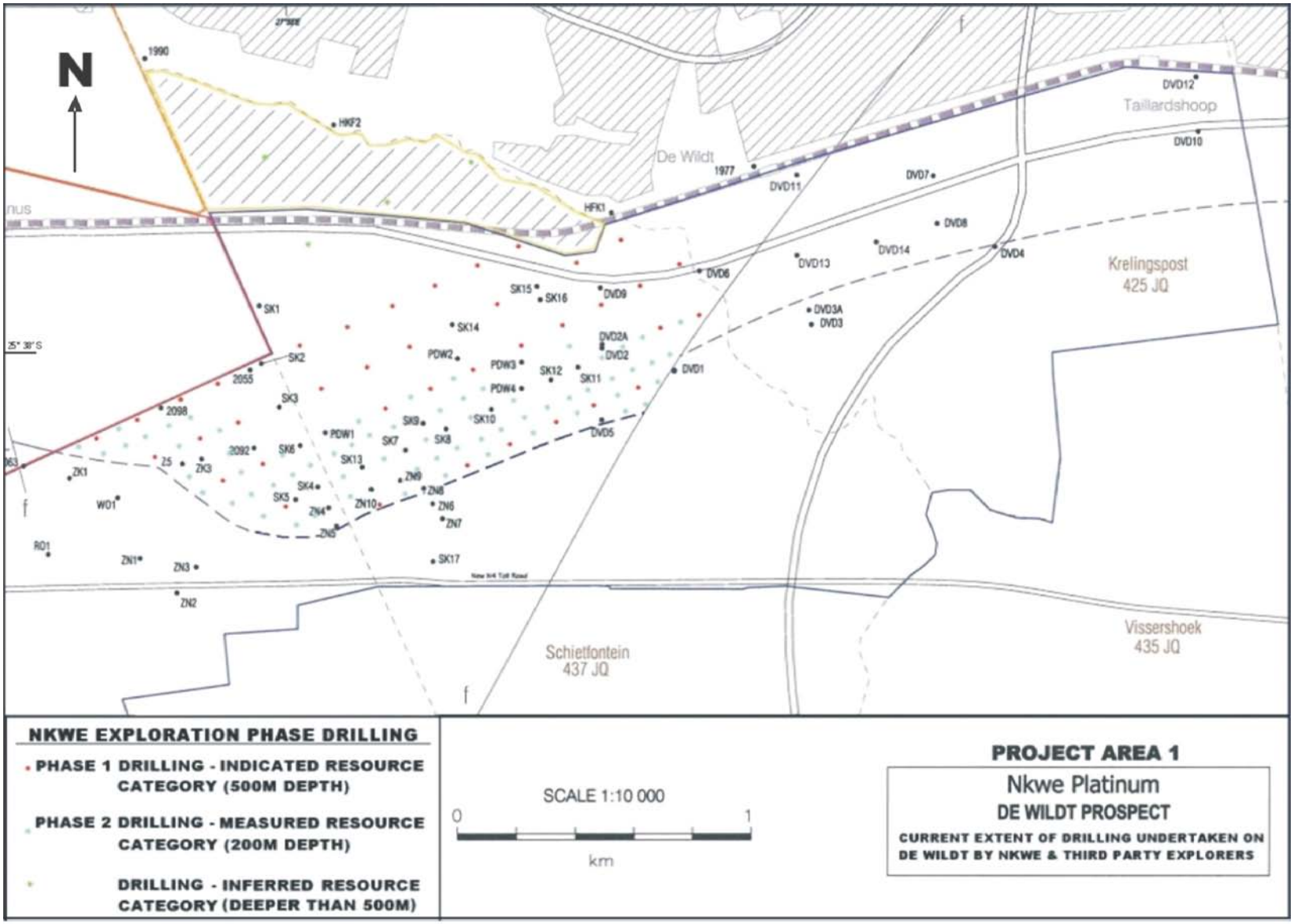


Figure 3. Diamond drill holes in and adjacent to the De Wildt prospect.

BHID	X COLLAR	Y COLLAR	Z COLLAR
BHID	**y**	**x**	**z**
GENCOR/IMPALA			
DH1960	98950	-2834605	1248
DH1977	94783	-2835129	1216
DH1990	90813	-2834376	1186
DH1995	92301	-2833692	1128
DH2046	88513	-2834081	1177
DH2055	91736	-2836535	1213
DH2063	90161	-2837257	1208
DH2092	91816	-2837219	1221
DH2098	91083	-2836830	1216
DHZ05	90860	-2837780	1222
DHZN5	91950	-2838080	1237
NKWE PLATINUM			
DWD01	94353	-2836954	1232
DWD02	93875	-2836791	1225
DWD02A	93861	-2836790	1225
DWD03	95295	-2836642	1233
DWD03A	95272	-2836561	1232
DWD04	96545	-2836114	1249
DWD05	93875	-2837289	1233
DWD06	94500	-2836297	1216
DWD07	96130	-2835651	1232
DWD08	96144	-2835954	1238
DWD09	93855	-2836405	1218
DWD10	97917	-2835324	1249
DWD11	95120	-2835673	1221
DWD12	97820	-2834924	1242
DWD13	95689	-2836067	1234
DWD14	95653	-2835593	1225
PDW01	91989	-2837374	1222
PDW02	92894	-2836886	1220
PDW03	93328	-2836889	1220
PDW04	93324	-2837090	1222
PHELPS DODGE			
SK01	91460	-2836630	1208
SK02	91470	-2836980	1214
SK03	91610	-2837280	1218
SK04	91850	-2837830	1228
SK05	91710	-2837900	1229
SK06	91725	-2837550	1223
SK07	92456	-2837599	1232
SK08	92730	-2837420	1228
SK09	91665	-2837321	1225
SK10	93010	-2837280	1222
SK11	93610	-2837010	1228
SK12	91450	-2837090	1228
SK13	92150	-2837700	1218
SK14	92764	-2836781	1218
SK15	93360	-2836450	1222
SK16	93380	-2836520	1225
SK17	92720	-2838200	1242
SK18	92850	-2837930	1238
ZK01	90237	-2837694	1209

Table 1: The location and collar positions of diamond boreholes drilled by different companies in De Wildt project area. Coordinates in WGS 84, Cape datum.

CHAPTER 2

REGIONAL GEOLOGY

2.1. Preamble

The Bushveld Complex (BC) is the world's largest layered igneous intrusion, exhibiting layering over millimetres to hundreds of metres (Eales and Cawthorn, 1996; Eales, 2001). It hosts over half the world's platinum, chromium, vanadium and refractory minerals, and arguably has ore reserves capable of lasting for a hundred to a thousand years (Vermaak, 1995). The complex was emplaced at 2061 ± 27 Ma based on single zircon age from felsic volcanic rock from the Rooiberg Volcanics (Walraven et al., 1990). The BC has an areal extent of approximately 65 000 km^2 (Tankard et al., 1982 and Cawthorn et al., 2006).

2.2. Stratigraphy of the Bushveld Complex

The Bushveld Complex consists of four main suites of igneous rocks namely, the Rooiberg Group, the Rustenburg Layered Suite, the Rashoop Granophyre Suite and the Lebowa Granite Suite (SACS, 1980; Cawthorn et al., 2006).

The BC intruded metasedimentary rocks of the Transvaal Sequence, largely along an unconformity between Magaliesberg Quartzite of the Pretoria Group (Walraven, 1997; Eriksson et al., 2007). The floor rocks of the BC exhibit considerable lateral variation and consist of meta-volcanic rocks (lavas), quartzite, shale and dolomite (Viljoen and Schürmann, 1998). The Bushveld Granite Suite consists of the Rashoop Granophyre and Lebowa Granites, and forms the bulk of the roof-rock assemblage, together with quartzite, hornfels and dolomite (Kruger, 2005).

The RLS crops out in five limbs/lobes (Fig. 1) including the Far Western Limb, Western Limb, the Eastern limb, the Northern Limb (also known as the Potgietersrus limb) and the Bethal Limb (Eales, 2001). The Bethal Limb does not crop out, but is known to exist from deep borehole data and positive gravity anomalies.

The lithological units of the northern, western and eastern limbs approach 8km in stratigraphic thickness and describe a saucer-shaped ellipse that extends over an east-west distance of approximately 370 km and a north-south distance of approximately 200 km (Cawthorn et al., 2006).

The Rustenburg Layered Suite (RLS) of the Western Limb (which host the Brits prospect) extends for 200 km along an arc from Thabazimbi in the north to Pretoria in the south (Eales and Cawthorn, 1996; Cawthorn et al., 2006). It is divided into northern and southern sectors that are separated by the intrusive Pilanesberg Alkaline Complex.

The RLS is subdivided into five zones (Fig. 4), the Marginal Zone overlain by Lower Zone, Critical Zone, Main Zone and the Upper Zone (Cousins, 1959 citing Hall, 1932, van der Merwe, 2008). The Critical Zone occurs only in the Western and Eastern Limbs of the BC where it is enriched in Platinum Group Elements (PGEs) in the Merensky Reef and UG2 reefs, relative to marginal cumulates (Cousins, 1959 citing Hall, 1932).

The Marginal Zone is the lowermost unit of the BC and ranges in thickness from 0 to 250 m in the western Bushveld. The zone generally comprises marginal contact rocks or arguably, the chill zone at the base of the BC (Kruger, 2005), i.e., it is mixed and contaminated by metasedimentary xenoliths. The zone consists of heterogeneous gabbronorite, norite and hybrid metasediments (Vermaak and Hendricks, 1976; Kruger, 2005).

The Lower Zone overlies the Marginal Zone and is characterized by cumulate pyroxene and olivine-rich layers including pyroxenites and harzburgite (Viljoen and Shurmann, 1998). The thickness of the Lower Zone has been influenced by the topography and structure of the sedimentary floor such that local attenuation of the ultramafic rocks occurs where floor-rock structural complexities exist (Cawthorn et al., 2006).

The Critical Zone overlies the Lower Zone. The base of the Critical Zone coincides with the first appearance of cumulus chromite in the sequence, while the top is defined by poikilitic anorthosite known as the Giant Mottled Anorthosite (GMA); it is situated a few metres above the Merensky Reef (De Klerk, 1995). The Critical Zone is subdivided into the Lower and Upper Critical Zones on the basis of cumulus plagioclase. The Lower Critical Zone consists entirely of ultramafic layers such as orthopyroxenite, harzburgite and chromite layers (Kruger, 2005). The Upper Critical Zone contains both ultramafic and mafic layers such as chromite, feldspathic orthopyroxenite, norite, and anorthosite layers with some olivine bearing layers (Kruger, 2005).

The Lower and Upper Critical Zones are well layered and contain extensive deposits of chromitite (Vermaak and von Gruenewaldt; 1986, Bristow et al., 1993; Viljoen and Schürmann, 1998). The chromitite layers have been subdivided into three groups (Viljoen and Schürmann, 1998). From the base, these are the Lower Group (LG), the Middle Group (MG) and the Upper Group (UG). A total of thirteen (13) chromitite seams of varying thickness are recognized (Cousins and Feringa, 1964; Viljoen and Schürmann, 1998) including:

- Seven LG seams with a total thickness of 3.5 m (LG1, LG2 and LG2A, LG3, LG4, LG5, LG6 and LG6A and LG7).
- Four MG seams with a total thickness of 4 m (MG1, MG2, MG3 and MG4).
- Two UG seams with a total thickness of 2 m (UG1 and UG2).

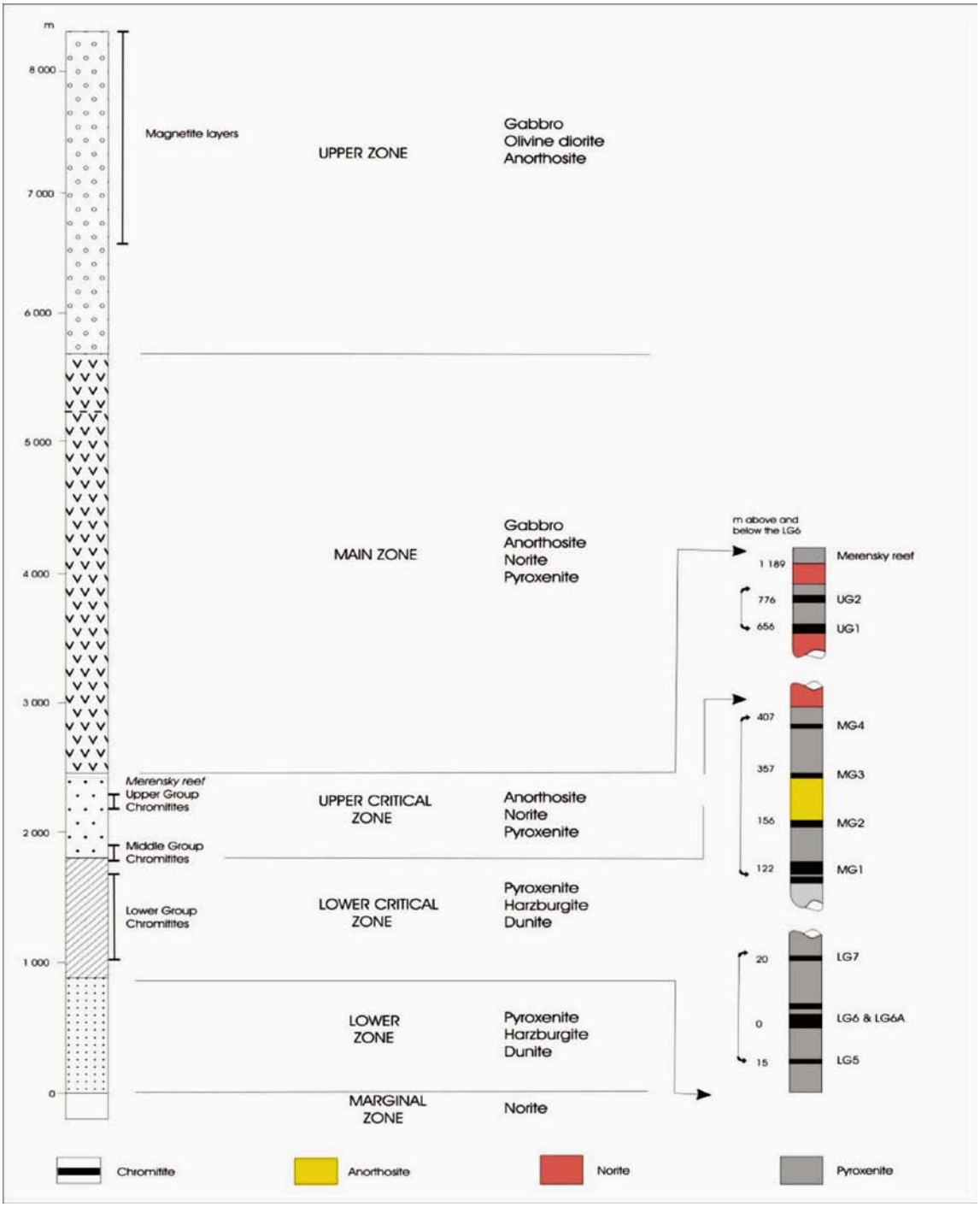


Figure 4. Stratigraphy of the Rustenburg Layered Suite of the BIC (after Schürmann et al., 1988).

The Lower Critical Zone hosts the LG, MG1 and MG2 seams (Fig. 4), while the upper Critical Zone hosts the MG3, MG4, UG seams, and the Merensky Reef. The UG2 chromitite seam and Merensky Reef are the main platiniferous units/horizons of the BC and are situated towards the top of the Upper Critical Zone (Viljoen and Schürmann, 1998). The Bastard Reef cyclic unit overlies the Merensky Reef cyclic unit and consists of thin layers of chromitite, pyroxenite, norite and anorthosite (Viljoen and Hieber 1986; Cawthorn et al., 2006). Near the township of Marikana (situated west of De Wildt project), the Bastard Reef occurs as a pyroxenite (~2 m) or norite (~12 m) (Davey, 1992). The Bastard Reef is located ~10 m above the Merensky Reef in some localities in the western BC (Farquhar, 1986, Viljoen and Hieber, 1986).

The Main Zone overlies the Critical Zone. The base of the Main Zone occurs at the top of Giant Mottled Anorthosite (GMA) and is marked by the appearance of cumulus clinopyroxene and a loss of chromitite. The Main Zone makes up almost half the thickness of the BC intrusion. It is characterized by a relatively monotonous sequence of norite that passes upward into gabbronorite, with occasional anorthosite and pyroxenite bands. Several mottled anorthosite layers occur in the lower portion of the Main Zone and a distinctive pyroxenite layer (Pyroxenite Marker) occurs two thirds of the way up. The middle to upper portions of the Main Zone are resistant to erosion and give rise to the distinctive hills that are evident throughout the Western Limb of the BC (Bristow et al., 1993). However, it should be borne in mind that some authors (Kruger, 2005) put the Main Zone-Critical Zone boundary at the Merensky Reef level based on different initial Sr-isotope compositions and the existence of an unconformity. Kruger (2005) explained the unconformity to be the result of major magma influxes concomitant to erosion of the existing cumulates. As such the Merensky Reef is regarded as the first layer at the base of the Main Zone. The first appearance of cumulus magnetite defines the top of the Main Zone (Bristow et al., 1993) or, the bottom of the Upper Zone. The Main Zone is one of the world's major sources of dimension stone.

The Upper Zone overlies the Main Zone and consists of gabbro, magnetite-gabbro, anorthosite and troctolite layers. The upper contact of the Upper Zone is non-conformable with the Bushveld Granite Suite or Transvaal Sequence. The Upper Zone hosts twenty-five layers of magnetite that make up approximately 8% by volume of Upper Zone rocks. It is thus relatively well layered (Eales and Cawthorn, 1996).

2.3. Metallogenesis of the Bushveld Complex

PGM mineralization occurs in 13 of the chromitite seams of the Critical Zone (LG1, LG2, LG3, LG4, LG5, LG6, LG7, MG1, MG2, MG3, MG4, UG1 and UG2) and increases progressively upward from the lowermost layer to the uppermost UG2 chromitite layer (Viljoen and Schürmann, 1998). The Merensky Reef, UG2 Chromitite and the Platreef are the main sources of platinum (PGEs) in the Bushveld Complex. In the western limb of the Bushveld Complex only economic PGE mineralization

occurs in the Merensky Reef and UG2 chromitite layers. The platinum to palladium (Pt: Pd) ratio of UG2 in the western Bushveld averages 2.5, while in the eastern limb the ration is 0.94. The grade (Pt+Pd+Rh+Au) of the UG2 at Rustenburg Platinum Mines Ltd is reported to be 5.49 g/t. The Pt:Pd ratio of the Merensky Reef in the western limb averages 2.6 (Viljoen and Schürmann, 1998).

At its base, the Merensky Reef consists of a dark pyroxenite unit (the Merensky pyroxenite) with the mineralized portion of the reef being referred to as the Merensky Reef Layer, i.e., that part of the Merensky pyroxenite that is economic to mine. The Merensky Reef pyroxenite is associated with thin chromitite stringers of variable thickness (Vermaak and Van Der Merwe, 2000). The Merensky Reef can be traced for considerable distance laterally: approximately 140 km in both western and eastern limbs. Seismic surveys suggest that the reef can be traced as far as 50 km down-dip and to a vertical depth of 6 km (Cawthorn and Eales. 1996). The reef dips 9° to 27° toward the centre of the complex.

Viljoen and Schürmann (1998) recorded that the Merensky Reef typically forms a heterogeneous pegmatoidal, feldspathic pyroxenite with scattered sulphide blebs. It is generally bound by narrow (± 1 cm) chromitite stringers. The footwall to the Merensky is typically noritic or anorthositic, though in some places, feldspathic pyroxenite or harzburgite are associated with pothole-type Merensky reef. The upper contact is gradational from feldspathic pyroxenite and norite, to anorthosite.

In the western lobe of BC, the Merensky Reef has been divided into the Swartklip facies due south of Pilanesburg, and the Rustenburg facies centred on the town of Rustenburg (Fig. 5), owing to regional variations in thickness and the abundance, size and type of potholes. The Swartklip facies consists of narrow pegmatoidal and potholed Merensky Reef of high PGE grade, while the Rustenburg facies consists of wider, generally non-pegmatoidal Merensky Reef of lower PGE grade. The Rustenburg facies extends from the eastern side of Rustenburg Section to the Brits area (close to the De Wildt project area); it widens from 1m in the Rustenburg Section to 14m in the Brits area where it becomes sub-economic in PGEs (Viljoen, 1994). Naldrett et al. (2009) explained that the Merensky Reef was the result of major magma influxes that gave rise to pre-Merensky and Merensky cyclic units. They show an upward decrease in Pt tenor and upward increase in Cu/Pd ratios across the pyroxenite of Merensky Reef and also laterally away from feeder zones (Naldrett et al., 2009).

The UG2 chromitite of the Upper Critical Zone is a massive continuous layer that hosts mineable grades of chromite, with interstitial base metal sulphides and PGM minerals. It has been traced for over 280 kilometres in strike, is 0.50 m to 1.50 m thick, and dips north from 10° at Rustenburg to 26° in the northwestern limb (Viljoen and Shürmann, 1998). Up to three thin chromitite stringers (leader seams) are situated a few tens of centimetres above the main chromitite layer in the hangingwall pyroxenite. The leader chromitite seams are known to bifurcate and coalesce (Leeb-Du Toit, 1986; Viljoen et al., 1986). The UG2 chromitite is generally underlain by a pegmatoidal

feldspathic pyroxenite that often displays a mottled appearance due to the presence of large bronzite grains within the chromite crystals (Leeb-Du Toit, 1986 and Viljoen et al., 1986).

PGE mineralization is concentrated on the upper and lower contacts of the UG2 chromitite (Maier and Barnes, 2008), with minor concentrations in the leader chromitites. Mineralization may also extend a few tens of centimetres into the hangingwall and footwall rocks. The top and bottom contacts of UG2 chromitite are characterized by high PGE contents that suggest the UG2 seam formed by injection of chromitite slurries into semi-consolidated footwall units (Maier and Barnes, 2008). However, Heimstra (1985) showed that the UG2 chromitite layer is made up of three layers representing distinct cycles with discrete Pt/Pd ratios; the uppermost cycle has the highest Pt/Pd ratio of about 3 while the lower two thirds or remainder has a Pt/Pd ratio close to 1.3. In the simple case, there is no silicate between the three layers and they appear as one, while in places they are separated by partings and are thus discrete (adapted by Cawthorn, 2004 from Hiemstra 1985).

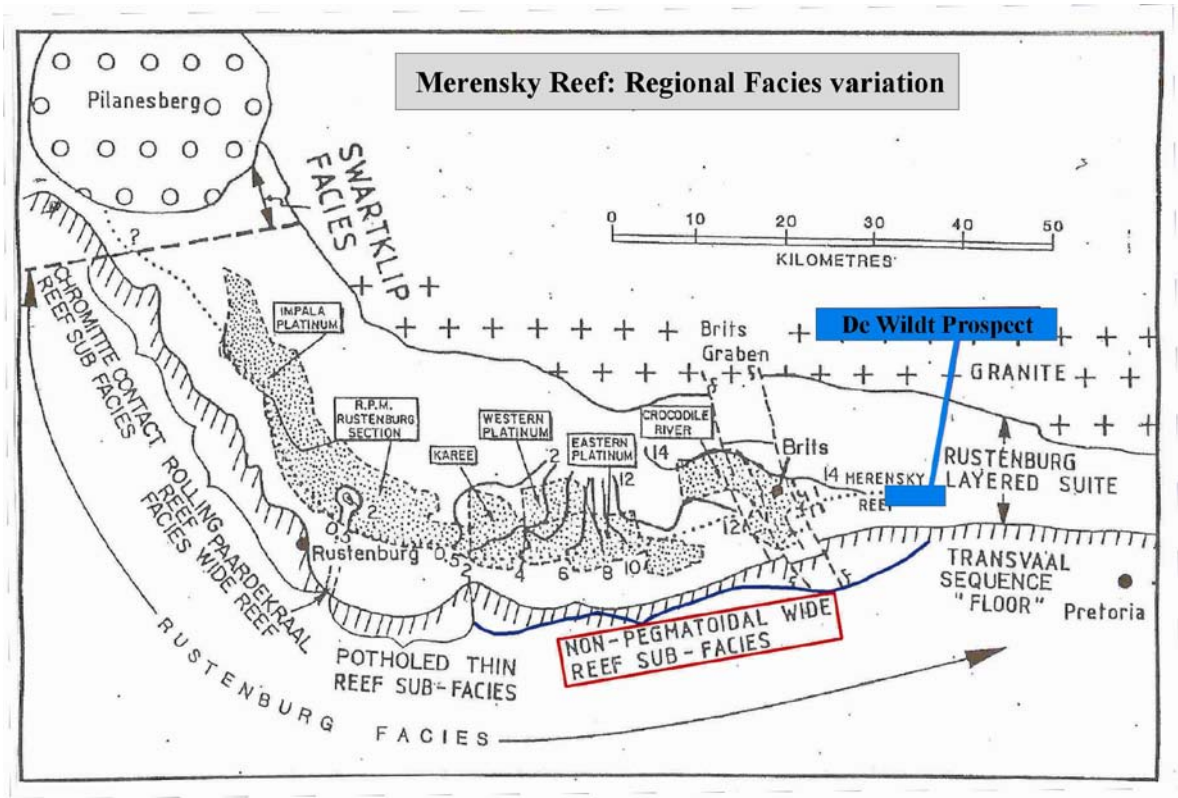


Figure 5: Regional geological variations in the nature of Merensky Reef (after Viljoen, 1994). The Swartklip facies is located due south of the Pilanesberg Complex while the Rustenburg facies is centred on the town of Rustenburg. The De Wildt project area lies due east of the town of Brits.

Recent models for the formation of massive chromitite seams involve magma mixing of relatively differentiated residual magma with a magnesium-rich primitive magma, in association with variations in the pressure of the chamber (Lipin, 1993; Cawthorn, 2005). Maier and Barnes (2008) suggested that the chromitite seams may have formed from flowing crystal mush that was injected along broadly bedding-parallel fractures into semi-consolidated footwall cumulates, along an inclined floor of the magma chamber. Mathez and May (2005) suggested that the chromitite may have acted as a barrier to ascending late magmatic fluids causing fluidization of the footwall cumulates. Maier and Barnes (2008) added that fluidization may have aided downward injection of the chromitite into the footwall. Variations in thickness, lithology and composition within the BC are controlled by proximity to the main feeder zone, such as at the Union Section (Maier and Eales, 1997). Scoon and Teigler (2005) noted that the Upper Group chromitites (UG2 and UG1) tend to be thicker in the distal facies (relative to the main feeder zone) while the Merensky Reef is well developed in the proximal facies but thicker and poorly mineralized in the distal facies. Teigler et al. (1992) and Scoon and Teigler (2005) observed that the Upper Critical Zone in the distal facies is thinner and dominated by plagioclase cumulates, while in the proximal facies it is thick, well developed and dominated by pyroxene cumulates.

2.4. Intrusive and discordant bodies

Rocks of the Rustenburg Layered Suite are intruded by lamprophyre and dolerite dykes and sills, and the Pilanesberg Complex (Leeb-Du Toit, 1986). Carbonate-rich dykes are exposed in the Amandelbult section of the Rustenburg Platinum Mines, and are brecciated and kimberlitic. In the Impala Mines lease area, micaceous (lamprophyre) dykes that range in thickness from centimetres to a few metres, are exposed in underground workings and are hosted by en echelon joint sets (Leeb-Du Toit, 1986). Vermaak and Von Gruenewaldt (1986) reported the presence of abundant NW-trending alkaline dykes of the Pilanesberg Complex that crosscut Transvaal metasedimentary rocks and the BC in the region immediately west of Brits Township.

The Pilanesberg Complex is a large body of intrusive and extrusive alkaline rocks with aerial extent of approximately 530 km^2. The complex is situated about 50 km NNW of Rustenburg at the contact of granitic and mafic rocks of the BC (Lurie, 1986) and has an east-west diameter of 28 km and a north-south diameter of 24 km. It forms a well-defined ring structure. The complex intruded the Western Limb of the BC ca. 1138 ± 45 Ma (Rb-Sr, in nepheline syenite; Harmer and Sharpe, 1985). It was emplaced during intrusion of syenite along ring fractures and the extrusion of lava and deposition of pyroclastite. The final volcanic events associated with emplacement were marked by the intrusion of foyaitic cone sheets and ring dykes. Alkaline dykes (syenitic) are associated with the ring complex (Lurie, 1986).

2.4.1. Iron Rich Ultramafic Pegmatoids (IRUPs)

IRUPs are discordant bodies in the BC that assume pipe-like/carrot-like, vertically elongate or irregular bodies (Eales, 2001). They are composed of clinopyroxene, olivine, ilmenite, amphibole, mica, and sulphide minerals together with Fe-Ti-Cr oxides. They are dark-brown to black in colour. Their width varies from a few centimetres to several kilometres (e.g. the Middellaagte Pipe at Amandelbult Section Mine is approximately two kilometres wide). The pipes are replacement bodies that passively replaced existing layered rocks by downward magmatic fluid percolation, particularly plagioclase-rich rocks such as norite and anorthosite (Eales and Cawthorn, 1996). In the western limb of the Bushveld, at Amandelbult, IRUPs are known from their pronounced magnetic signature (Eales and Cawthorn, 1996). They are spatially associated with dykes and faults but preferentially replace anorthosite layers between the UG2 and Merensky Reef. Elements that are a product of replacement include Fe, Ti, V and Ca. A marked excess of Fe is expressed by a high percentage of magnetite.

2.4.2. Potholes

Potholes are considered as disruptions of normal magmatic layering (Viljoen, 1994) and significantly and/or deleteriously impact mining of the UG2 and Merensky Reef layers. A pothole is a feature in which the unit truncates its footwall and forms a basin-shaped depression. The disrupted magmatic layer occurs within the pothole in a modified form when compared to its regional character (Viljoen, 1994, Lomberg et al.; 1999). Models for pothole formation have included:

- Injection of magma at specific feeder points followed by gravity sagging and chemo-thermal activity (Campbell, 1986).
- Kinloch et al. (1990) and Boudreau (1992) postulated that pothole formation resulted from development of significant intercumulus liquid and gas over-pressure in solidifying cumulates. By escape of gas or fumarolic activity these regions of gas over-pressure eventually remove cumulus material to form potholes, as suggested by the presence of hydrous minerals in potholes.
- Potholes are rolls (Lomberg et al., 1999). A roll is a feature in which there is a small change in strike and dip of a layer due to small-scale slumping. The affected layer only registers a small drop in elevation with little discernable change compared to layers affected by potholes. Rolls are common both to the UG2 and Merensky Reef but seldom disrupt mining operations.

Van der Merwe and Cawthorn (2005) documented the existence of irregular basal contacts on the UG2 and Merensky Reef. They summarized a number of processes that could account for small-scale structural features at the base of UG2 and Merensky Reef including redissolution, interference ripples, diapirism, gas-escape structures and impact generated dimples. Vermaak (1976) ascribed the undulating contacts to the base of Merensky Reef to impact-generated dimpling. The dimpled surface of the basal chromitite stringer of the Merensky Reef overlying an anorthosite footwall is the result of

impact of boulder-sized aggregates of pyroxenite onto unconsolidated chromitite and the underlying anorthosite (Vermaak, 1976). Kinnaird et al. (2002) citing Carr et al. (1999) suggested that potholes are the result of downward collapse of crystal mush into pull-apart sites, the pull-apart forming during tensile stress and magma loading, and that the texture is similar to dish-shaped potholes on the base of the chromitite units.

2.5. Structure and Metamorphism

2.5.1. Structure of the Bushveld Complex

Regionally, the emplacement of the BC magma into Kaapvaal Craton was facilitated by craton-wide lateral extension following plume-related underplating and gravitational loading (Uken, 1998). The subsequent isostatic adjustment in response to subsidence of the RLS is considered to have resulted not only in the formation of the current lapolithic shape of the BC (Gerya et al., 2004), but also its lobate character (Uken, 1998). The structures developed in response to magmatic loading; large basement domes (~100 km in diameter) around the perimeter of BC, medium sized domes (~40 km in diameter) within the BC and extending to the base of the Transvaal Supergroup, and small-scale domes and diapers (~8 km in diameter) occurring only within the contact metamorphosed floor rocks in the metasedimentary units of the Pretoria Group in the north-eastern BC (Uken and Watkeys, 1997; Uken, 1998). Kruger (2005) concluded that the BC is lobate, interconnected, wide but shallow, and a sill-like intrusion with upturned margins. This is supported by Clarke et al. (2008) who showed that the BC is a sill-shaped sequence of mafic-ultramafic rocks.

During the emplacement of the BC, contact aureole tectonism was expressed by sagging and up-folding/doming of the floor with formation of local basins, and this exerted a significant influence on the subsequent development of the Critical Zone (Hatton and Von Gruenewaldt, 1985). The up-folds/domes are described by Clarke et al. (2008). The intrusion of the essentially sill-like RLS resulted in the heating (thermal metamorphism) of the underlying floor rocks; the heated, plasticized and molten rock rose diapirically into the overlying crystallizing magma (Uken and Watkeys, 1997; Uken, 1998). Davey (1992) suggested that floor folds in the western BC within the Magaliesberg Quartzite (e.g., the Kookfontein and Spruitfontein upfolds) could be the reason why the Lower Critical Zone is absent from the Critical Zone (Fig. 6). Viljoen (1994) attributed lateral stratigraphic variations in chromitite layers and the thickening of the Merensky Reef pyroxenite east of Rustenburg Section to syn-emplacement folding/doming. Davey (1992) postulated that the Spruitfontein up-fold might separate two magma sub-chambers in which similar, but not identical, processes took place during the development of the Critical Zone.

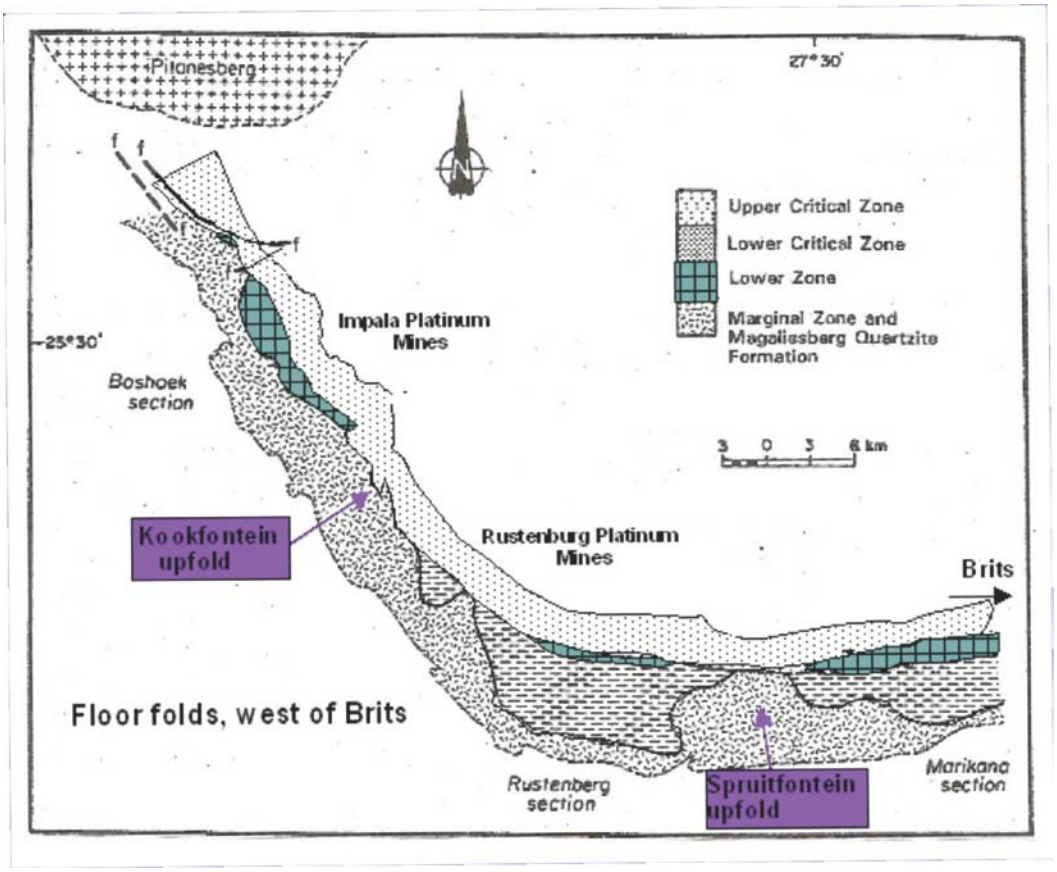


Figure 6: Floor folds in the Magaliesberg Quartzite Formation in the south-western Bushveld Complex, west of the De Wildt project area (modified after Davey, 1992). Floor folds include the Kookfontein and Spruitfontein upfolds.

2.5.2. Contact metamorphism

Heat released from cooling of the BC magmas is associated with metamorphism of the country rock at a lateral distance of up to 50 km from the contact (Cawthorn et al., 2006). Regionally, the contact aureole in the floor rocks to the BC thickens from south of Pretoria toward the east, west and north. The peak average thermal gradient estimated across the aureole was 80 ± 20°C/km with pressures of 2.1 ± 0.4 kbar in the upper part of the Pretoria Group (Gerya et al., 2004).

Contact metamorphism of Transvaal Supergroup wall rocks was described by Hartzer (1995) from the Crocodile River, Marble Hall and Dennilton domes: contact metamorphism is generally low- to medium-grade. However, rocks in the inner contact aureole attained pyroxene-hornfels facies, as characterized by the presence of augite and hypersthene (Hartzer, 1995). In contrast, xenoliths of meta-argillite (of the Transvaal Supergroup) within the BC are characterized by the assemblage sapphirine, mullite, spinel and corundum (Sharpe and Chadwick, 1982), which is common for high grade hornfelses adjacent to mafic intrusions (Pattison and Tracy, 1991).

In argillitic units of the Crocodile River dome, contact metamorphism attained 410-510°C and 2.5 kbar pressure, as expressed by the development of the metamorphic assemblage andalusite, biotite, muscovite and quartz (Hartzer, 1995). Carbonate rocks attained 530°C and <2.5 kbar pressure with

development of the calc-silicate mineral assemblage tremolite ± talc, calcite, quartz and dolomite. Volcanic rocks are characterised by the metamorphic assemblage hornblende, plagioclase, quartz, muscovite and biotite, which is characteristic of hornblende-hornfels facies metamorphism. Sedimentary rocks at the contact with Bushveld granite in the Rooiberg fragment underwent contact metamorphism to albite-epidote hornfels facies (Rozendaal et al., 1986).

Buick et al. (2000) citing Wallmach et al. (1989; 1995) reported that the RLS contains numerous calc-silicate xenoliths that were initially metamorphosed at ~1200-1300ºC and later retrogressed by hydrous fluid infiltration at ~700ºC. The occurrence of hydrothermal vein systems (comprising calcite at low temperature, hornblende and plagioclase) throughout the RLS has been attributed to the ingress of hydrous C-O-H bearing fluids at ~350-700ºC (Schiffries and Rye, 1990). Buick et al. (2000) showed through stable oxygen isotope work that the fluids were derived by dehydrating the country rocks in the floor of the BC intrusion. They suggested that the retrogression was a result of channelled infiltration of fluid into cooling RLS mafic rocks where it exchanged ^{18}O with low ^{18}O RLS mafic rocks. Stevens et al. (1997) documented the occurrence of high grade mid-crustal granulite facies metamorphism that may have resulted from the intraplating of Bushveld Complex-related ultramafic magmas before the Vredefort impact event.

2.6. Regional Geophysics

Geophysical surveys including gravity, seismic and magnetic have been conducted by Davison and Chunnett (1999) and Viljoen (1999) to investigate the structure and emplacement of the BC. The complex exhibits a 30 km long major gravity high immediately northeast of the Pilanesberg and a second 9 km long gravity high northeast of Rustenburg in the western Bushveld (Fig. 7). These gravity highs correspond with thickening of mafic units and are interpreted as indications of feeder sites for mafic magma in the western BC (Viljoen, 1999). Small gravity highs occur over the Brits graben and in the area between Brits and Pretoria adjacent to the De Wildt project area.

Regional gravity interpretation in which there was a lack of positive gravity anomaly at the central area of the BC led to a disregard of the possible connection of the western and eastern limbs at depth (Cawthorn and Webb, 2001). However, based on petrographic and stratigraphic similarities in the UG1, UG2, middle group chromitites, Merensky Reef, Upper Zone/Middle Zone transition it is assumed that the two major limbs are connected and form part of one large magma chamber (Cawthorn and Webb, 2001). Cawthorn and Webb (2001) suggested that the depression of the continental crust under the BC by up to 6 kilometers was the result of isostatic readjustments due to the enormous mass of overlying mafic rock.

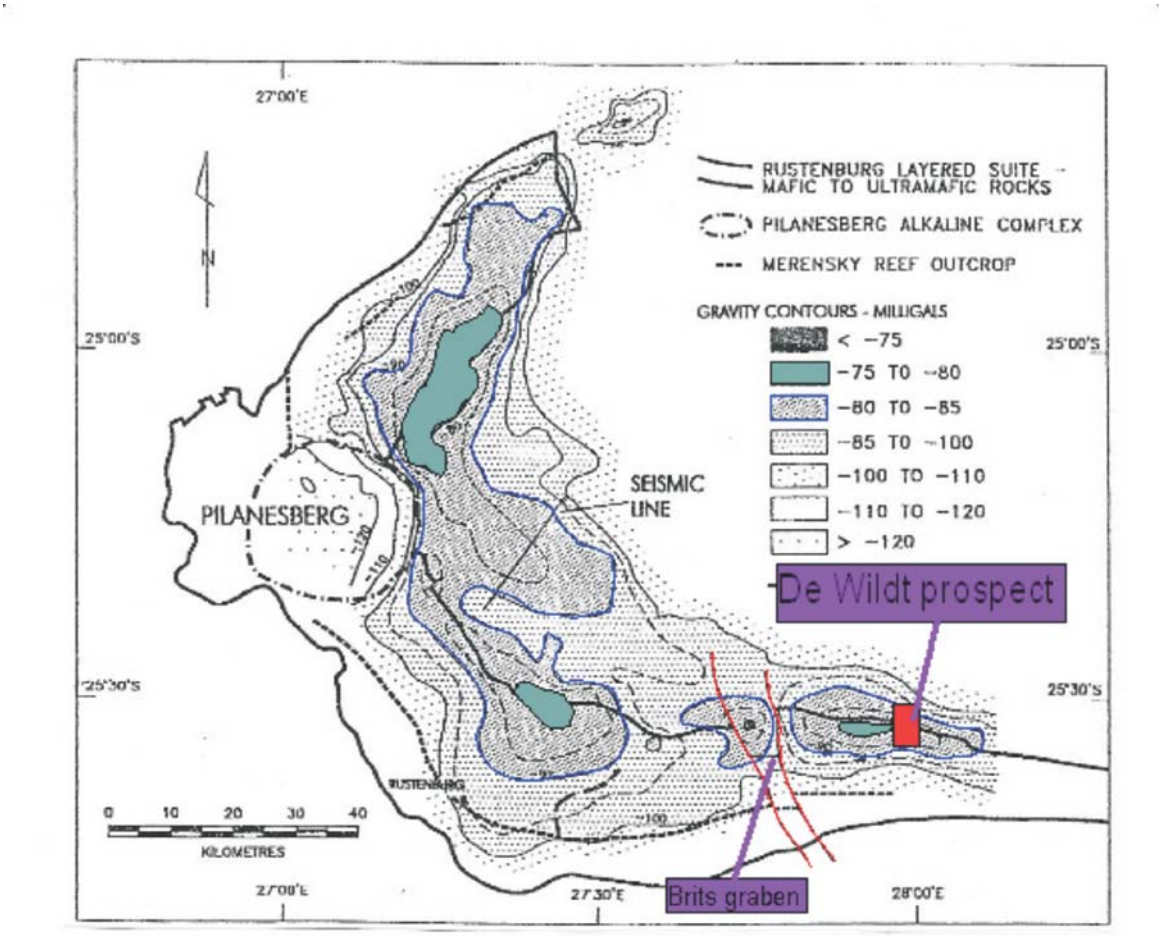


Figure 7: Major gravity anomalies in the western BC (modified after Viljoen, 1999). Gravity highs occur north of Pilanesberg, north of the town of Rustenburg and due west of the De Wildt project area. The gravity highs correspond with thickened mafic units that may represent feeder sites.

2.7. Floor Rocks to the Bushveld Complex

The BC intrudes the Transvaal Supergroup which is composed of a 10-15 km thick sequence of relatively undeformed sedimentary and volcanic rocks (Button, 1986; Eriksson et al., 1995, 1993; 2007). The complex intruded the Transvaal Supergroup along an unconformity above the Magaliesberg Formation of the Pretoria Group (Walraven, 1997; Eriksson et al., 2007). The floor to the Rustenburg Layered Suite of the BC consists of intercalated mudstone-sandstone units, andesite lava and subordinate conglomerate beds, diamictite and minor carbonate units of the Pretoria Group (Hatton and Schweiter, 1995; Eriksson et al., 2007).

The Transvaal Supergroup (Table 2) has been correlated to Griqualand West basins of South Africa and the Kanye basin of Botswana by Eriksson et al. (1993; 2007). The Transvaal basin is dated at ca. 2.5-2.2 Ga, but the age of the Pretoria Group is constrained to ca. 2.35-2.20 Ga based on a Rb-Sr whole rock age of 2224 ± 21 Ma for the Hekpoort Formation of the Pretoria Group (Burger and

Coertze, 1973-1974), and an unpublished 2350 Ma age (Eriksson et al., 1995; Frimmel and Minter, 2002) for the Timeball Hill Formation of the Pretoria Group.

2.8. Local Geology – the Brits area

The De Wildt area is situated approximately 5 km east of the Brits graben (Figs. 1 and 5). The graben is the main structural lineament within the immediate surrounding area and extends from the Crocodile River fragment in the NNW to the edge of the Johannesburg Dome in the SSE (Wilhelm et al., 1997). The graben contains sub-graben blocks that are bounded by the steeply dipping, NNW-trending Bokfontein and De Kroon faults (Judeel and Hartmann, 2008), with normal block displacements in the order of 600 m. The trend and dip of igneous layers in the graben varies from one block to the next. Several fault-controlled syenite and dolerite dykes crosscut the graben (Lomberg et al., 2006). Iron-rich pegmatoids (IRUPs) and potholes have been mapped SE of the De Wildt prospect in the graben in the Elandsfontein property (Tiegler et al., 1992; Scoon and Mitchell, 1994; Lomberg et al., 2006) as indicated from aeromagnetic data and disturbed UG2 chromitite and Merensky reefs intersected in boreholes.

Published data for the UG2 chromitite and Merensky Reef in the region of the De Wildt project is limited and includes Maier and Bowen (1996) citing Moen (1989) who documented the UG2, and Butcher and Merkle (1991) who studied with Upper Zone rocks. Maier and Bowen (1996) citing Moen (1989) recorded that the UG2 chromitite layer on the Schietfontein farm overlies a large meta-sedimentary footwall block, but did not investigate the cumulate sequence between the UG2 and the base of the complex. It is thus not known if the sequence in the De Wildt region is different from that present at Rustenburg and Amandelbult in western BC. Maier and Bowen (1996) reported that the UG2 hanging-wall pyroxenite was separated from the UG2 chromitite by a 15 m norite layer in the Schietfontein farm portion. Lomberg (1991) reported that the UG1 chromitite layer is poorly developed to the east of the Zilkaatsnek 439-JQ farm portion (Fig. 2) and consists of numerous thin chromitite lenses, with no development of the Lower Zone.

Maier and Bowen (1996) noted that in the western BC, the UG2-Merensky Reef interval is situated about 100 m below the Critical Zone-Main Zone boundary. However, the UG2-Merensky Reef relationship east of Brits is not known as a result of poor exposure and a large number of faults. Roberts (1992) documented that in the area bounded by Rosslyn, Hartbeespoort Dam and Pretoria the cumulate succession of BC, which includes the De Wildt project area, is broadly similar to other BC localities, except for the absence of Lower Group chromitites, the appearance of cumulus plagioclase below the Middle Group chromitites and an exceptional thick Merensky Reef (12 m). The western limb of the BC has been shown to thin eastwards towards Pretoria (Cawthorn and Webb, 2001).

Further to this, the 2527 Brits Geological Series map records the presence of dykes and faults throughout the Brits area and within the De Wildt prospect (Chief Directorate: Survey and Mapping, 1996). Faults are less pronounced away from the graben and towards the east. A NE-trending dyke intrudes the Magaliesberg Quartzite hills about 5 km south of the De Wildt prospect. A NE-trending sinistral (apparent) strike-slip fault also occurs south of the De Wildt prospect, with a calculated sinistral displacement of approximately 250 m. Quartzite outcrops occur in the centre the prospect, while two parallel ridges of the Magaliesberg Quartzite occur on the eastern margin of the prospect.

With respect to radiometric data over the De Wildt area, Antonie (2004) reported that the spectrometer uranium channel is flat while those of thorium and potassium showed disparate anomalies. Zones of increased gamma radiation in the K channel correlated with areas where floor rocks were mapped and thus could be used to indicate potential inliers.

Group	Formation	Age (Ma)	Lithology
	Loskop	2060 (U-Pb)	Mudrock sandstone
Rooiberg	Selonsrivier and Damwal	2090	Felsites
	Dullstroom,Leeuwpoort	2089+/-15 (Rb-Sr)	Mafic & felsic lavas clastic sediments
	Rayton/Woodlands		Mudrock sandstone pyroclastic carbonate rock
	Magaliesberg		sandstone
	Silverton		Mudrocks volcanics carbonate rock
	Dasport		sandstone
Pretoria	Strubenkop		Mudrock sandstone
	Dwaalheuwel		Sandstones conglomerates
	Hekpoort	2224 +/-21 (Rb-Sr)[1]	Basaltic andesites
	Boshoek		Conglomerate sandstone
	Timeball Hill	2263 (Rb-Sr)	Mudrocks sandstone tilloid
	Rooihoogte		Breccias conglomerates sandstone
	Duitschland		
	Penge	2432+/-31 (U-Pb SHRIMP)	Iron Formation
	Frisco		Dolomite chert
Chuniespoort	Eccles		Dolomite chert
	Lyttelton		Dolomite chert
	Monte Christo		Dolomite chert
		2550± 3 Ma4(Single zircon Pb-evap)[3] 2583 ± 5 Ma2(U-Pb SHRIMP)[2]	
	Oaktree	2588 ± 7 Ma2(U-Pb SHRIMP)[2]	
Black Reef	**Black Reef**		Sandstone/conglomerate
	Buffelsfontein		Sandstone mafic felsic lavas mudrock
	Godwan Group		Sandstone lavas
Pre-Transvaal	Wachteenbeertje Fm.		Mudrock carbonate sandstone
	Woikberg Group		Mudrock sandstone basalts
	Upper Groblersal Group		Sandstone lavas
	Lower Groblersal Group		Metamorphic rocks

Table 2: Simplified stratigraphy of Transvaal Supergroup and age data (modified after Eriksson et al. (1993) and Dankert and Hein (2010).
(1) Burger and Coertze (1973-1974; Rb-Sr whole rocks age).
(2) Martin et al. (1998; single zircon U-Pb SHRIMP).
(3) Walveren and Martini (1995; single zircon Pb-evaporation).
(4) Unpublished; vvvvv = volcanic or pyroclastic unit.

CHAPTER 3

METHODOLOGY

3.1. Research approach

This research attempts to investigate and establish the structural setting of UG2 and Merensky Reef;

- Photogrammetry: Black and white aerial photographs were combined into a photographic mosaic for the De Wildt region and interpreted. This was overlain with Google Earth imagery. The interpretation was validated with surface mapping to establish the position of faults and dykes.
- Aeromagnetic data (1st vertical magnetic derivative and total magnetic intensity, 2nd vertical magnetic derivative, Fig. 8; see Appendix) yielded insight into the underlying geology by depicting magnetic horizons and anomalies. A magnetic interpretation map was compiled.
- Geological data from diamond drill core and surface plans was incorporated to provide a comprehensive model for the litho-stratigraphic and structural setting of the Merensky Reef and UG2 chromitite layers.
- Petrographic and mineralogical studies of selected samples from boreholes were investigated to establish lithologies (Fig. 3, borehole map).
- The strato-structural setting of UG2 chromitite and Merensky Reef in the De Wildt area was correlated and compared with the strato-structural setting of the UG2 chromitite and Merensky Reef in the adjacent Rustenburg facies to the west of the De Wildt project area to establish similarities and differences in the nature of the reefs, and to develop an overall model for reef variation.
- An interpretive map based on combined photogrammetric, magnetic, topography, borehole data and historic geology for the De Wildt area was compiled.

3.2. Photogrammetry

Black and white digital aerial photographs (rasters) and a flight plan of the study area were obtained from the photographic database at the University of the Witwatersrand Johannesburg. The 1:36 000 aerial photographs were captured on 14-25 July 1961 using a Wild 15 AG 39 No.296 camera or lens, with a focal length of 152.37 mm and in a 9 x 9 inches format. From these images, a photographic mosaic was created using Arc-GIS version 9.0. Geo-referencing of the raster images was completed using georeferenced topo-cadastral sheet 2527DB Brits (Chief Directorate: Survey and Mapping, South Africa, 1996) in which the study area is located.

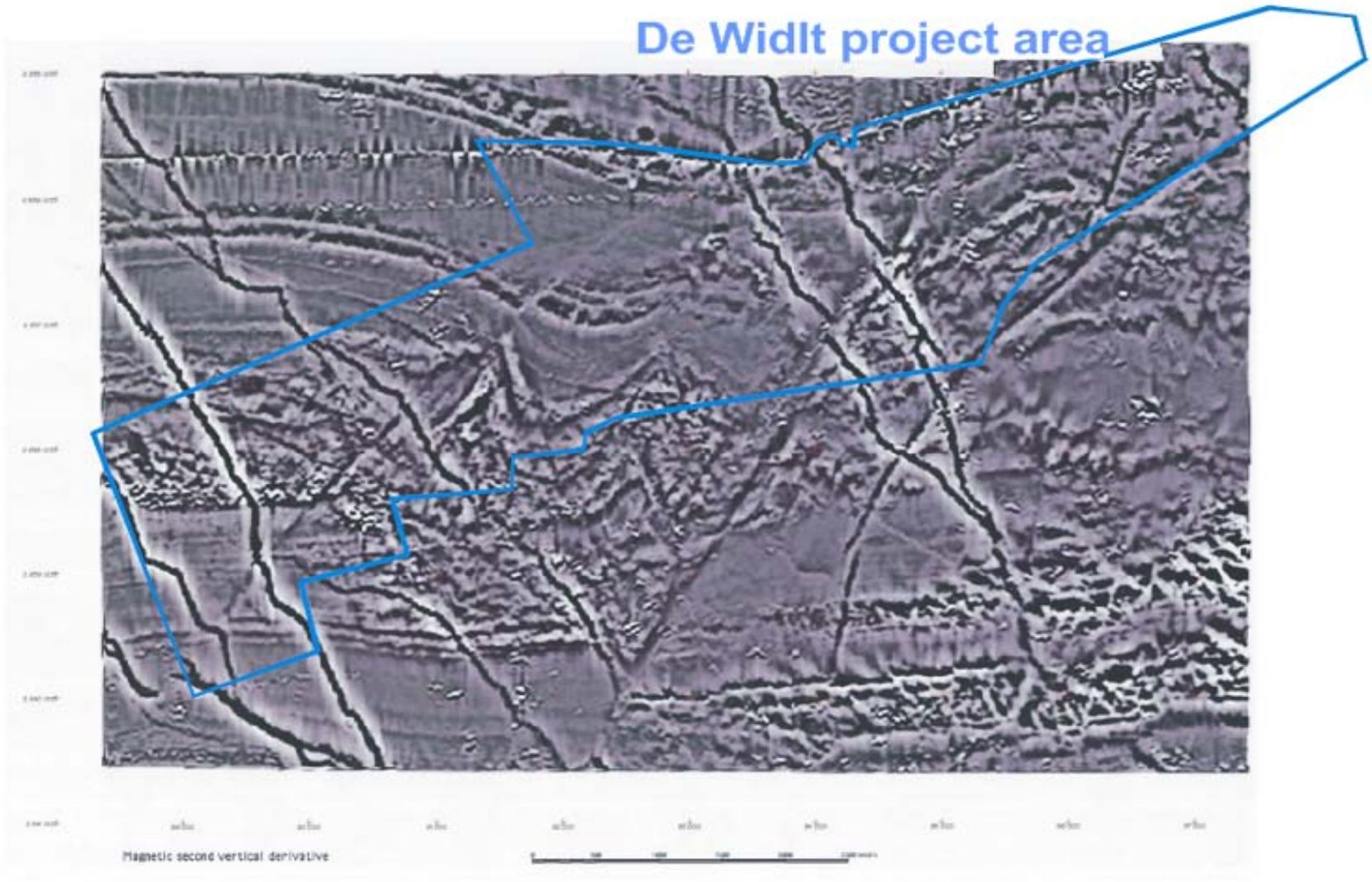


Figure 8. The second vertical magnetic derivative map across the De Wildt project (Antoine, 2004). Structures such as dykes and faults, which disrupt the mafic layers of BC, were discerned from this plan. The De Wildt project area is marked in blue.

3.3. Aeromagnetic data

A detailed aeromagnetic survey over the De Wildt area was flown on 13-14 November 2003 by Fugro Airborne Surveys (Pty) Ltd on behalf of Nkwe Platinum (SA) (Pty) Limited, using a horizontal gradient mode magnetometer mounted on a Bell 206 helicopter. A total of 1012 line kilometres were acquired using a line spacing of 50 m. A sensor to ground clearance of 20 m was used for both the magnetometer and gamma ray spectrometer data. A north-south line direction was used with orthogonal control lines flown at an interval of 500 m. The magnetic data was sampled at 10 Hz, while spectrometer and navigation (GPS) data were acquired at 1 Hz. Additional survey specifications are given in Table 3. Total magnetic intensity data was enhanced using a second vertical derivative filter that preferentially sharpened the magnetic signatures of shallow sources. The resulting 2nd vertical magnetic derivative map was interpreted and found to be useful in delineating the extent of various lithological units, and dykes and faults masked by overburden.

The data from the aeromagnetic plan was extracted using the methodology of Hammond (1998);

- "when a number of essentially parallel units can be discerned, a relatively intact block of layered rock might have been imaged''.
- "where two magnetic units cross each other with little effect, an interpreter is limited to relatively few geological relationships that have this pattern (e.g., joint sets, dykes)".
- "unless a given discontinuity is a major structure with a very large displacement, then a chance exists that some correspondence between units on either side of the fault can be discerned"

Survey specification	Detail
Magnetic data recording interval	0.1sec, approximately 5 meters
Radiometric data recording interval	1 sec, approximately 50 meters
Sensor Mean Terrain Clearance	20 meters
Flight line spacing	50 meters
Tie line spacing	500 meters
Flight line trend	090 degrees
Tie line trend	000 degrees

Table 3: Specifications of airborne magnetic survey conducted over the De Wildt project area (after Antoine, 2004).

Mitchell and Manthree (2002) documented the occurrence of a high iron-rich zones associated with the transition from Critical Zone to Main Zone of the BC. Ashwal et al. (2005) detailed that anorthositic rocks, particularly within the Main Zone, show higher magnetic susceptibility than any other polyphase cumulates as a result of the presence of intercumulus magnetite and dust-like inclusions of magnetite. Thus, it has been possible to separate the Giant Mottled Anorthosite (GMA) from other mafic rocks in the region.

3.4. Mapping and logging

Geological surface mapping was conducted throughout the project area as delineated by the farm boundaries. Sites of outcrop were measured and recorded using a GPS (Garmin) instrument (UTM, WGS 84). The mapping exercise involved general mapping principles that included rock description and identification, structural measurements such as dip and strike of bedding, layering and banding. A geological surface plan was compiled using the collected data.

All diamond boreholes drilled by Nkwe Platinum were logged at the core-shed at De Wildt. The logging involved recording borehole depth, lithological descriptions according to BC standards (SACS, 1980), description of mineralization, alteration and structures such as faults, fractures and joints. Also, photographs of reef intersections and other lithologies of interest were made. The data log for each borehole was captured into several Excel™ spreadsheets and subsequently exported into Golden Software Grapher™ (version 5) from which stratigraphic columns were compiled (Figs. 9-11). Grapher ™ together with Corel DRAW™ (version 9), were used to compile diagrams and illustrations. The construction of UG2 chromitite isopachs and isochons used Golden Software Surfer™. Drill core data from historic logs (SK boreholes) was presented to Nkwe Platinum in the form of manuscripts which were then captured into Excel™ spreadsheets after relogging. The data was later incorporated into the Nkwe Platinum database and used for analysis and interpretation.

The geological data obtained from more than 40 diamond holes (inclusive of historical boreholes) drilled in the project area was used to investigate the structural setting as well as the geology of the Merensky Reef and UG2 layers. Cross-sections of the project area were drawn to interpret structures such as faults and dykes that displace the Merensky Reef and UG2 reefs, and also to establish the lateral continuity of the Merensky Reef and UG2 layers across the project area.

The UG2 isopach and isochon maps of UG2 chromitite data from boreholes were drawn and used to depict the variation of the UG2 chromitite layer across the project area in terms of width and grade. The investigation of the PGE value distribution along the UG2 chromitite reef, based on assay results, was also conducted. This helped delineate the portions of the UG2 chromitite reef that were enriched in PGEs. In addition, prill splits, which are a percentage break down of the individual PGE constitution within the UG2, was calculated from assays of the UG2 chromitite samples. Attention was paid to establishing the Pt:Pd ratio of the UG2 chromitite reef at De Wildt prospect. The Pt:Pd ratios

were chosen as these are commonly calculated for the BC by mining and exploration companies in South Africa and allowed comparisons to published Pt:Pd ratios from various localities within the BC.

3.5. Petrography and mineralogy

More than 35 samples of NQ drill-core (not orientated) were taken from boreholes that had features of interest and not normally encountered in the BC mafic rocks. The core was split using a Costor core-splitter at Nkwe Platinum's core yard to obtain half core samples of between 10-20 cm lengths. The samples were labelled and bagged, and details of the depths at which the sampling took place were recorded. The samples were submitted to SGS Laboratory in Booysens Johannesburg for preparation of polished thin sections and these were used for mineralogical and micro-structural analysis**.**

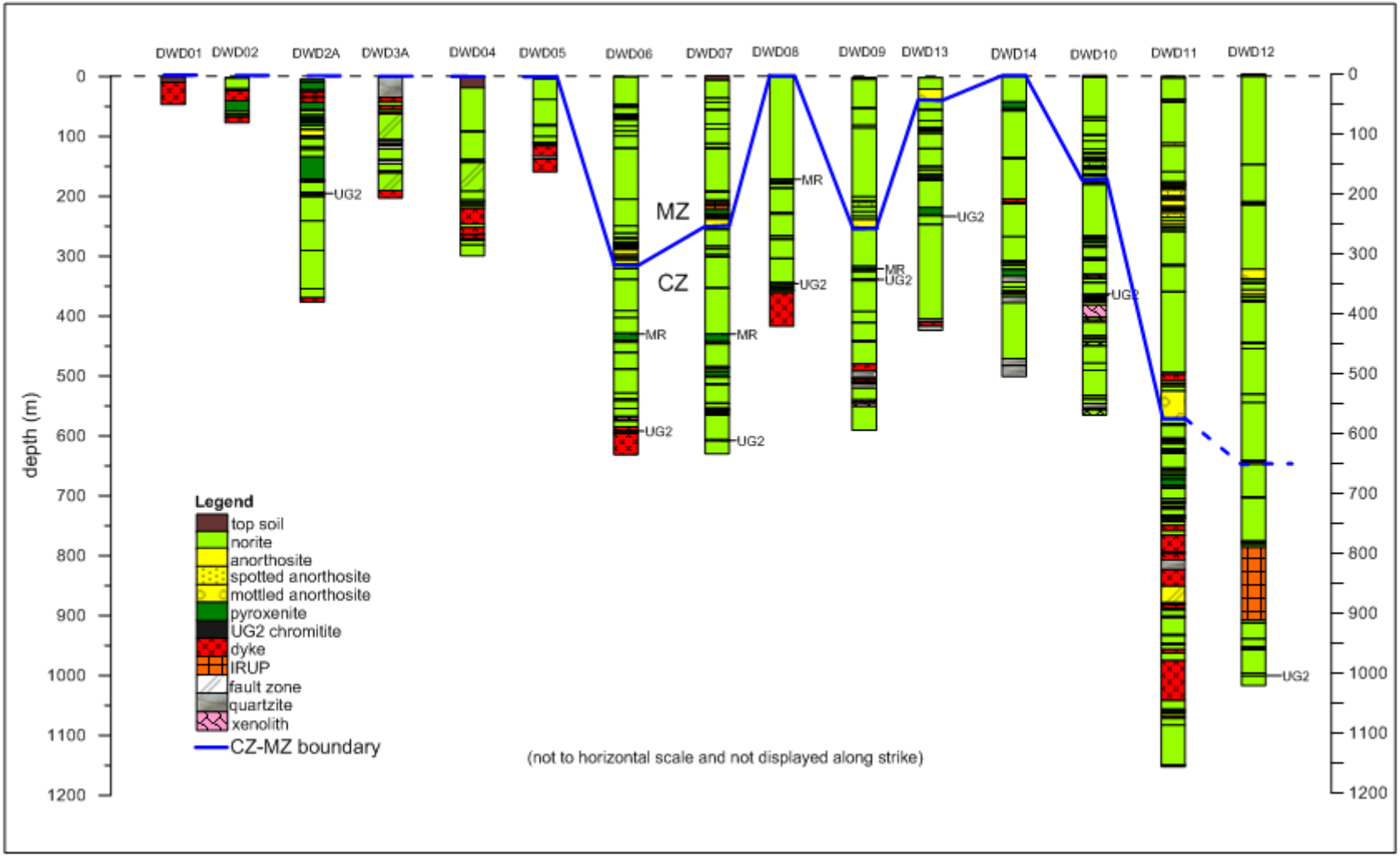


Figure 9: Schematic representations of borehole logs drilled in the De Wildt project area by Nkwe Platinum. The boreholes were used in the study to characterize the distribution and continuance of the Merensky Reef (MR) and Upper Group 2 chromitite (UG2) layers.

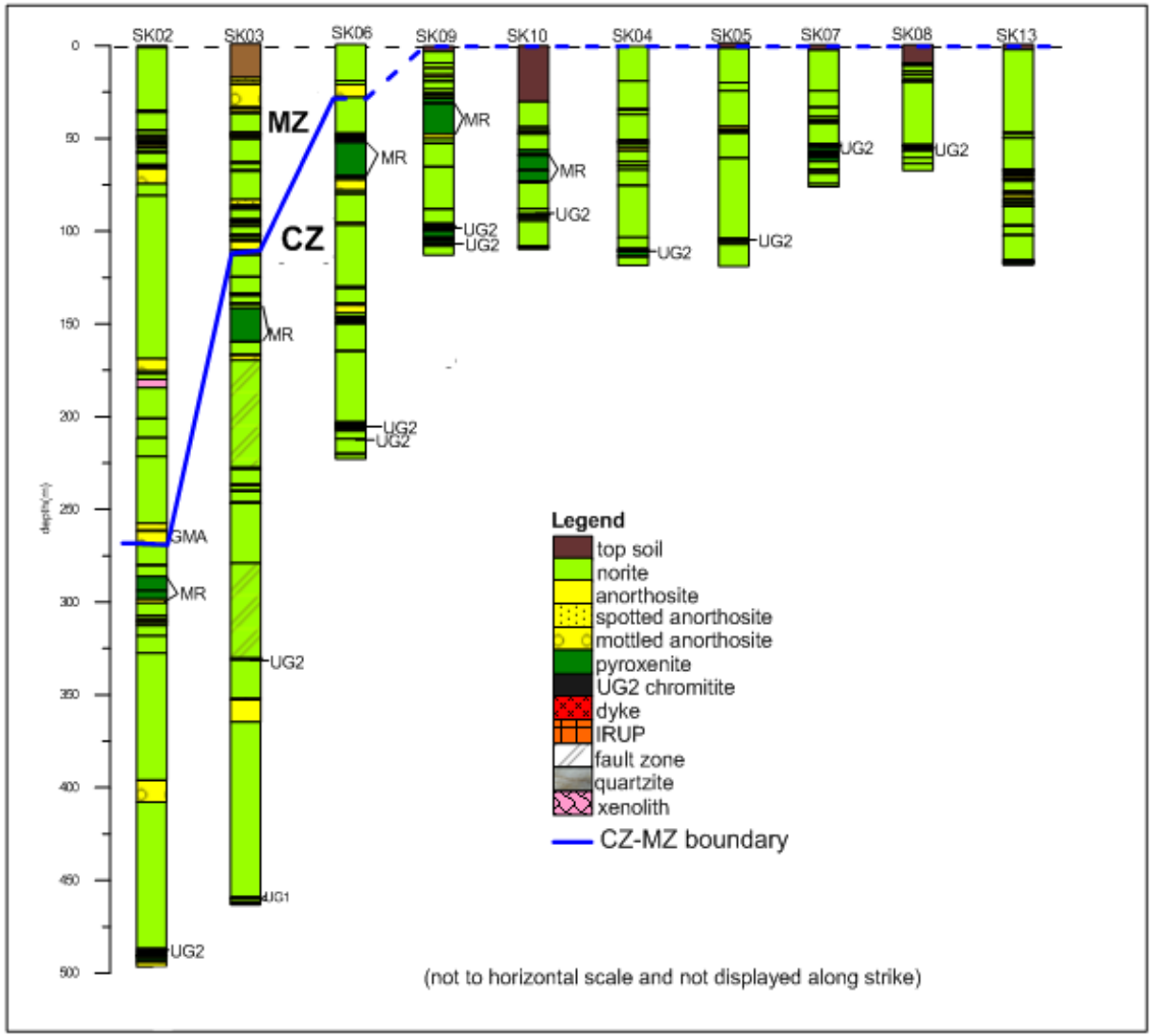


Figure 10: Stratigraphic logs drawn from historical diamond boreholes that were re-logged and used in the study (MR=Merensky Reef, UG2=Upper Group 2 chromitite and UG1=Upper Group 1 chromitite layer).

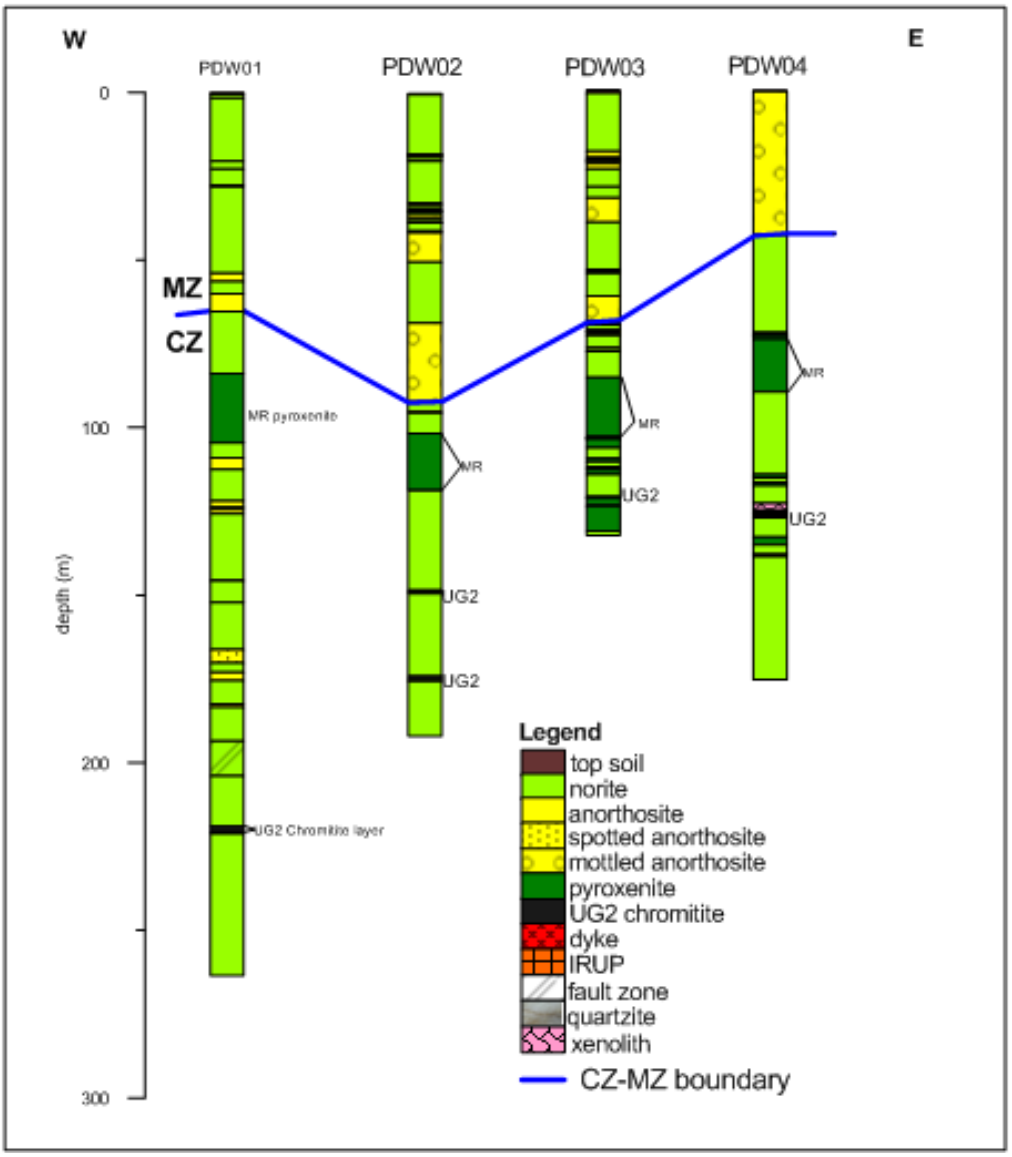


Figure 11: Schematic representation of logs of boreholes drilled by Nkwe Platinum in the western portion of the De Wildt project area (MR=Merensky Reef, UG2=Upper Group 2 chromitite layer)

CHAPTER 4

REMOTE SENSING & FIELD INVESTIGATION RESULTS

4.1. Surface Mapping

The De Wildt project area is covered by black turf, with minimum exposure of the Rustenburg Layered Suite. Limited outcrop of the Bushveld Complex rocks occur along the Magaliesberg mountain ridge, which is situated at the southern boundary of Visserhoek, Schietfontein and Zilkaatsnek farm portions (Figs. 2, 12). The Magaliesberg mountain ridge consists of sandstone (and quartzite) of the Magaliesberg Formation of the Transvaal Supergroup. The southern part of project area is generally marked by relatively fine-grained norite units that are tentatively correlated with the Marginal Zone of the BC. Fine to medium-grained norite and gabbronorite boulders subcrop in the northern part of the prospect and define the Main Zone in the De Wildt project area. Rugged hills to the far north characterise Main Zone gabbronorites. Norite (leuco-norite) units (with a strong NW trending mineral lineation defined by plagioclase crystals) and scattered pyroxenite subcrop were confined to a narrow zone in the centre of the study area. This zone is interpreted to overlie the Critical Zone of BC (Fig. 12). The rocks in the study area generally trend E-W and dip 18-28°N.

In the east of the study area, pyroxenite and melanorite units of the BC crop out and contact the Magaliesberg quartzite floor rocks. The quartzite units trend E-W and dip approximately 28º N. The contact between the BC and Transvaal metasedimentary floor rocks is marked by recrystallized and contact metamorphosed quartz veins.

4.2. Photogrammetry

In the photographic mosaic, the east-west trending Magaliesberg Quartzite units are readily defined in the south of the study area (Fig. 13). The Main Zone Hills, which are composed of gabbro-norite, lie to the north. Settlements that make up the township of Ga-Rankuwa are situated north and northeast of the study area. Two ridges of quartzite encroach into the eastern portion of the study area. Northeast-trending lineaments crosscut the study area east and west of the Main Zone Hills. Numerous NNE and NNW-trending master joints crosscut the Magaliesberg Quartzite in the south of the project area. A railway line that traverses east-west along the northern boundary of the study area, and local roads, are also evident in the mosaic. Farm portions are also partially discernable within project area and throughout the surrounding areas. Open cast pits occur west and east of the De Wildt project area.

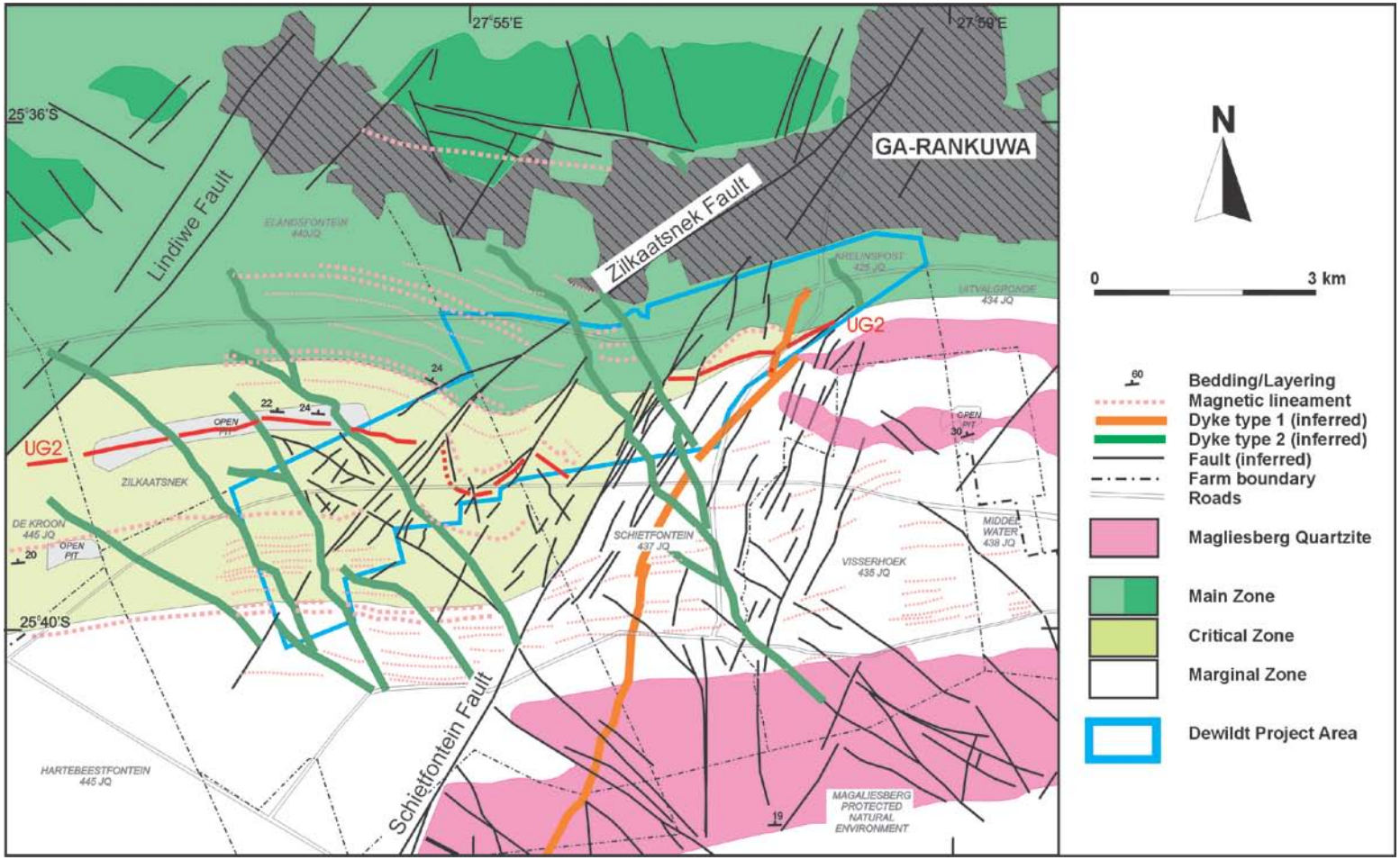


Figure 12: Schematic map that combines interpretations of black and white aerial photographs and Google Earth images of the De Wildt project area (blue) with those of topography and 1st and 2nd vertical derivative aeromagnetic data. West-trending lineaments are evident in the BC mafic units, and these are crosscut by an array of NE and NW-trending faults and two dyke sets. Displacement on the Schietfontein, Zilkaatsnek and Lindiwe fault is sinistral (apparent) but the faults are most likely scissor faults with normal displacement and west block down. The BC mafic units dip north.

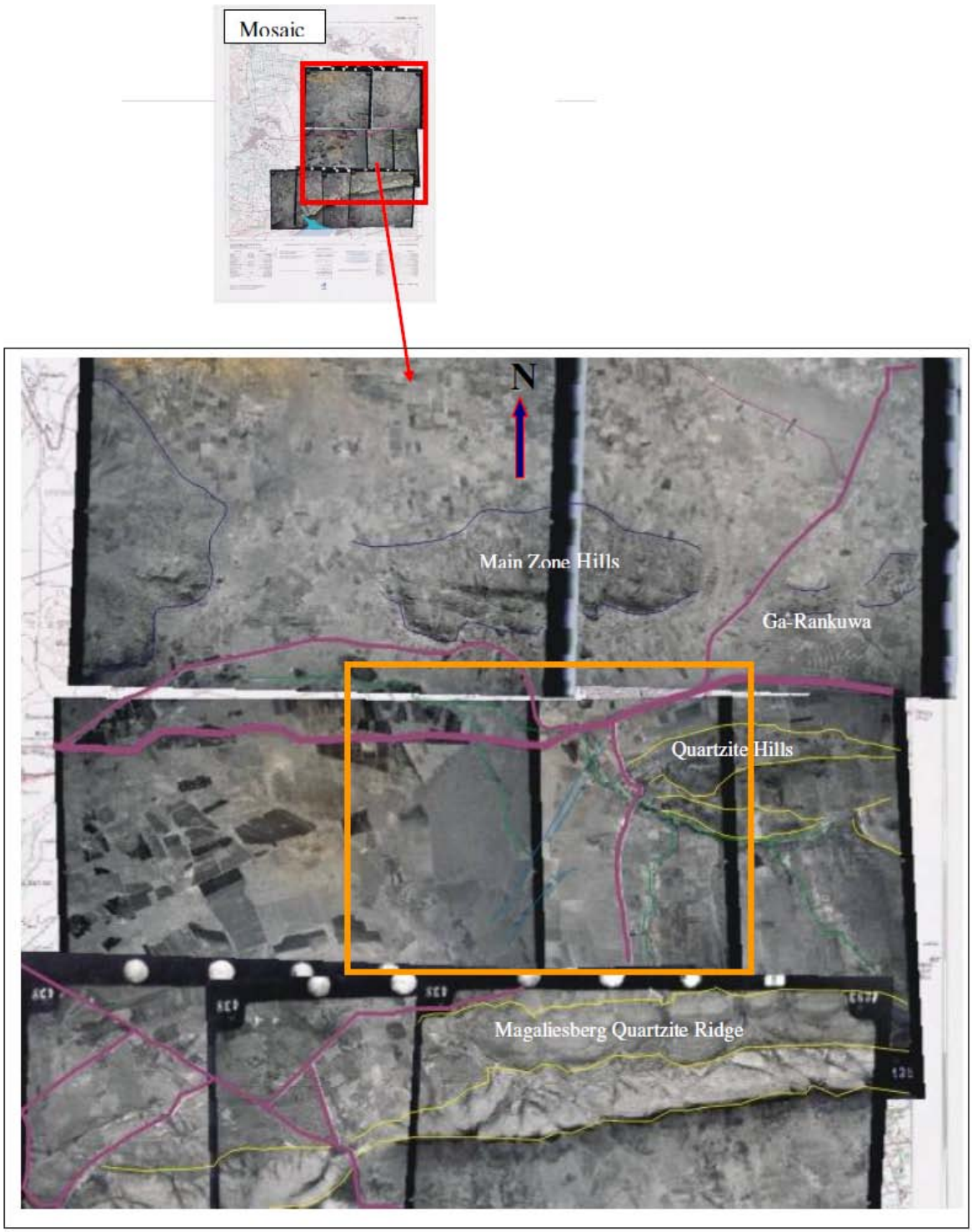


Figure 13. Photographic mosaic of De Wildt area (orange box). NE trending lineaments (faint blue) are apparent across the prospect. Quartzite hills occur to the east and south of the project and are crosscut and displaced by NW and NE-trending fractures. Small streams are marked in green.

4.3. Aeromagnetic Interpretation

The 2nd vertical derivative aeromagnetic map for the De Wildt region (c.f. Fig. 8) was interpreted using the methodology of Hammond (1998). North-south orientated lineaments were ignored to avoid flight line stitch mismatch (flight lines were north-south). Three distinct zones (i.e., western, central and eastern zone) were defined on the basis of lithological character and fault/fracture patterns. The zones are bounded by NNE-ENE trending faults that are hereafter termed the Zilkaatsnek and Schietfontein faults (Fig. 12). The position of the Schietfontein fault coincides with the position of NE-trending fault on the 2527 Brits Geological Series map of the De Wildt region and a NE-trending lineament that passes east of the Main Zone Hills (Figs. 13, 12). A NE-trending fault, termed the Lindiwe Fault, can be interpreted from topographic data.

NNW-trending magnetic highs (shown in dark green lines in Figs. 14, 12) are interpreted as mafic dykes that crosscut all BC mafic units and the Zilkaatsnek and Schietfontein faults. Based on crosscutting relationships the dykes were emplaced after the BC mafic units and after deformation associated with fault formation.

The western zone covers the Zilkaatsnek farm portion and is marked by relatively undisturbed E-W trending linear magnetic highs and lows that are interpreted as mafic units of the BC. Within these units, the Giant Mottled Anorthosite (GMA) is resolved as two distinct parallel high-low couplets, as marked by two yellow lines in Figure 14. The couplets are interpreted as the boundary between the Main Zone and Critical Zone in the De Wildt area. An anorthosite unit is also interpreted higher up (and northward) in the Main Zone stratigraphy (on the top edge of the magnetic image, Fig. 14).

The central zone is characterized by folded mafic units of the BC. NNW and NE-trending lineaments that crosscut the mafic units are interpreted as fractures and joints. The Zilkaatsnek fault (apparent) displaces the Giant Mottled Anorthosite unit by a maximum of approximately 150 m in an (apparent) sinistral sense, but displacement is unequal along the length of the fault being lesser in the northeast and greater in the southwest. The Zilkaatsnek fault is thereby interpreted as a scissor fault that is hinged in the northeast. However, the kinematic of the Zilkaatsnek fault have yet to be established.

The eastern zone underlies the Krelingspost Farm and part of the eastern portion of Schietfontein farm. The zone is bounded by the NE-trending Schietfontein Fault and is crosscut by NE and NNE-trending magnetic lineaments (low) that are interpreted as mafic dykes (termed the Older Dykes). The Older Dykes are crosscut by NW-trending dykes and were thus emplaced before them. The Schietfontein Fault has a calculated sinistral displacement of approximately 300 m, but again, is hinged in the northeast and displacement is unequal along the length of the fault. The Schietfontein fault is thereby interpreted as a scissor fault.

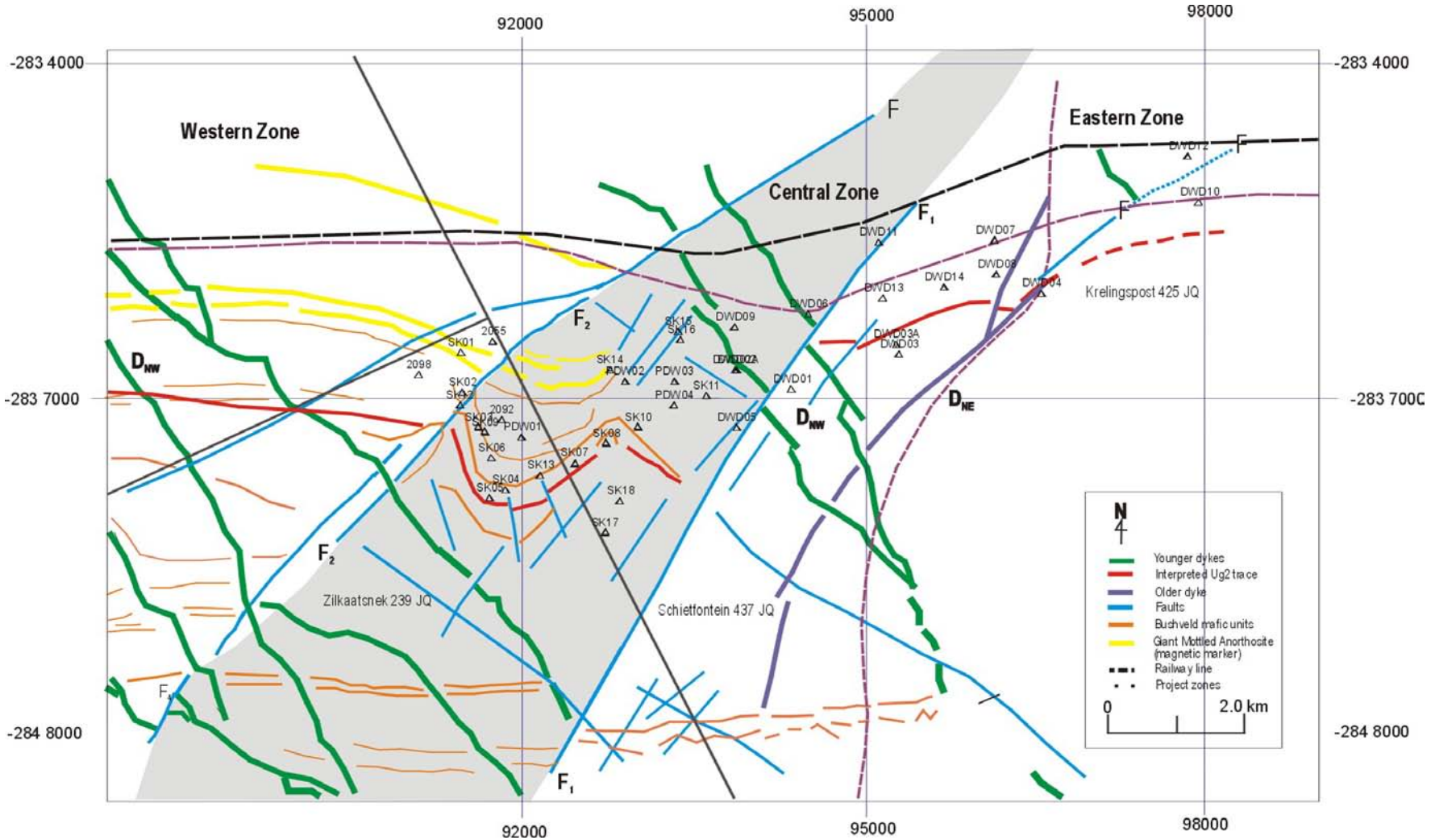


Figure 14: Geological interpretation of the magnetic signatures from the 1st and 2nd vertical aeromagnetic data. The Central Zone shaded in grey is highly disturbed and characterized by faults and fractures. NW-trending dykes traverse the prospect (interpreted from aeromagnetic data from Antoine, 2004).

Furthermore, the average dip of BC mafic units across the Schietfontein and Zilkaatsnek faults (i.e., from east to west) decreases from ~28°N to ~18°N suggesting that the western blocks were displaced normally rather than laterally; the surface projection of shallowly north-dipping BC mafic units in the western zone (relative to the eastern zone) resolves an apparent sinistral sense across the faults.

The BC mafic units in the eastern zone are discontinuous, with numerous interpreted fractures or joints. A series of subordinate NE and NW-trending magnetic lineaments transects the De Wildt region and weakly displace the BC mafic units and NW-trending lineaments (dykes). They are interpreted as mesoscopic faults.

4.4. Radiometric Survey

The company, Nkwe Platinum, commissioned a high-spatial resolution airborne magnetic and spectrometer survey over the De Wildt project area in November 2003. Gamma-ray spectrometer data for potassium (K), thorium (Th) and uranium (U) were made available to Nkwe Platinum. The interpretation of the radiometric data is shown in Fig. 15. Very high K-Th levels were registered in the south of the study area. The western and central zones were characterised by predominately high Th levels, while the eastern zone was characterised by moderate K and Th: the latter approximately coincides with ridges of the Magaliesberg Quartzite in the east of the De Wildt project area. The zone of high K and Th to the south of the prospect does not coincide with the east-west trending Magaliesberg Quartzite Mountain ridge of the Transvaal Supergroup: its meaning needs further investigation.

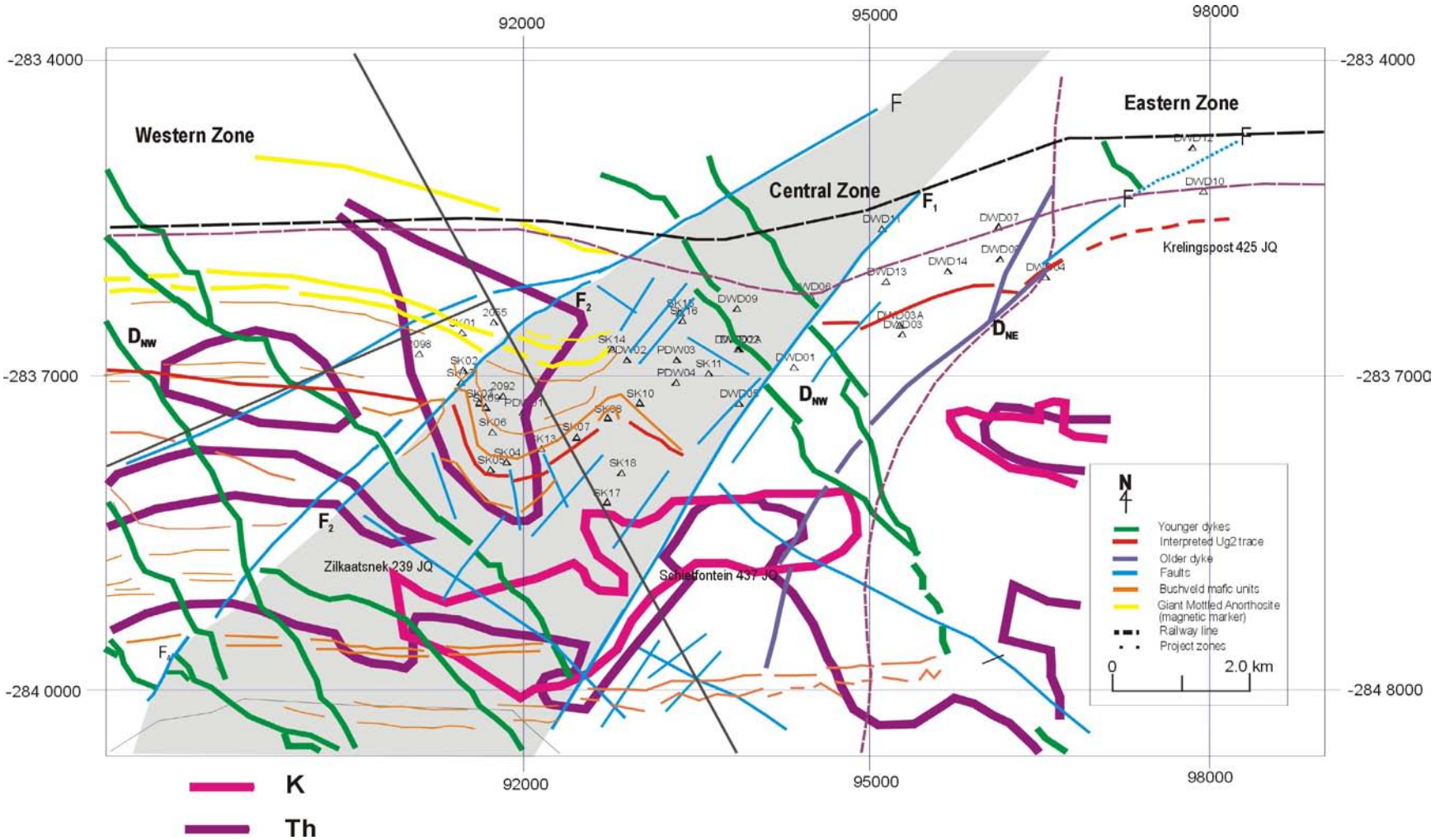


Figure 15: Interpretation map of Potassium and Thorium radiometrics across the project area. Zones of high Th-K radiation occur in the central and western parts of the De Wildt Project area (interpreted from aeromagnetic data from Antoine, 2004).

CHAPTER 5
STRATIGRAPHY OF DE WILDT AREA

Boreholes drilled by Nkwe Platinum were collared in the Main Zone and Upper Critical Zone of the BC in the De Wildt project area. The Upper Critical Zone becomes increasingly disturbed towards the eastern parts of the project. The Lower Zone is absent. Fine-grained norite with abundant metasedimentary xenoliths forms the Marginal Zone in the De Wildt project area.

5.1. Character of the Main Zone

In the De Wildt project area, the Main Zone is characterized by sequences of gabbronorite, norite, and anorthosite, with a maximum thickness of 640 m (Fig. 16). Two mottled anorthosite layers occur about 250 m above the Giant Mottled Anorthosite (GMA) within a sequence of norite. In this study the GMA has been used as stratigraphic marker delineating the Main Zone-Critical Zone boundary. The base of GMA thus marks the top of the Critical Zone (Mitchell, 2002). The GMA could be traced across the prospect from the west to the east and hence was used as a marker horizon. However, it should be borne in mind that in some literature, the MZ/CZ boundary is taken at the base of the Merensky Reef (Kruger, 2005).

5.2. Character of the Critical Zone

The Merensky Reef at De Wildt is located at between 40 m and 180 m below the GMA, i.e., 40-180 m below the Main Zone. The (true) distance between the GMA and the Merensky Reef increases from the west to east. To the west of the project area at Zilkaatsnek Farm and in the far-western boundary of the Schietfontein Farm, the Merensky Reef pyroxenite is located approximately 40 m below the GMA, while in the east of Schietfontein and Krelingspost farms, it is 105 m to 180 m below the GMA. The Bastard Reef unit is not developed.

The Merensky Reef pyroxenite was correlated from borehole to borehole throughout the project area and thus formed an important marker horizon in the CZ. The Merensky Reef-UG2 interval was dominated by a sequence of leuconorite, anorthosite and mottled anorthosite with gradational contacts. In general, the Merensky Reef-UG2 vertical separation ranged from 114 m to 188 m (Table 4, Fig. 17). However, in boreholes PDW02 and DWD09, the Merensky was intersected at greater depths than expected such that the Merensky Reef-UG2 stratigraphic interval was significantly reduced in thickness to 29.57 m and 16.38 m respectively. In borehole DWD13, the Merensky Reef pyroxenite overlay a feldspathic pyroxenite with disseminated chromite and chromitite slivers instead of a UG2 chromitite layer, while in borehole DWD12 the Merensky Reef pyroxenite was not intersected. Instead, the interval hosted IRUPs.

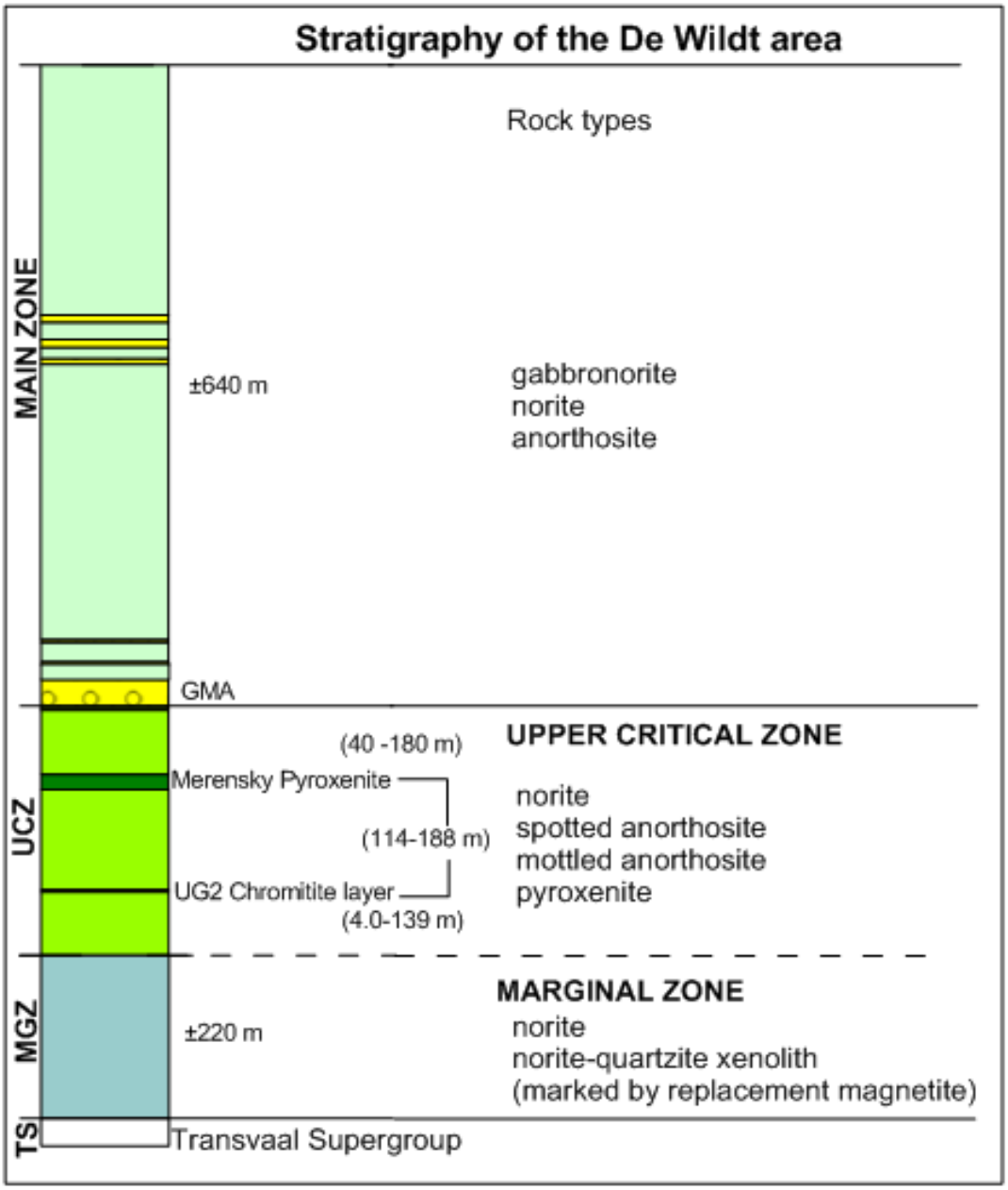


Figure 16: Provisional local stratigraphy of De Wildt prospect. The base of the GMA is interpreted as the boundary between the Main Zone and the Critical Zone. The vertical separation between the Merensky Reef and UG2 chromitite layer ranged from 114 m to 188 m.

With respect to the UG1, the layer was intersected about 128 m below UG2 layer in borehole SK03 in the far west of Zilkaatnesk Farm, but drilling at Schietfontein and Krelingspost farms did not intersect the UG1 below the UG2 reef, despite drilling to depths of 190 m and 250 m. Rather, a sequence of fine-grained quartz-norite and quartzite (often intruded by dolerites) was intersected.

Furthermore, boreholes drilled at De Wildt did not intersect the Lower Critical Zone and Lower Zone. Instead, they intersected a thick sequence of fine-grained melanorite which alternated with quartzite and norite-quartzite hybrid rocks, and metasedimentary rocks. In borehole PDW4 (Fig. 18), a large calc-silicate xenolith overlay a poorly developed UG2 layer. The UG2 reef had a very poor PGE content.

Borehole	UG2-Merensky Reef interval (m)
DWD06	151.90
DWD07	164.22
PDW01	114.56
SK02	188.61
SK03	170.66
SK06	132.63

Table 4: The UG2-Merensky Reef interval in the De Wildt project area. The data records the disturbed Merensky Reef-UG2 interval from the boreholes where layers were disrupted by potholing. Faults were omitted.

5.3. Character of the Marginal Zone

A zone consisting of very fine norite, similar to the chill-margin norite at the base of the BC rock succession, was intersected in several boreholes (Table 5). The norite hosts abundant metasedimentary xenoliths (mostly quartzite) and hybrid rocks. The norite, together with abundant metasedimentary xenoliths and hybrid rocks, is similar to the Marginal Zone documented by Vermaak (1976) and Cawthorn et al. (2006) and is thus tentatively classified as the Marginal Zone (MgZ) in the De Wildt project area. The metasedimentary units (Transvaal Supergroup metasedimentary sequences) are interpreted as blocks that were lifted off the floor during the emplacement of the BC.

Furthermore, numerous fine-grained magnetic melanorite units in the MgZ were intersected in borehole DWD10. The units are characterized by discontinuous magnetite stringers and blebs. Intercalations of quartz dominate the MgZ in boreholes DWD10 and DWD11 (Figs. 19-20). In borehole DWD12, the UG2 layer effectively overlies the MgZ, being separated from it by coarse-grained meso-norite (4.16 m in thickness) that hosts chromitite blebs and slivers. The MgZ is crosscut by numerous diabase dykes and sills, some of which are magnetic.

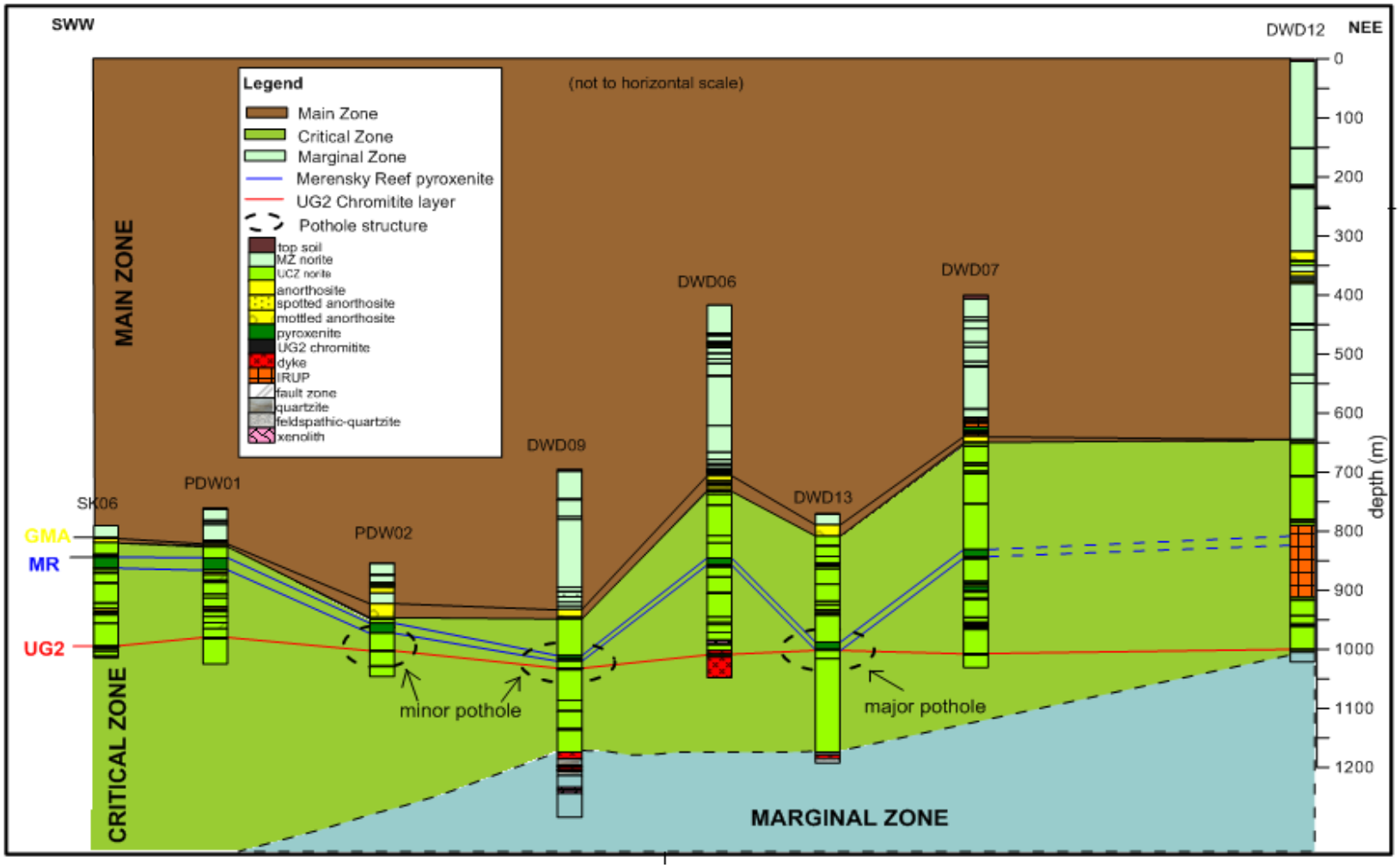


Figure 17: Schematic borehole cross section depicting of the separation between Merensky Reef and UG2 across the De Wildt project area. In the intersections in which the UG2 reef was multi-layered, the top reef contact of the first UG2 chromitite unit was used for correlation. Pothole interpretations were based on transgressed/missing footwall layers, thickened hangingwall layers of MR, steep dips and overall stratigraphic attenuation of the MR-UG2 interval without any discernable evidence of faults.



Figure 18: A calc-silicate xenolith that is rich in epidote (shown in red line) within a BC norite sequence in borehole PWD4. Part of the disturbed UG2 footwall with flow structures as defined by chromite and magnetite stringers is delineated by the dashed green lines.

BHID	Marginal Zone thickness (m)
DWD09	110.68
DWD10	188.43
DWD11	221.44
DWD13	177.09
DWD12	16.61

Table 5: Thickness of the Marginal Zone intersected in several boreholes. The boundary between the Critical Zone and Marginal Zone is tentatively taken at the level of the first appearance of the fine-grained 'chill-margin' contact-type norite.



Figure 19: Diamond drill core of sedimentary xenoliths (in yellow) in core of the BC within Marginal Zone of the BC at De Wildt project. Below the xenoliths is part of the Transvaal Supergroup quartzite intersected in borehole DWD11.

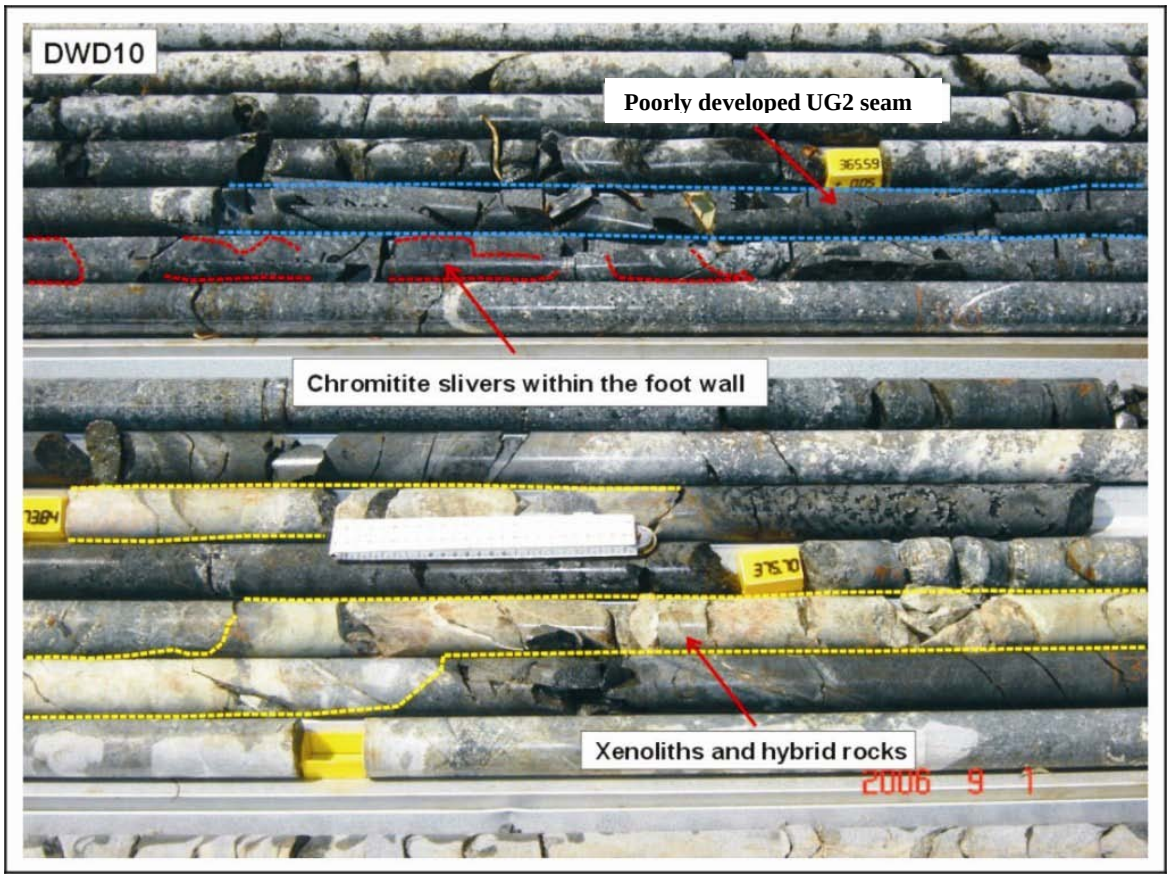


Figure 20: Poorly developed UG2 chromitite layer intersected in borehole DWD10. The UG2 is underlain by metasedimentary xenoliths (borehole DWD10 intersection).

5.4. Merensky Reef at De Wildt

The Merensky Reef was intersected in boreholes drilled mainly on Zilkaatsnek 439 JQ and Schietfontein Farm portions and includes boreholes PDW01, PDW02, PDW03, PDW04, DW06, DWD07 and DWD09 drilled by Nkwe Platinum (Table 6). In most borehole intersections, the Merensky feldspathic pyroxenite was jointed, moderately chloritized and serpentinized. The measured width of normal Merensky Reef ranged from 11.6 m to 20.5 m, while that of possibly potholed Merensky Reef was typically less than 5 m. The reef consists of a medium to coarse-grained feldspathic pyroxenite with a bottom chromitite stringer/layer of variable thickness (Fig. 21). The feldspathic pyroxenite is characterized by distinct euhedral to subhedral orthopyroxene crystals that constitute over 80% of the unit (Fig. 22a). Intercumulus plagioclase makes up approximately 20% of the unit. Biotite is present as an accessory mineral. The bottom chromitite stringer/layer ranged from 0.2 cm to 2.0 cm in thickness. The contact with the overlying Merensky pyroxenite was often very irregular.

In all boreholes studied, the upper contact of the Merensky Reef was gradational through feldspathic pyroxenite into melanorite and anorthosite. The gradational upper contact was marked by disseminated sulphide, consisting predominantly of pyrrhotite and chalcopyrite. In contrast, the immediate footwall to the Merensky Reef was composed of norite, anorthosite (mottled/poikilitic) or, pyroxenite of variable thickness (Figs. 22b-d; 23).

In borehole PDW04, the Merensky Reef has a well-defined basal chromitite layer about 2.0 cm in thickness, while the upper portion was marked by a relatively narrow zone of scattered sulphide (blebs). In boreholes PDW02 and PDW01, the Merensky Reef basal chromitite stringer/layer was not well developed. Instead, the basal contact was defined by irregular and diffuse chromitite stringers with minor chromite blebs and disseminated chromite over a 1.0-2.5 cm interval. Disseminated sulphide mineralization was apparent in the Merensky Reef intersected in borehole PDW01 near the upper contact of the Merensky reef pyroxenite. Here, sulphide extended upward for 50 cm into the hangingwall norite. Sulphides were not found in the footwall. However, in borehole SK06 the anorthosite (mottled/poikilitic) in the immediate footwall to the Merensky Reef hosted disseminated sulphides.

Merensky Reef							
Borehole	Thickness (m)	Merensky Reef-lithology	Hanging wall	Upper Contact	Footwall	Bottom Contact	3E+Au (g/t)
PDW01	20.59	feldspathic pyroxenite	norite	gradational	anorthosite	Irregular chromitite stringer	<0.1
PDW02	16.94	feldspathic pyroxenite	norite	gradational	pyroxenite	Irregular chromitite stringer (potholed)	<0.1
PDW03	17.75	felspathic pyroxenite	norite	gradational	norite	sharp contact	
PDW04	15.70	feldspathic pyroxenite	norite	gradational	anorthositic	2 cm chromitite stringer	<0.1
DWD06	11.61	feldspathic pyroxenite	norite	gradational	anorthosite	0.2 cm chromitite stringer	0.33
DWD07	12.25	feldspathic pyroxenite	norite	sharp	anorthosite	sharp contact	<0.1
DWD09	5.03	feldspathic pyroxenite	norite	gradational	melanorite	pot-holed	<0.1
SK02	12.04	feldspathic pyroxenite	norite	gradational	anorthosite	chromitite stringer not developed	0.88
SK03	17.90	feldspathic pyroxenite	norite	gradational	anorthosite	chromitite stringer not developed	0.30
SK06	18.47	feldspathic pyroxenite	norite	cut by a vein	anorthosite	irregular chromitite stringer	3.51
SK09	16.53	feldspathic pyroxenite	norite	gradational	anorthosite	sharp contact	
SK10	13.7	feldspathic pyroxenite	norite	gradational	norite	sharp contact	

Table 6: Merensky Reef intersections within the De Wildt project.

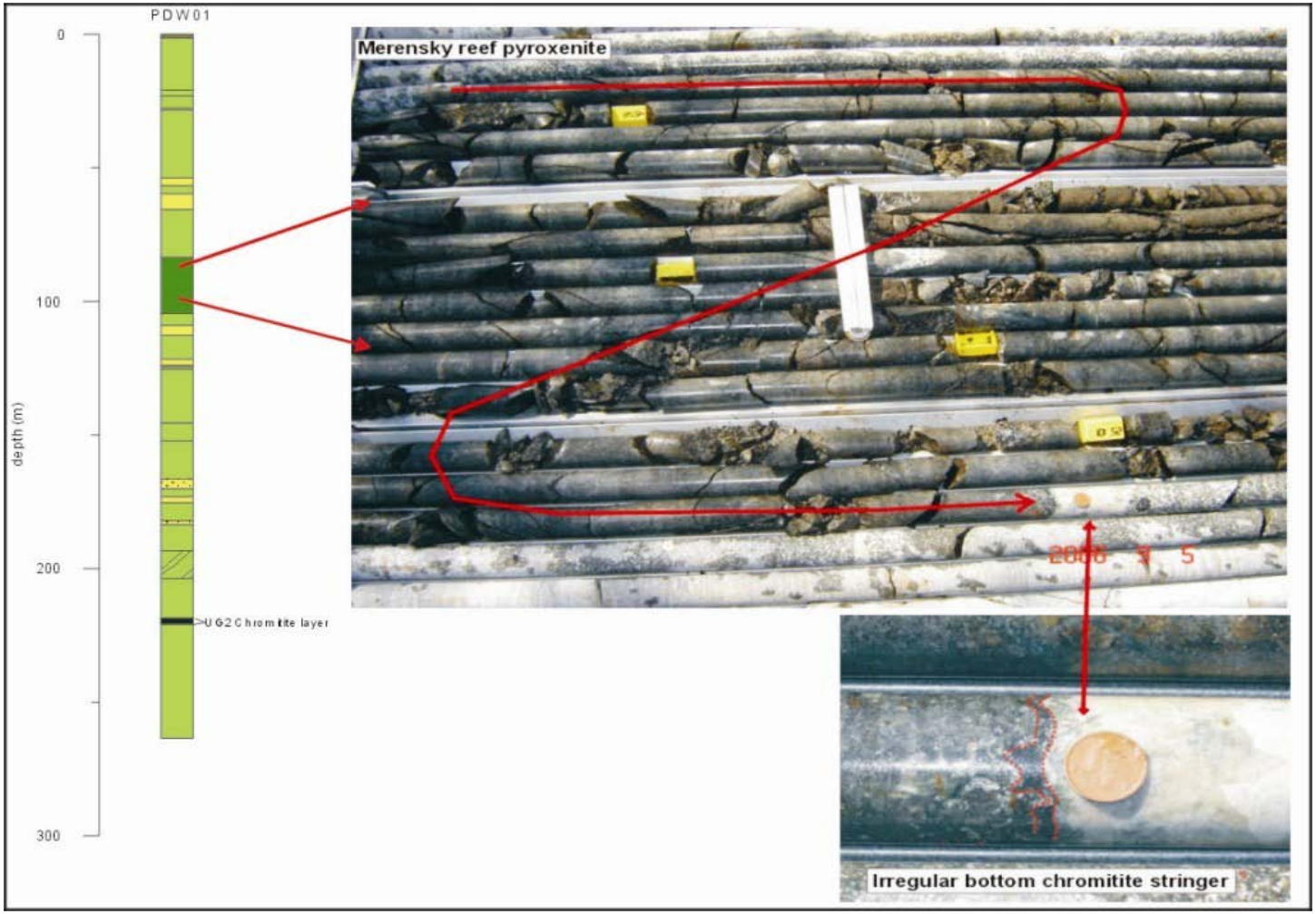


Figure 21: Typical Merensky Reef intersection of greater than 20 m thickness at De Wildt together with schematic of the borehole (PDW01). The MR is altered with chlorite and serpentinite filled joints.

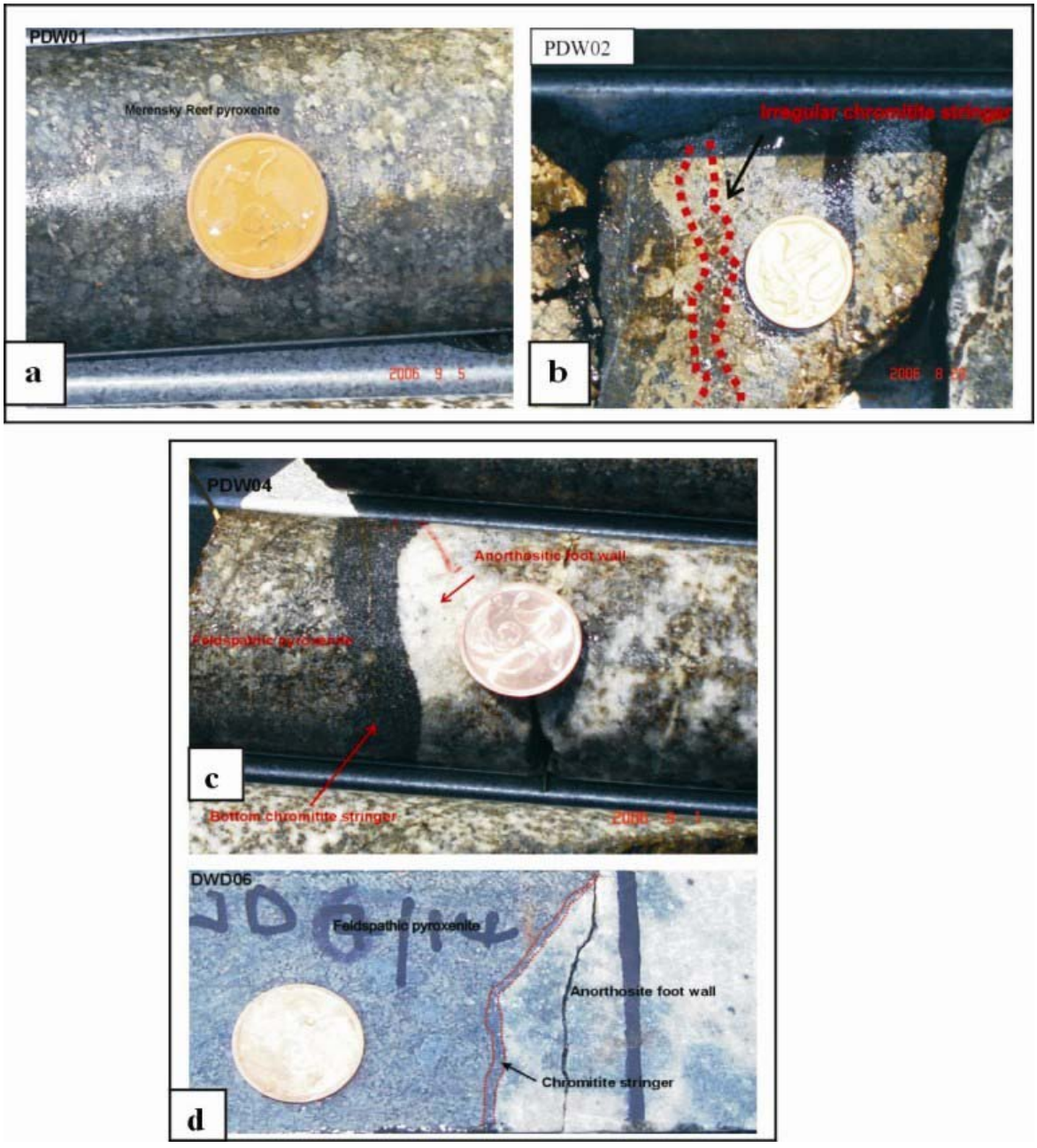


Figure 22: Merensky Reef pyroxenite and the different footwall units intersected in borehole. Image **a** is of a medium crystalline feldspathic pyroxenite layer making up the MR. Image **b**, is of a poorly defined basal chromitite stringer that defines the bottom contact of MR. The MR pyroxenite is weathered and chloritized. Image **c**, shows a well developed basal chromitite stringer of MR, the undulating contact between the chromitite stringer and the footwall anorthosite is defined. Image **d**, shows a half NQ core section of an irregular basal chromitite stringer of MR in contact with mottled anorthosite footwall.

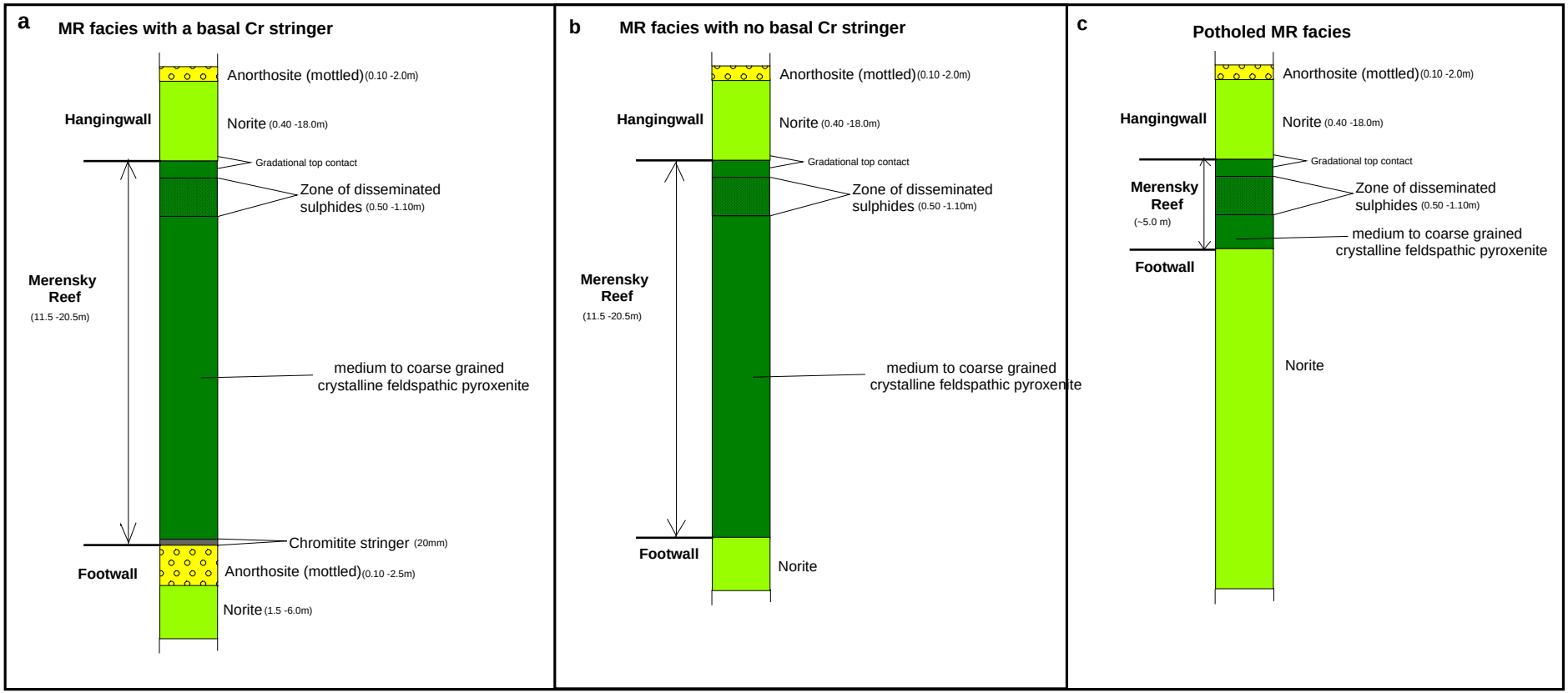


Figure 23: A schematic of the different Merensky Reef facies intersected at De Wildt. In (**a**) the MR is characterized by a medium crystalline feldspathic pyroxenite that has a basal chromitite stringer. In **(b)** the MR is wide but devoid of a basal chromitite stringer. In the potholed facies (**c**), the MR pyroxenite is significantly thinned (in this case down to ~5.0 m).

5.5. UG2 Chromitite layer at De Wildt

The UG2 chromitite layer intersected in boreholes in the De Wildt project area is highly variable in character; it is multi-layered, poorly developed (Table 7) and is not overlain by the triplets or leader seams. The UG2 layer also displays a lack of lateral continuity. The chromitite underlies the Merensky Reef at a (true) depth range of 114 to 188 m in boreholes and is composed of ~ 90 % chromite by volume and 5-10% plagioclase. Pyroxene, magnetite, pyrrhotite, chalcopyrite and pyrite form accessory minerals. Magnetite occurs in the form of discontinuous stringers and lenses.

The UG2 chromitite layer is also crosscut by quartz-biotite veins and fractures and is generally altered, often with magnetite lenses and blebs in places (Figs. 24a-b). However, in boreholes collared on the west of the project area, diffuse pyroxene crystals enclose chromite grains and give the UG2 reef a poikilitic texture. The thickness of the reef varies from 0.40 to 1.25 m.

The UG2 chromitite dips generally dips at 19-25° as measured from the core-bedding angle using a clino-ruler, however, is steeply dipping (about 60°) at Krelingspost Farm. The relationship is consistent with block rotation along the Schietfontein Fault (c.f. Section 4.2).

5.6. UG2 Chromitite facies

Two main facies were noted in the UG2 chromitite layer; the **'A type' normal facies** and the **split-reef facies** (Fig. 25). The split reef facies is characterized by a UG2 chromitite layer that has partitioned into two or more chromitite units. The chromitite units are separated by an intervening chromitiferous norite or feldspathic pyroxenite layer. The split reef facies can be further divided into four sub-facies depending on the number of massive chromitite seams developed including;

'B type' - consists of two discrete chromitite units.
'C type' – consists of three discrete chromitite units.
'D type' - consists of one chromitite unit underlain by a chromitiferous pyroxenite/norite.
'E type' – consists of chromitiferous pyroxenite, devoid of massive chromitite units.

The 'A type' normal reef facies occurs only in the western zone of the De Wildt project area, while split-reef facies occurs in the central and eastern zones (Fig. 26). The distribution of the split-reef facies throughout the project area does not follow a well defined pattern and as such, a closely spaced drill program was needed to constrain the UG2 chromitite reef setting.

De Wildt UG2 Chromitite layer intersections

UG2 reef					UG2 Foot wall			
BHID	**From**	**To**	**Thickness (m)**	**Facies type**	**From**	**To**	**Thickness(m**	**Rock type**
SK02	486.85	488.10	**1.25**	A 'normal type'	488.10	491.32	**3.22**	feldspathic pyroxenite
SK03	331.28	331.83	**0.55**	D' type				
SK04	109.53	110.63	**1.10**	A 'normal' type	110.64	113.31	**2.67**	feldspathic pyroxenite
SK05				B type'	none			
Upper chromitite unit	106.48	107.07	**0.59**					
Lower chromitite unit	107.14	107.57	**0.43**					
SK06				B 'split reef'	204.85	206	**1.15**	feldspathic pyroxenite
Upper chromitite unit	203.91	204.60	**0.69**					
Lower chromitite unit	204.75	204.85	**0.10**					
SK07				A 'normal' type				
UG2 leader?	53.77	53.81	**0.04**					
UG2 leader?	53.82	53.92	**0.10**					
UG2 chromitite layer	53.95	55.07	**1.12**					
SK08				B 'split reef'	57.35	58.01	**0.66**	meso-norite
Upper chromitite unit	55.93	56.64	**0.71**					
Lower chromitite unit	57.04	57.12	**0.08**					
SK09				C 'split reef'	99.57	107.84	**10.43**	feldspathic pyroxenite
Upper chromitite unit	96.37	97.74	**1.37**					
Middle chromitite unit	98.78	98.90	**0.12**					
Lower chromitite unit	99.26	99.57	**0.31**					
SK10	90.67	91.19	**0.52**	D' type	92.08	94.58	**2.5**	feldspathicpyroxenite
SK13				B 'split reef'	117.76	118.05	**0.29**	meso-norite
Upper chromitite unit	116.41	117.22	**0.81**					
Lower chromitite unit	117.36	117.42	**0.06**					
DWD2A	194.67	194.82	**0.15**	D type				
DWD06	591.89	592.09	**0.20**	D type	592.09	596.59	**4.50**	pegmatoidal feldspathic pyroxenite
DWD07				C 'split reef'				
Upper chromitite unit	607.68	608.00	**0.32**					
Middle chromitite unit	608.75	608.83	**0.08**					
Lower chromitite unit	608.90	609.82	**0.92**					
DWD08	345.21	345.81	**0.60**	D' type	359.06	362.27	**3.21**	coarse grained norite
DWD09				B 'split reef'	339.32	340.00	**0.68**	meso norite
Upper chromitite unit	337.12	337.84	**0.72**					
Lower chromitite unit	339.11	339.32	**0.21**					
DWD10				B 'split reef'				
Upper chromitite unit	367.07	367.18	**0.11**					
Lower chromitite unit	368.05	368.19	**0.14**					
DWD12				B 'split reef'	1000.61	1004.77	**4.16**	coarse grained meosnorite
Upper chromitite unit	999.90	999.98	**0.08**					
Lower chromitite unit	1000.29	1000.61	**0.32**					
PDW01				B 'split reef'				
Upper chromitite	218.97	219.80	**0.84**					
Lower chromitite unit	220.43	220.66	**0.23**					
PDW02				B 'split reef'?				
Upper chromitite unit	148.22	148.83	**0.61**					
Lower chromitite unit	173.92	175.02	**1.10**					
PDW03								
Upper chromitite unit	121.61	121.76	**0.15**	D type				
Lower chromitite unit	123.96	124.17	**0.21**					
PDW04				B 'split reef'				
Upper chromitite unit	126.00	126.60	**0.60**					
Lower chromitite unit	127.07	127.49	**0.42**					

Table 7: UG2 chromitite reef intersections within the De Wildt project area

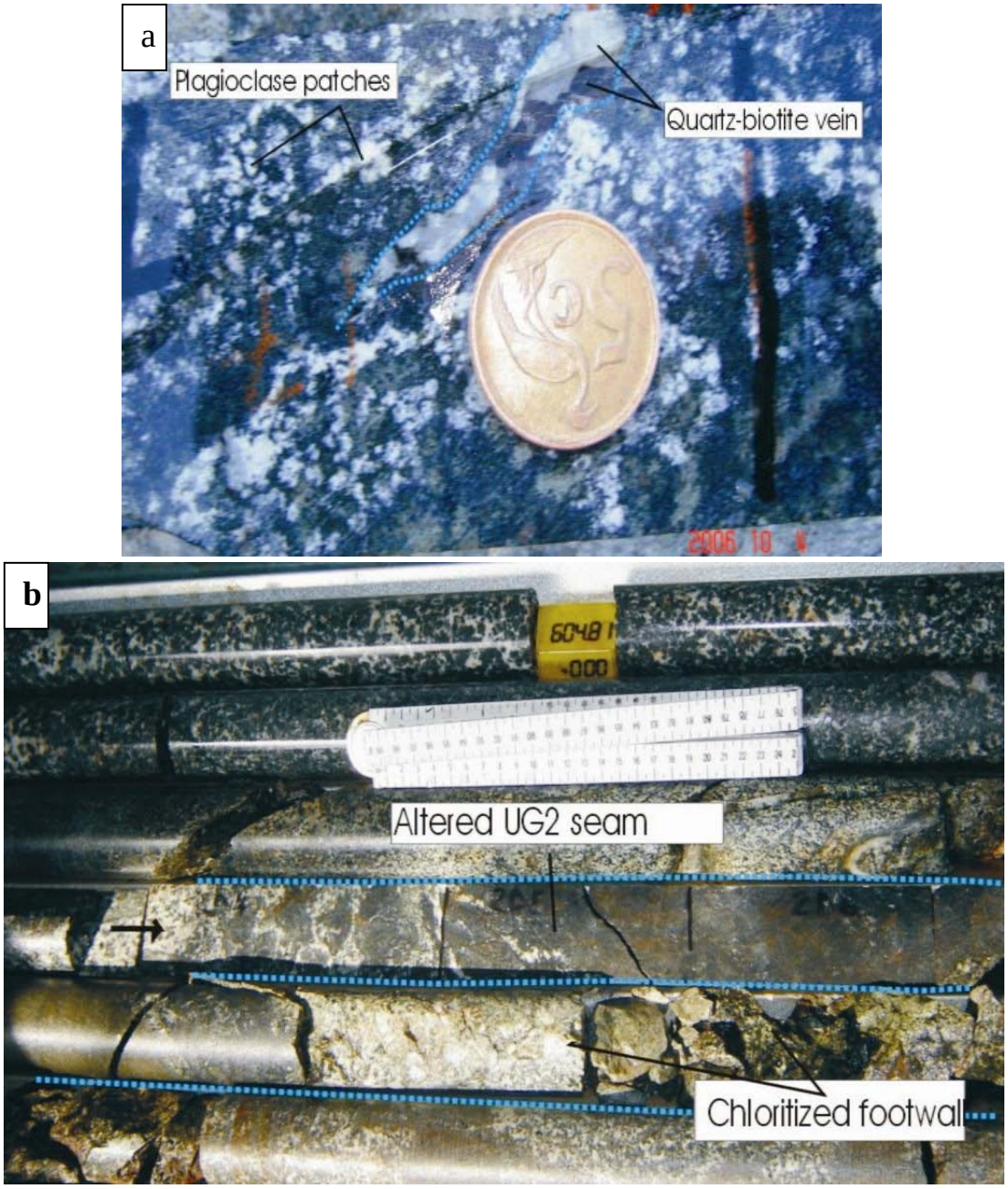


Figure 24: (**a**) UG2 seam intersected in DWD07, the seam is cut by quartz-biotite veins and marked by a generally high content of interstitial plagioclase. (**b**) Altered UG2 seam intersected at a depth of > 604 m, the top reef contact is poorly developed, marked by vague plagioclase lenses and anorthosite patches. The footwall pyroxenite has been heavily altered to chlorite giving the rock a dark green appearance.

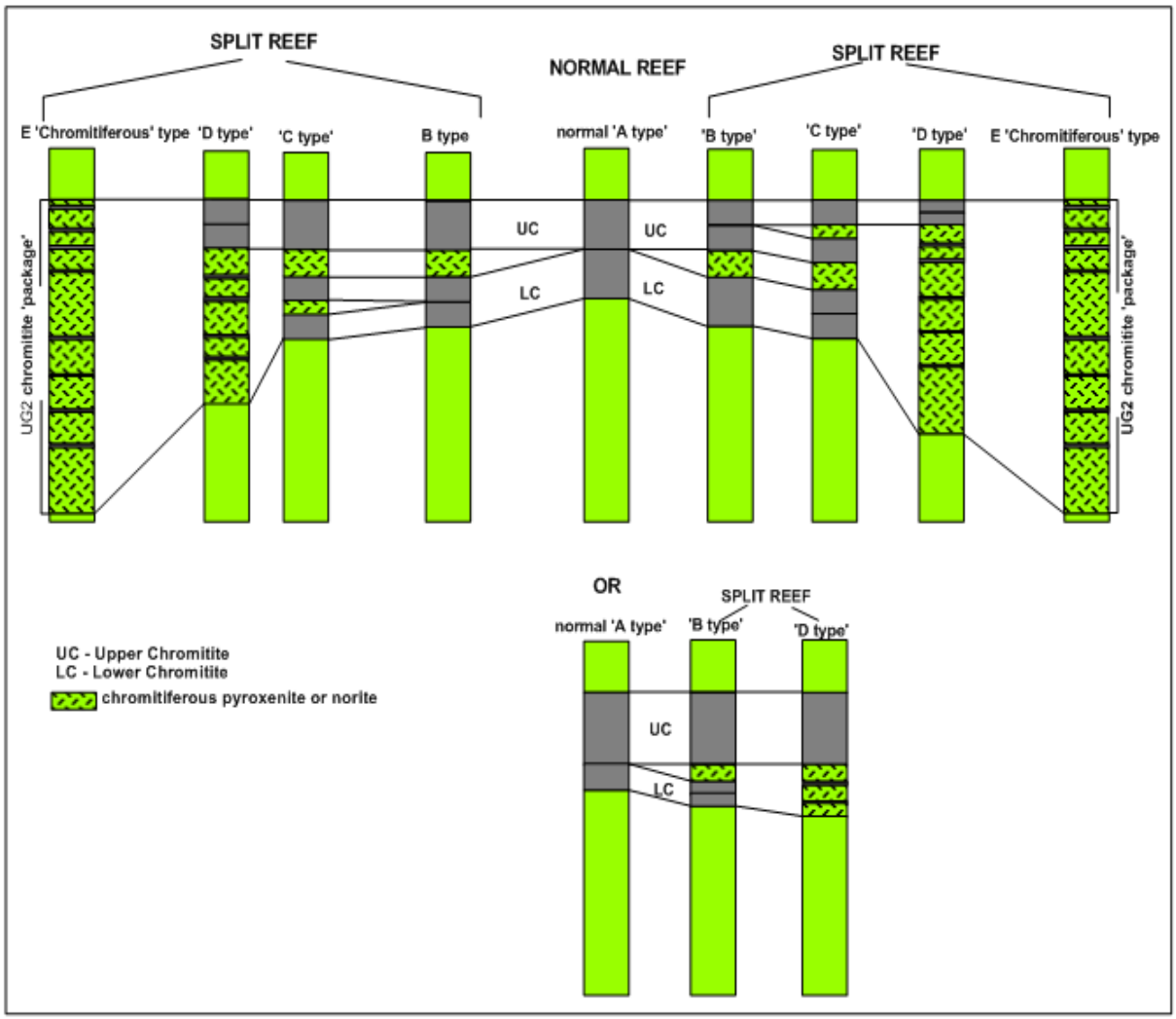


Figure 25: Schematic depiction of boreholes in the De Wildt project area showing the UG2 facies types in each borehole. Normal and split-reef facies occur in the area but the split-reef facies can be further subdivided into B, C, D, and E types.

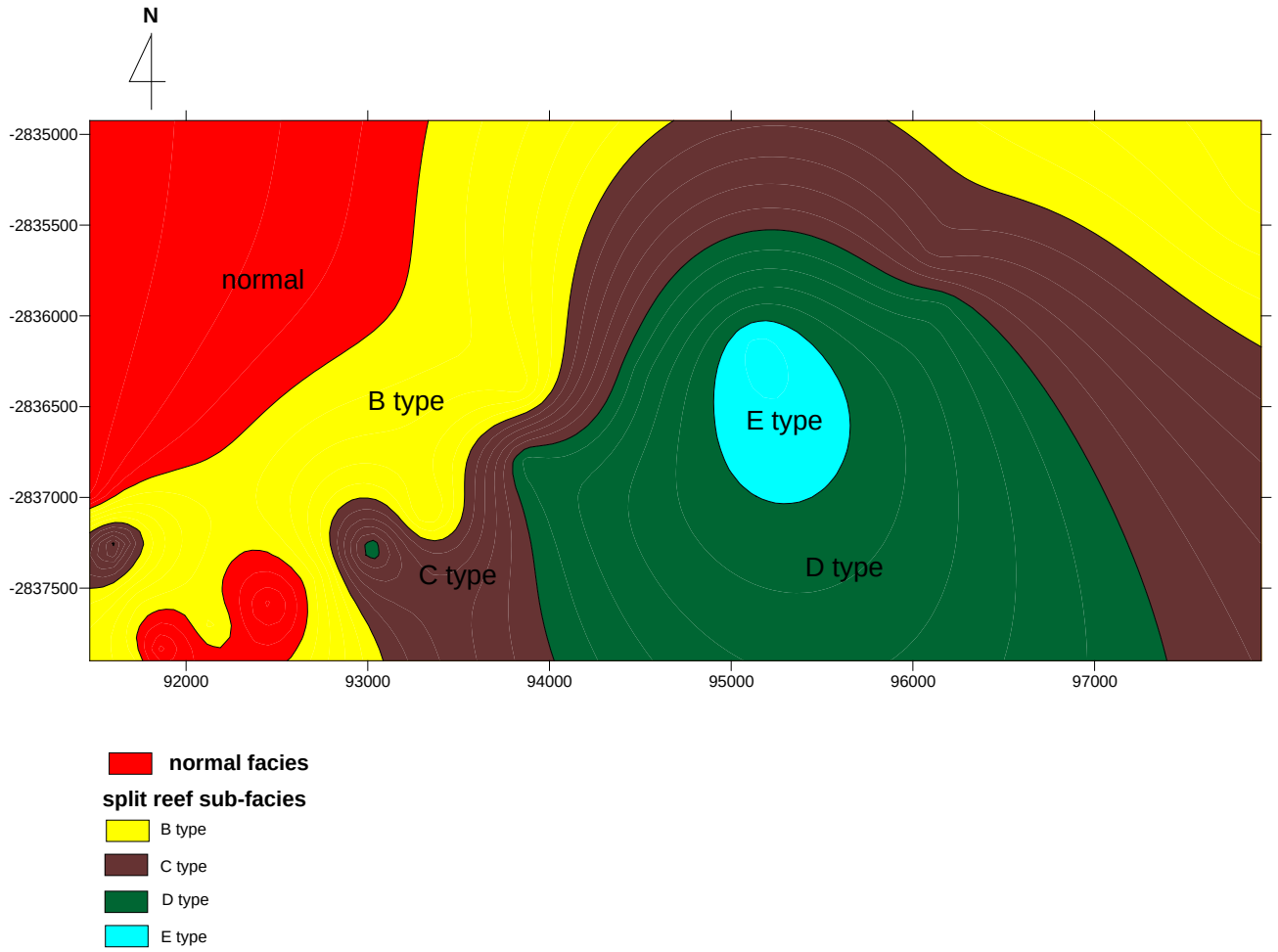


Figure 26: UG2 facies distribution in the De Wildt project area.

The **normal facies 'A type'** was intersected in boreholes SK02, SK04 and SK07 at the Zilkaatsnek Farm and consists of a 1.10-1.25 m massive chromitite layer. The chromitite unit is fine-crystalline with minor sulphide. The UG2 leader seams are absent or poorly developed in borehole SK04 (Fig. 27a). In borehole SK02, the massive chromitite layer is overlain by a 1.0 cm thick chromitite stringer about 6 cm into the hangingwall norite. It is possible that this stringer may be part of the UG2 leader seams. In boreholes SK04 and SK07, weakly disseminated chromite was present in the immediate overlying hangingwall of the UG2 chromitite seam. As such there is a possibility that the disseminated chromite may be part of the remnants of the triplets that are poorly developed. In the case where the leader seams were not developed at all, it is suggested that the leader seams coalesced with the UG2 layer. Such coalescence may have contributed in the widening of the UG2 chromitite layer or package.

The 'B type' split reef sub-facies was intersected in boreholes SK05, SK06, SK08, DWD09, DWD10, DWD12, PDW01, PDW04 and PDW02 and consists of an upper and lower chromitite layer, that is separated by a chromite-rich pyroxenite or norite unit (Fig. 27b). The upper chromitite layer is 59-84 cm thick while the lower layer from 8-42 cm thick. However, in the east Krelingspost Farm, the B' type facies consists of relatively narrow upper and lower chromitite layers; 11-15 cm thick for the upper layer and between 14-32 cm for the lower layer as intersected in boreholes DWD10 and DWD12.

The upper chromitite layer is poikilitic and characterised by pyroxenite lenses and irregular feldspar veins, whereas the lower chromitite layer is fine-grained and hosts norite lenses (Figs. 28-29). The poikilitic texture of the upper chromitite layer of the UG2 could be the result of crystallisation of orthopyroxene (part of the UG2 pyroxenite) around and enclosing the pre-existing chromite crystals during chromitite formation.

The chromite-rich feldspathic pyroxenite separating the chromitite layers ranges from 8 cm to 63 cm in thickness. However, in borehole DWD09, the chromitite layers are separated by a 1.3 m thick, coarse-grained norite with irregular chromitite stringers. The norite hosts a 14 cm thick anorthosite layer.

The 'C type' split reef sub-facies was intersected in boreholes DWD07 and SK09 and consists of three chromitite layers/units separated by either a chromite-rich pyroxenite or norite (Fig. 30). The chromitite layers are variable in thickness and host norite and/or pyroxenite as internal waste. The middle chromitite layer is typically narrow (8-12 cm in thickness). In these boreholes the upper chromitite layer is 32-137 cm thick, while the lower layer is 31-92 cm thick. In borehole DWD07, the three layers are separated by pegmatoidal mesonorite that coarsens towards the lower contact. The mesonorite hosts irregular chromitite stringers/slivers and disseminated chromite. In borehole SK09, the chromitite layers are separated by fine-grained porphyritic feldspathic pyroxenite with blebs of chromite.

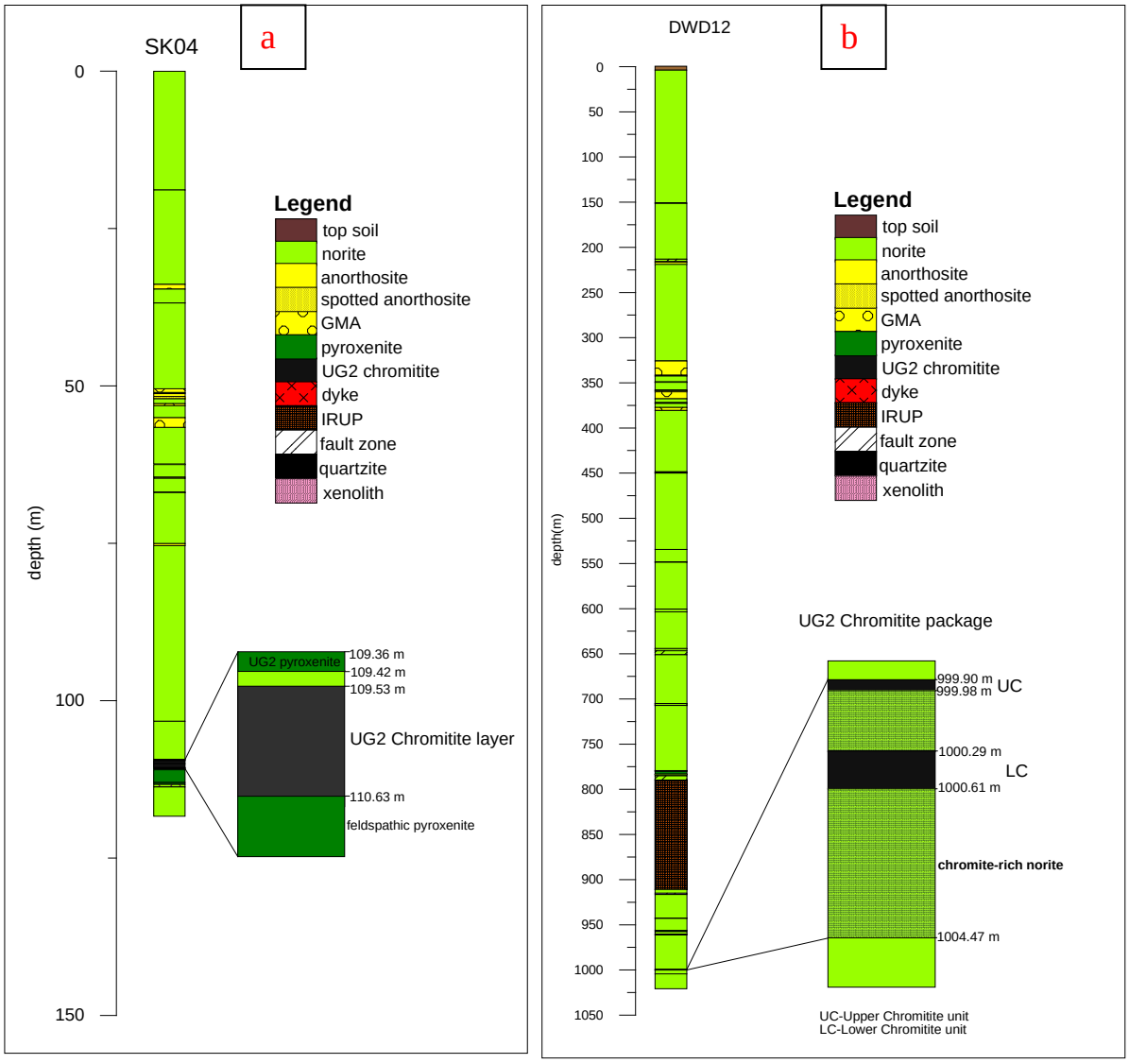


Figure 27: (a) UG2 normal facies. **(b)** The narrow B type sub-facies of UG2 split-reef facies.

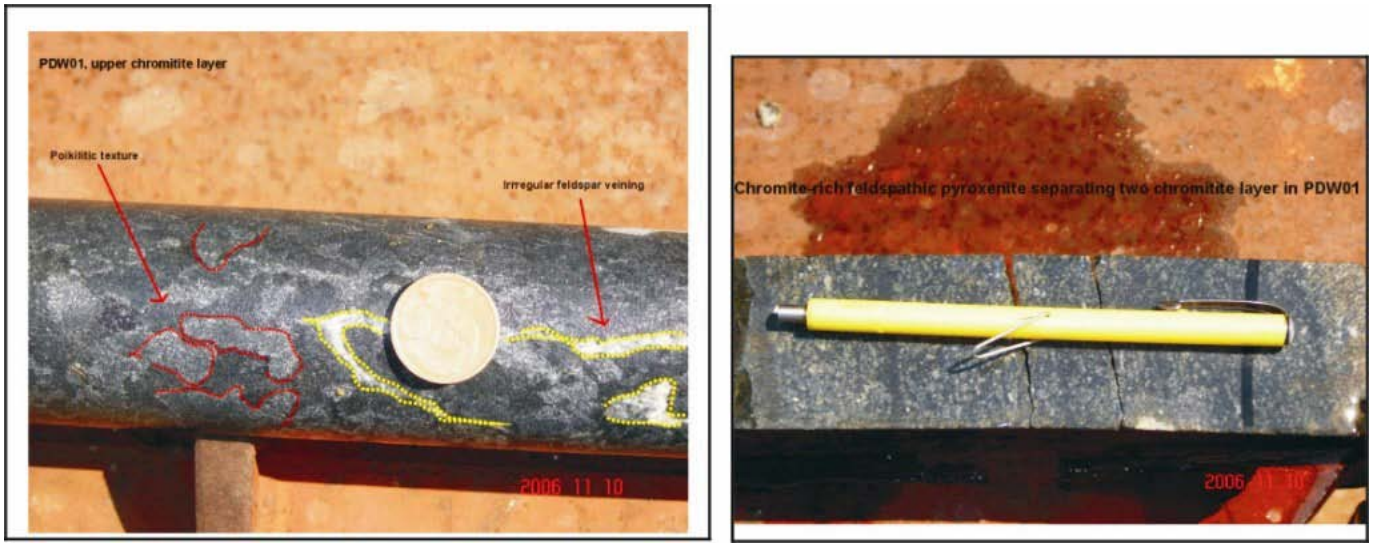


Figure 28: Upper chromitite layer of the UG2 package, and the chromite-rich feldspathic pyroxenite that separates the two chromitite layers.



Figure 29: Part of the UG2 package showing the chromite bearing norite unit. The chromite occurs in the form of blebs and irregular stringers. The lower chromitite layer in is poorly packed (intersected in borehole DWD12).

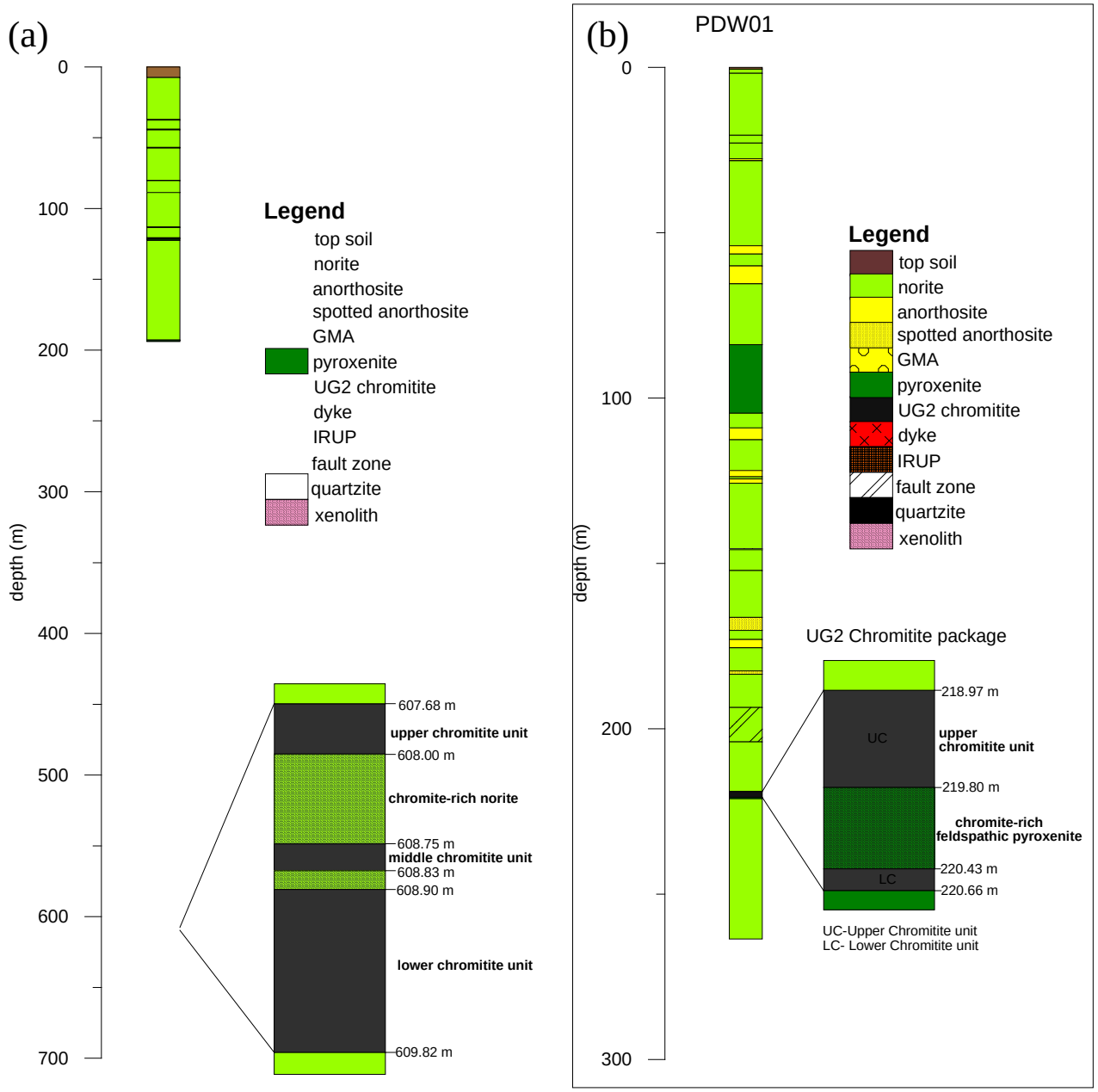


Figure 30: Stratigraphic logs showing the different UG2 split-reef. Figure (**a**) presents the C type sub-facies intersected in borehole DWD07.Figure (**b**) presents the thick B type sub-facies intersected in borehole PDW01.

The ‘D type’ split reef sub-facies was intersected in boreholes SK03, SK10, DWD2A and DWD06 (Figs. 31-32), and comprises a massive, but relatively narrow chromitite layer that is 15-55 cm in thickness. It is underlain by chromite-rich feldspathic pyroxenite. The contact between the chromitiferous footwall and the overlying chromitite layer is defined by irregular chromite lenses and/or stringers at scales of centimetres and less. The chromitite layer of the D type’ sub-facies is interpreted as coalesced leader seams (and or with part of the upper portion of the UG2 chromitite layer), while the underlying chromitiferous footwall is interpreted as the remnants of the rest of the UG2 chromitite layer.

The ‘E type’ split reef sub-facies of the UG2 Chromitite was intersected in borehole DWD13 (Fig. 33) that was collared in the central part of Schietfontein Farm. The facies is devoid of any massive chromitite layers/units. Instead, it consists of a chromite-bearing feldspathic pyroxenite ~150 cm in thickness) that hosts highly disseminated chromite and irregular chromitite blebs and stringers. The chromitite slivers are arranged randomly or, in a disordered fashion. The E-type sub-facies is tentatively interpreted as the remnants of the UG2 reef within a major pothole because stratigraphic layers are missing and the Merensky Reef-UG2 interval (in borehole) is attenuated. The pothole arguably led to the transgression of the mafic units within the Merensky pyroxenite-UG2 reef interval such that the Merensky pyroxenite rests directly on this chromite-bearing unit.

5.7. UG2 chromitite isopach

An isopach map of thickness of the UG2 chromitite layer is presented in Fig. 34. In the case of the split-reef facies in which the lower part of the seam consists of disseminated chromite within a feldspathic pyroxenite/norite, only the upper chromitite layers were used to construct the isopach map. The units with disseminated chromite were classified as part of the footwall. The intersections in borehole DWD13 are devoid of massive chromitite units, but consist of feldspathic pyroxenite that hosts disseminated chromite; it was thus was excluded from the map.

For the isopach map, a UG2 layer thicker than one metre is confined to the western zone of the project area, primarily in the Zilkaatsnek Farm. The central and southern parts of the project areas are characterized by UG2 layer that is 0.0-0.75 m in thickness. The north of the prospect area is characterised by UG2 reef which is 0.75-1.0 m in thickness, with isolated regions of greater than a metre in thickness. In summary, the UG2 in the De Wildt project area is laterally variable and thins towards the east and south.

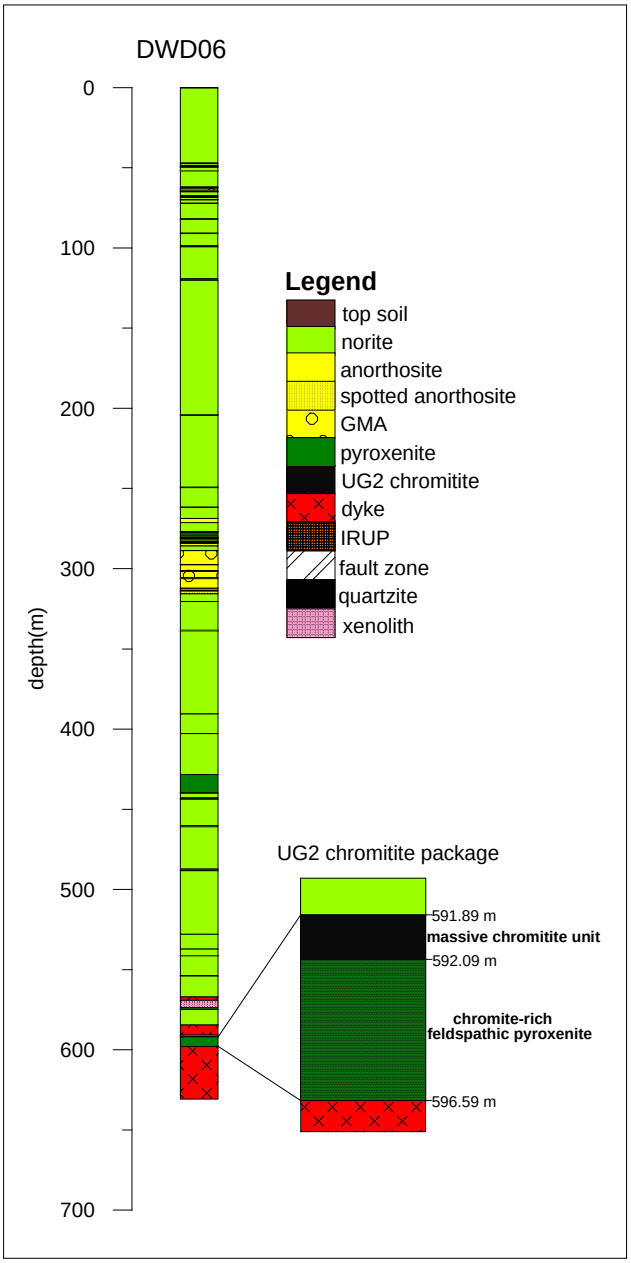


Figure 31: Borehole log showing the UG2 Split reef D-type sub-facies.

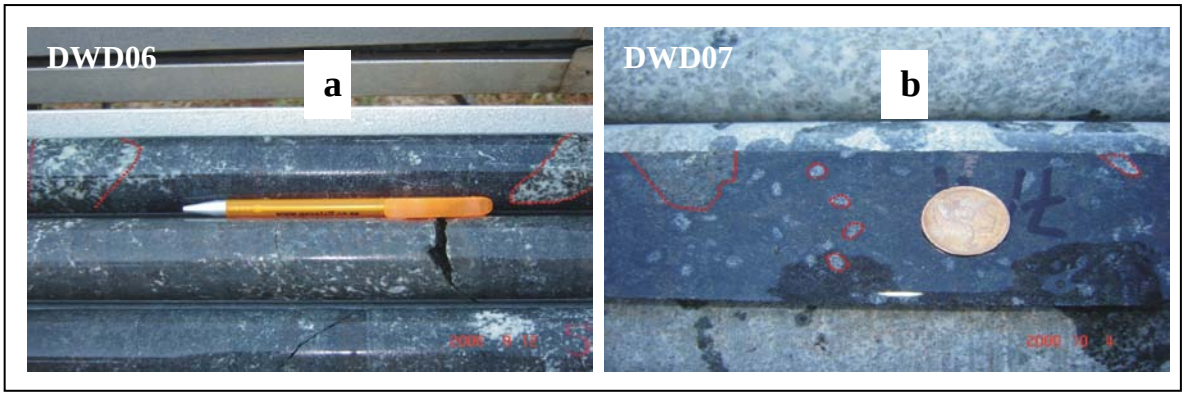


Figure 32: Narrow UG2 chromitite layer (a) and the upper UG2 chromitite layer with feldspar inclusions giving it a spotted texture (b).



Figure 33: Chromite-rich feldspathic pyroxenite with chromite blebs immediately above the pencil (borehole DWD13).

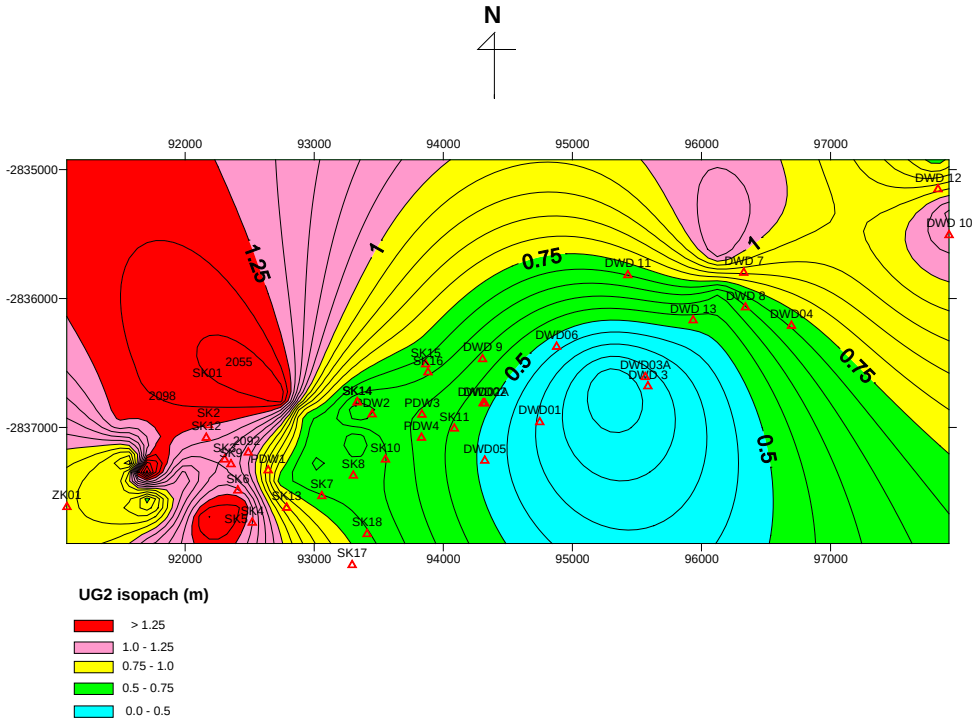


Figure 34: UG2 chromitite isopach map for De Wildt. Areas in which the mineralized footwall is not developed have thicknesses less than 1.0 m.

5.8. UG2 hangingwall units

The UG2 chromitite layers in the De Wildt project area are predominantly overlain by coarse-grained mesonorite layers whose thickness varies from 0.5 to 51 m (Table 8). The contact between the UG2 and the overlying mesonorite is sharp or irregular, and in some instances may be gradational through mesonorite, with increasing proportion of disseminated chromite. In some boreholes from Zilkaatsnek Farm, the UG2 is overlain by a feldspathic pyroxenite unit which ranges from 0.05 m to 3 m in thickness. The UG2 pyroxenite intersected is feldspathic with minor biotite, while in boreholes SK04 and SK13 the pyroxenite hosts disseminated chromite minerals and minor sulphide mineralization (in borehole DWD06).

5.9. UG2 footwall units

The UG2 Chromitite layer is predominantly underlain by a pegmatoidal feldspathic pyroxenite that is less than 1.0 m in thickness. The pegmatoidal pyroxenite is also known as the UG2 pegmatoid (c.f., Hiemstra, 1985, Penberthy and Merkle, 1999). The contact between UG2 and the UG2 pegmatoid is irregular. In the De Wildt project area the pegmatoidal feldspathic pyroxenite hosts disseminated chromite, chromitite lenses and chromite blebs. The UG2 pegmatoid is gradational downwards into a medium-grained pyroxenite that hosts disseminated chromite and diffuse chromite lenses/blebs. PGE mineralization extends into the footwall pyroxenite unit. However, not all boreholes intersected the UG2 pegmatoid.

5.10. Dykes, sills and replacement rocks at De Wildt project area

Dolerite dykes and sills were intersected in boreholes throughout the project area. The dykes trend NW. The dykes are variable in thickness ranging from 0.2 m to 55.73 m. They are associated with fracture zones and small-scale fault displacement. The dykes are associated with metasomatism of the BC mafic rocks, with alteration extending only a few centimetres from the intrusive contacts.

A number of iron-rich ultramafic pegmatoids (IRUP) were intersected in boreholes across the prospect. The IRUPs occur as centimetre to metre-scale, dark grey-black patches or irregular zones within norite and anorthosite layers. The IRUP zones are composed of large crystals of clinopyroxene, plagioclase and biotite with accessory replacement magnetite, sulphide and olivine. Of significance, was the 100 m thick (apparent thickness) IRUP zone intersected in borehole DWD12, which replaced the normal mafic rock succession of the Upper Critical Zone with an irregular iron-rich ultramafic pegmatoid in the depth interval 790.34 - 911.37 m.

UG2 hangingwall and footwall lithologies, and UG2 pyroxenite layer

BHID	Hanging wall	Thickness(m)	Foot wall	Thickness(m)	UG2 pyroxenite (thickness, m)	Nature of pyroxenite
SK3	Leuconorite	51.17	Norite, with disseminated chromite	0.11		
SK4	Melanorite	0.42	Pyroxenite, pegmatoidal	2.68	0.06	Feldspathic pyroxenite with disseminated chromite
SK5	Melanorite	0.48	Melanorite	1.08	0.06	Feldspathic pyroxenite
SK6	Melanorite	0.21	Felsdapthic pyroxenite, chromite-rich	1.81	0.06	Feldspathic pyroxenite
SK7	Melanorite	11.28	Felsdapthic pyroxenite	7.97		
SK8	Feldspathic pyroxenite	0.05	Norite	0.02		
SK9	Feldspathic pyroxenite	3.22	Feldspathic pyroxenite	0.51		
SK10	Feldspathic pyroxenite	0.07	Feldspathic pyroxenite	0.89		
SK13	Melanorite	13.49	Feldspathic pyroxenite	0.14	0.2	Feldspathic pyroxenite with disseminated chromite
DWD2A	Norite	4.95	Feldspathic pyroxenite	41.47		
DWD6	Norite	16.91	Feldspathic pyroxenite	4.95	1.08	Feldspathic pyroxenite with sulphide mineralization
DWD7	Norite	41.1	Norite, chromite-rich	20.9		
DWD8	Norite	39.91	Lueconorite, pegmatoidal	0.19	1.09	Feldspathic pyroxenite
DWD9	Norite	12.33	Norite	0.68	3.33	Feldspathic pyroxenite
DWD10	Melanorite, chromite-rich	27.9	Melanorite, coarse grained	0.23	0.57	Feldspathic pyroxenite
DWD12	Norite	38.34	Norite	4.16	0.74	Feldspathic pyroxenite
PDW01	Norite	15	Pyroxenite, pegmatoidal	0.44		
PDW02	Norite	29.86	Norite, pegmatoidal	0.32		
PDW03	Norite	0.16	Feldspathic pyroxenite	0.17		
PDW04	Norite	8.22	Norite	5.83	0.96	Feldspathic pyroxenite

Table 8: Immediate hangingwall and footwall lithologies to the UG2 chromitite layer.

5.11. Summary

- The intersection of the Marginal Zone directly below the Upper Critical Zone implies the absence of the Lower Critical Zone and Lower Zone stratigraphic horizons of the BC at De Wildt.
- The Merensky Reef intersected ranges from 11.6 m to 20.5 m and may sometimes have a basal chromitite developed. The reef was characterized by low PGE contents averaging less 1g/t with top and bottom PGE value peaks associated with the top and bottom contacts respectively.
- The UG2 chromitite layer within the prospect exhibited lateral variation from the east to west. The UG2 layer changes from being a single massive chromitite seam into a multi-layered and sometimes only consisting of only disseminated chromite and chromite stringers within a feldspathic pyroxenite. Also, the UG2 layer was characterized by a mineralized immediate footwall extending down to 4 m in some portions of the prospect

.

CHAPTER 6
PETROGRAPHY

A summary of petrographic descriptions of the lithologies deemed unsual or not so common within the RLS encountered (particularly in close proximity to the UG2 layer) in the study area is presented, such as the numerous quartzite units and other xenoliths, and replacement magnetite. The objective is to assess whether the UG2 layer at De Wildt may have formed or, been subjected to, any modifying conditions arising from possible contact metamorphism, deformation and alteration related to the emplacement of dyke swarms or, during cooling of the BC intrusion. Also, a petrographic overview is presented of the wider than normal UG2 footwall layer made up of a feldspathic pyroxenite with disseminated chromite and chromite blebs/slivers.

6.1. Quartzite xenoliths

Photomicrographs of quartzite intersected in borehole in the De Wildt project area are presented in Figures 35a-b. The polished sections are characterized by sub-rounded to anhedral quartz crystals and are weakly sericitised. Micro-faults crosscut the quartz grains with micro-displacement of the crystals. They are in-filled by oxide minerals.

The quartzite units are interpreted as xenoliths into the BC mafic rocks and have suffered brittle deformation and contact metamorphism to form feldspathic quartzite. Some of the rocks intersected at De Wildt are highly deformed to quartzite hornfels (Fig. 35c). Plagioclase is saussuritized giving a dusty appearance to the thin sections.

6.2. Hornfels

Hornfelsed metasedimentary rocks where intersected in several boreholes in contact with dolerite. In general, the hornfels are composed of recrystallized feldspathic quartzite. In borehole DWD3A/D (Fig. 35d), a zone of biotite (yellowish-reddish tint) characterised the contact between dolerite and hornfels, and granoblastic clinopyroxene characterised the chilled margins of dolerite. Suturing of quartz along grain boundaries occurred.

In borehole PDW4 (drilled in Schietfontein Farm), hornfelsed metasediments was composed of relatively equal proportions of chlorite (35%), epidote (30%) and actinolite (30 %) (Fig. 35e). The anhedral crystals are diffuse and distorted. Elongate needles of accessory sillimanite (5%) were randomly orientated throughout the matrix and together with chlorite, actinolite and epidote, suggest that an aluminosilicate-potassic protolith was subjected to hornblende-hornfels contact metamorphism during emplacement of the BC.

In one or two samples, the protolith is decidedly quartzo-feldpathic and composed of coarse plagioclase, medium-grained quartz and biotite (Fig. 35f). Quartz occurs in anhedral-subhedral and interconnected aggregates. Plagioclase crystals and their ghosts (remnants) are randomly orientated. Diffuse intergrowths of quartz-plagioclase occur in some samples. Biotite is formed within interstitices. Anhedral quartz crystals sometimes present together with highly deformed plagioclase and fractured orthopyroxene suggesting a higher grade of contact metamorphism and crystal deformation (Fig. 35g).

6.3. Chromite-rich feldspathic pyroxenite

A photomicrograph of the poorly developed UG2 seam composed of feldspathic pyroxenite and hosting disseminated chromite is presented Figures 35h-i. It consists of euhedral grains of chromite (opaque crystals) embedded within intercumulus plagioclase (white) and orthopyroxene crystals. The crystal margins are crosscut by chromite crystals. Orthopyroxene crystals exhibit small-scale fractures. Clusters of chromite grains occur in intercumulus plagioclase within feldspathic (plagioclase-rich) pyroxenite i.e., coarse-grained feldspathic pyroxenite hosting disseminated chromite (Fig. 35i).

6.4. Replacement pegmatites

Replacement pegmatites predominantly consist of large (~6 mm in diameter) prismatic, twinned plagioclase crystals (45%), together with subhedral to anhedral clinopyroxene crystals (35%), othopyroxene (10%), oxides (7%) and biotite (3%) (Fig. 35j). The random plagioclase laths define a sub-ophitic texture. Opaque minerals occur at existing minerals boundaries and are interpreted as replacement magnetite and/or ilmenite.

6.5. Summary

- Chromite grains are disseminated within pyroxenes and intercumulus plagioclase.
- Deformed feldspathic quartzite and hornfels rocks are micro-fractured and micro-faulted. They are characterised by recrystallized quartz crystals. The rocks have undergone brittle deformation.
- Two alteration types occur at De Wildt and include sericitisation and saussuritization of feldspars. Significant alteration is associated with contact metamorphism. Metamorphic assemblages consisting of random crystals of chlorite, epidote and actinolite are consistent hornblende-hornfels facies. Hornfels assemblages are interpreted as metasedimentary xenoliths of the Transvaal Supergroup.

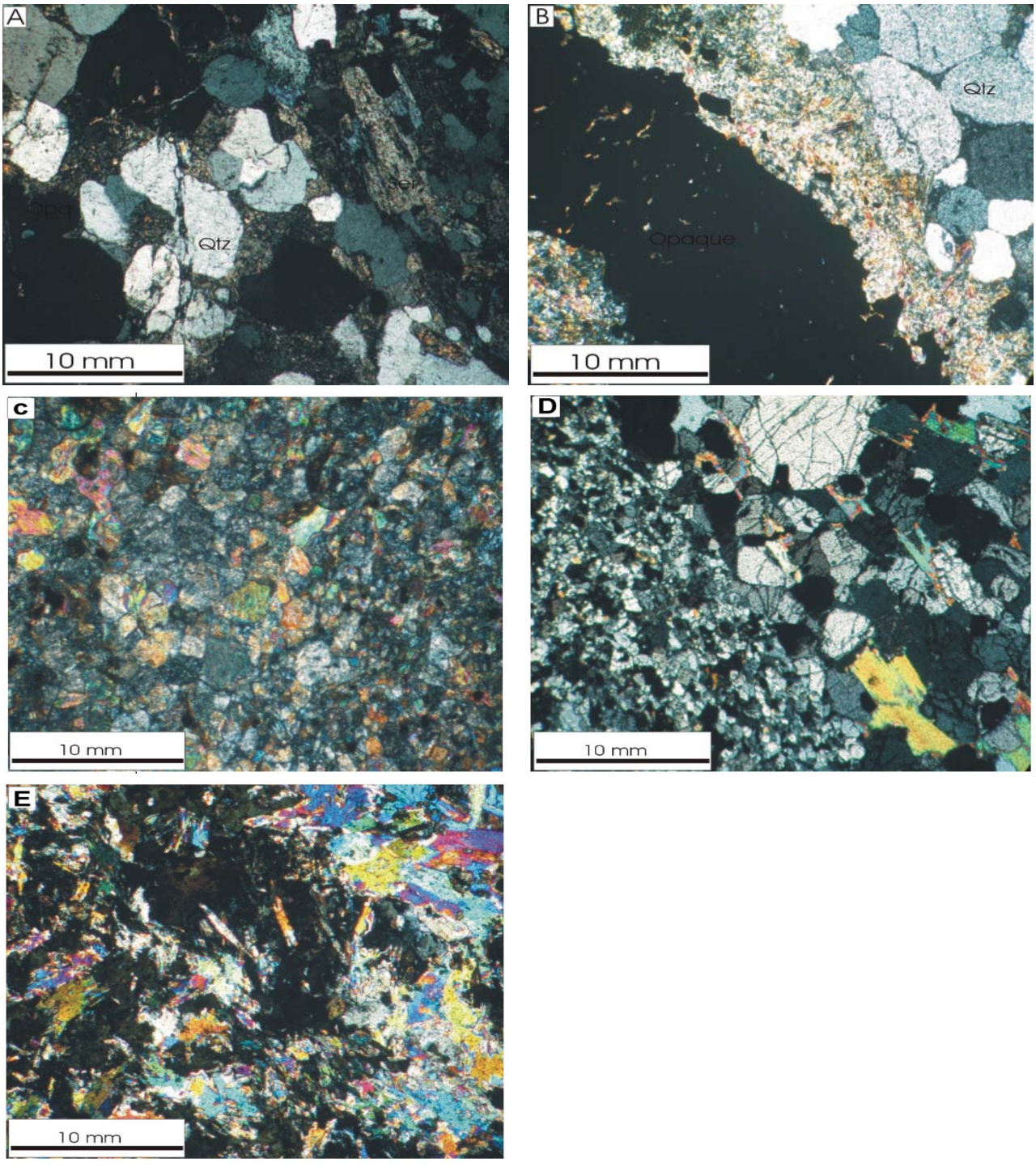


Figure 35: Photomicrographs of polished thin sections of selected core samples from various boreholes at De Wildt. All images are under crossed polars. Images **A** and **B** are quartzite characterized by veins composed of secondary oxide minerals. Sericite defines a zone around an (unidentified) opaque in image **B**. Image **C** shows a highly altered rock in which saussuritized plagioclase gives the rock a dusty appearance. Image **D** characterize contacts between recrystallized quartzite and dolerite: secondary mineral such biotite have formed between the contact and define contact metamorphism to hornblende-hornfels facies. Image **E** was derived from a metasedimentary xenolith that underwent low-grade metamorphism (borehole PDW04).

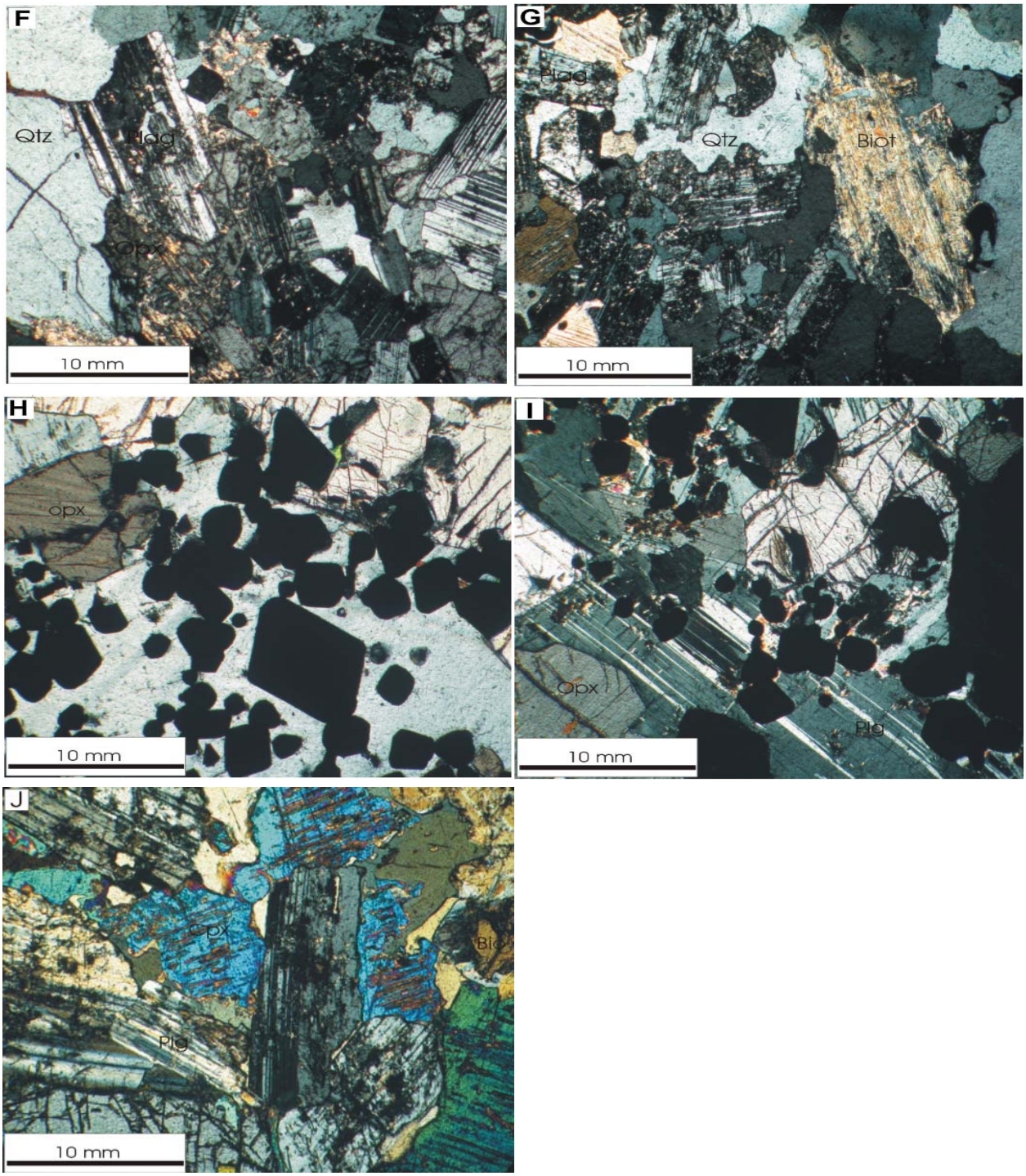


Figure 35: Photomicrographs of polished thin sections of selected core samples from various boreholes at De Wildt. All images are under crossed polars. Images **F** and **G** are hornfelses marked by the presence of fractured quartz, plagioclase, biotite and vague pyroxene crystals. The deformation in image F is interpreted to be localized and a result of magmatic fluids associated with intrusion of the dolerite dykes prominent within the De Wildt project area. Images **H** and **I** are of feldspathic pyroxenite hosting disseminated chromite, intersected where the UG2 seam was anticipated. The chromitite grains do not exhibit a preferred orientation but are scattered throughout the crystal mass. Image **J** is of pegmatite consisting of plagioclase, clino and othopyroxene and biotite crystals with oxides minerals in interstitices.

CHAPTER 7

MINERALIZATION

A summary of the PGE mineralization within the Merensky Reef and UG2 chromitite layers is presented. Also the mineralized UG2 footwall layers consisting of a feldspathic pyroxenites/norite hosting disseminated chromite and chromite blebs/slivers are outlined.

7.1. Merensky Reef PGE content

In the Dewildt project area, two major zones of PGE's occur along the Merensky Reef; an upper zone near the top gradational contact and a lower zone associated with the basal chromitite stringer/layer. However, the average PGE values for the Merensky Reef (or Merensky pyroxenite) in boreholes drilled by Nkwe Platinum were less than 0.1 g/t for Pt, Pd, Rh and Au (also known as 3E + Au, in South African platinum industry). The Merensky Reef intersections from historical drill core averaged close to 1g/t (3E+Au) over widths of less than 1.0 m near the top and bottom contacts (Fig. 36).

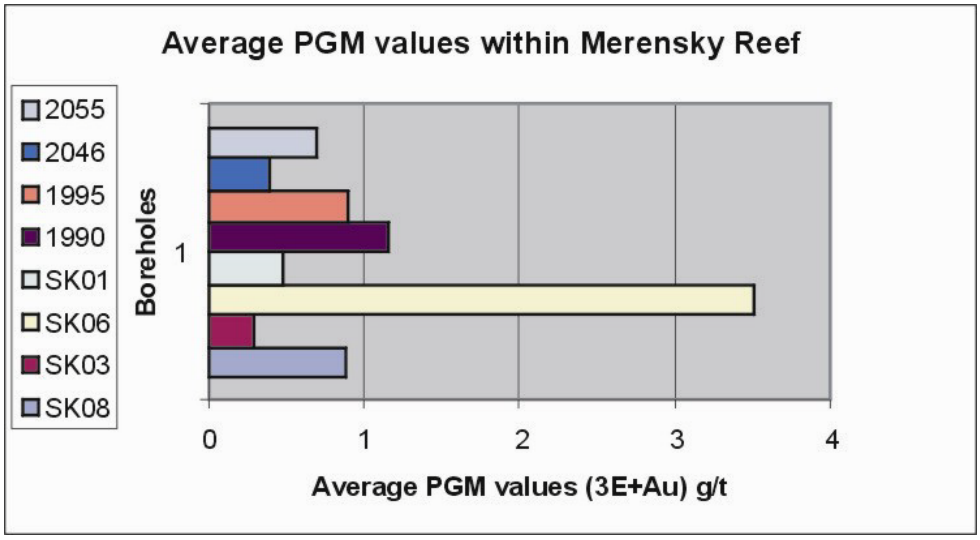


Figure 36: Average PGE values for Merensky Reef over 1 m from the bottom contact. In most of the boreholes drilled by Nkwe Platinum the grades were less than 0.1 g/t over widths of less than one metre near the top and bottom contacts

7.2. UG2 chromitite Isochon

The UG2 isochon map (Fig. 37) presents the five PGE's and gold distribution or grades (5E + Au, grams per tonne) of the UG2 layer across the De Wildt project area; there is a decrease in grade from the west to the east. The relatively higher grades of 3.0 g/t in the western zone coincide with the distribution of normal facies across the De Wildt project area. The central and eastern zones are characterized by grades less than 2.0 grams per tonne (g/t), coinciding with the zone in which the split-reef facies is dominant.

7.3. PGM value distribution along the UG2 chromitite

The top and bottom contacts, and the middle part of the normal facies UG2 chromitite layer, display elevated PGE values, while the immediate hangingwall and footwall units have relatively low PGE values (Fig. 38a). The highest PGE peaks are exhibited by the bottom contact and middle part of the UG2 layer. Prill splits of the UG2 chromitite show that the reef has a high Pt:Pd ratio of 3:1, i.e., the platinum content of the UG2 chromitite is more than three times that of palladium (Fig 38b, Table 9) and the Pt:Pd ratio show a general upward increase within the UG2 chromitite layer. Pt, Rh and Ru show similar variations with peak values in the middle of the chromitite layer. The average Pt/Pd ratio for the mineralized UG2 footwall is 1.7 (Table 9). In contrast, prill splits of the UG2 from the western Bushveld show that the platinum content is twice that of the palladium (Pt:Pd ratio of 2:1). This may indicate that the UG2 chromitite layer at De Wildt may have been subjected to late stage fluid activity with subsequent remobilization of Pd.

A plot of the centimetre grams per tonne of the PGEs distribution within the UG2 chromitite layer across the prospect is presented in Fig. 39. The western zone is characterized by relatively high PGE value distribution, with values greater than 400 cmg/t (5E + Au). Some locations within the western zone have values that exceed 600 cmg/t. The eastern zone and part of the central zone record values less than 200 cmg/t PGE distribution. Generally, the PGEs distribution decreases from west to east such that the eastern zone of the project area record relatively poor PGE values. The poor values in the eastern zone coincide with the presence of narrow ‘B type’ split reef sub-facies, in which the UG2 chromitite seams are poorly packaged (intersections in boreholes DWD10 and DWD12), while the western zone hosts predominantly normal facies and ‘B type’ split reef sub-facies which are massive and relatively well packed.

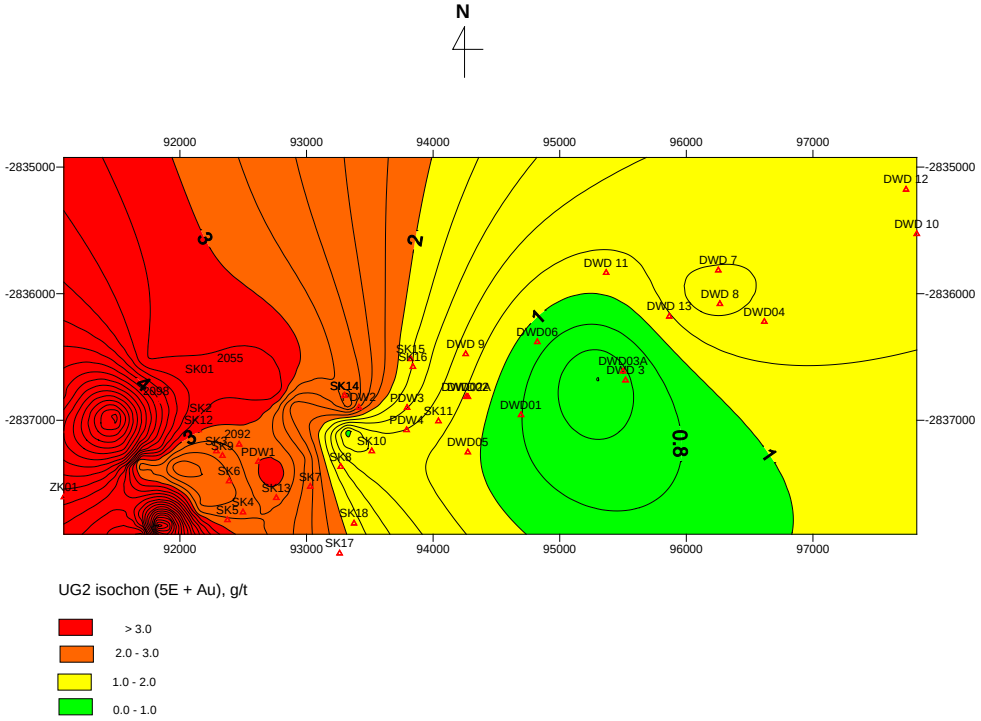


Figure 37: UG2 chromitite isochon map over the De Wildt project area.

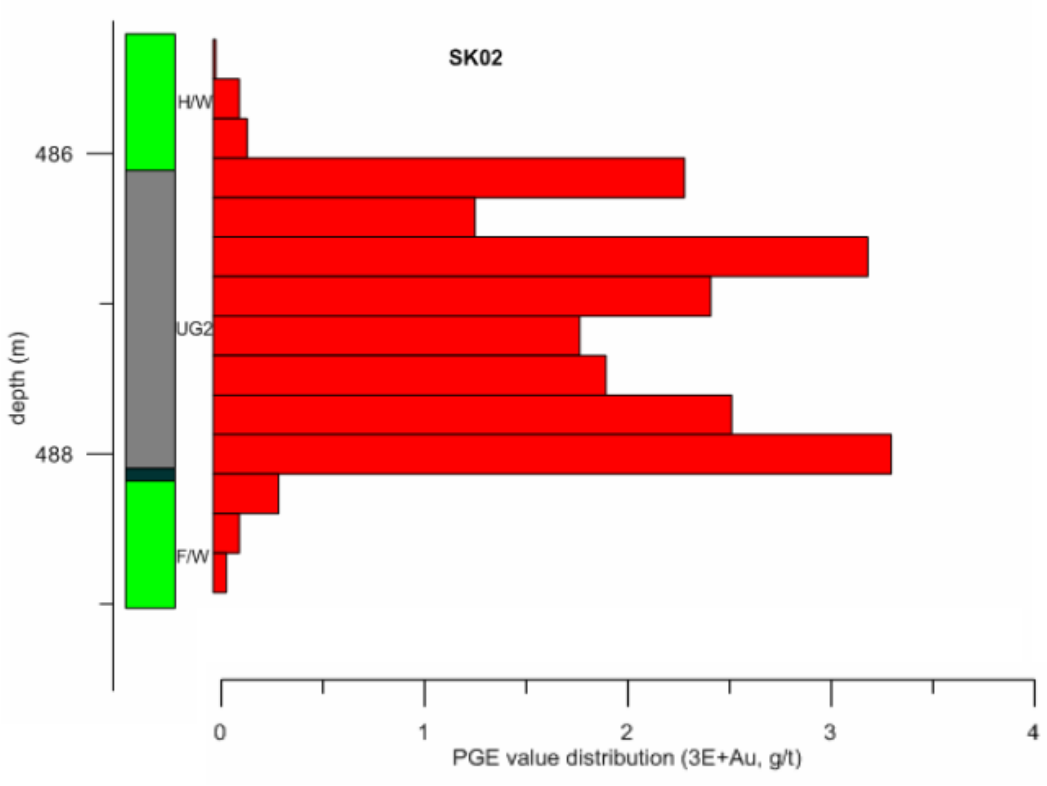


Figure 38a: PGM value distribution within the UG2 chromitite layer (normal facies type) in borehole SK02.

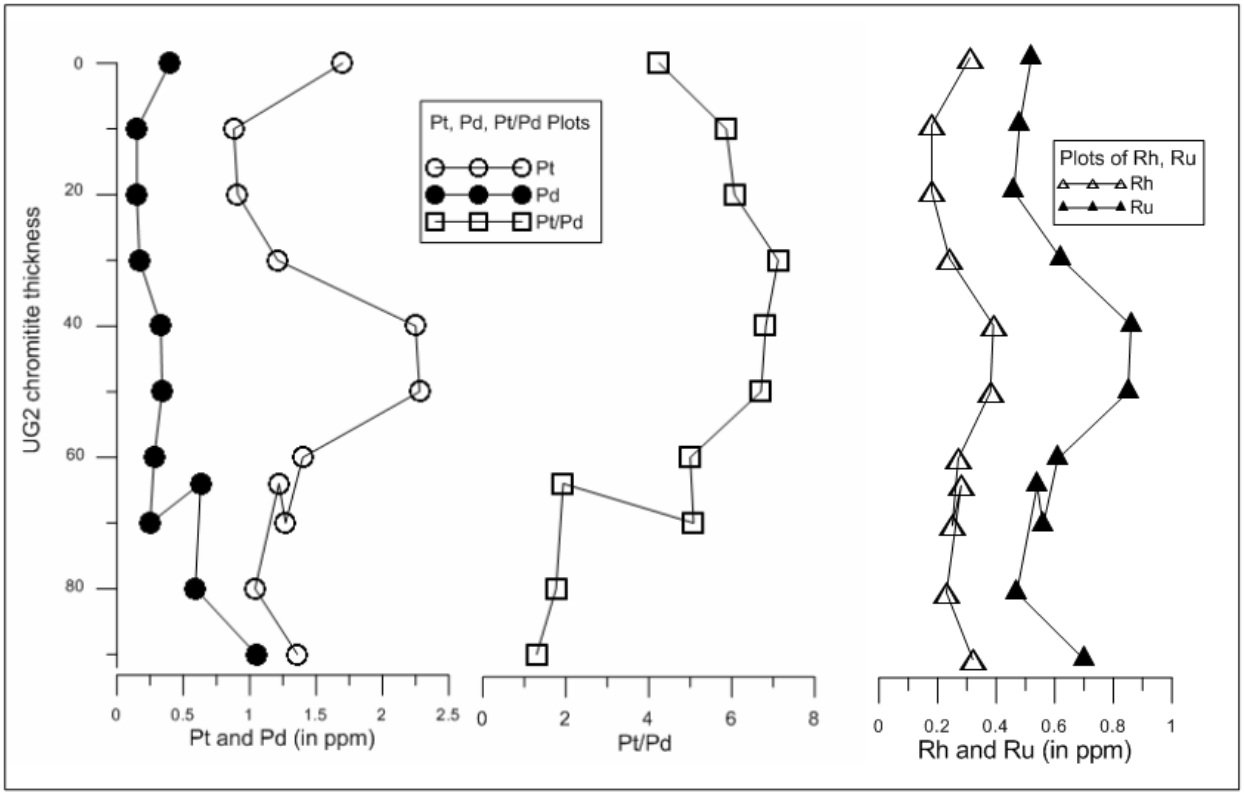


Figure 38b: Plots of Pt, Pd, Rh, Ru and Pt/Pd ratios of UG2 chromitite layer (from borehole PDW01). The Pt/Pd ratio values display an overall upward increase within the chromitite layer.

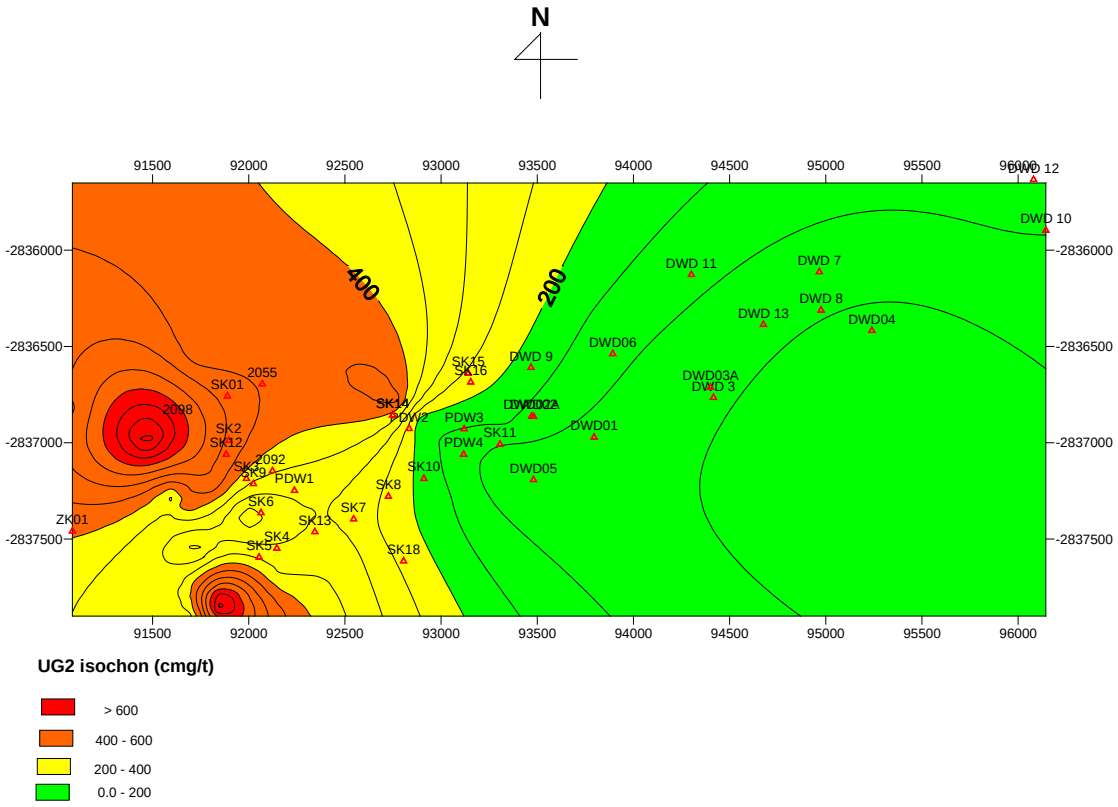


Figure 39: UG2 chromitite isochon map showing the plot of centimetre grams per tonne (5E + Au) across the De Wildt project area.

De Wildt Project - Prill Splits (5PGE)

UG2 Chromitite Layer

BHID	Farm	%Pt	%Pd	%Rh	%Ru	%Ir	%Au
PDW1D1	Schietfontein	53.27	13.93	10.14	16.82	5.18	0.67
PDW2D1	Schietfontein	57.66	8.76	10.46	18.73	3.89	0.49
PDW3D1	Schietfontein	51.32	13.67	11.02	18.69	4.32	0.98
2092 D3	Zilkaatsnek	42.22	34.73	7.26	11.92	2.72	1.14
2098 D1	Zilkaatsnek	59.34	8.60	9.26	16.69	5.62	0.5
1977 D4	Krelingspost	62.75	7.84	10.46	13.07	4.25	1.63
Average		54.43	14.59	9.77	15.99	4.33	0.90
Pt/Pd		**3.73**					

Lower UG2 Chromitite Layer (of the split-reef facies)

BHID	Farm	%Pt	%Pd	%Rh	%Ru	%Ir	%Au
2098 D1	Zilkaatsnek	56.86	10.62	9.96	15.93	4.42	2.21
1977 D4	Krelingspost	51.54	22.03	7.93	12.78	4.85	0.88
Average		54.20	16.33	8.95	14.36	4.64	1.55
Pt/Pd		**3.32**					

Chromite-rich UG2 footwall layers

BHID	Farm	%Pt	%Pd	%Rh	%Ru	%Ir	%Au
PDW1D1	Schietfontein	55.17	17.24	10.34	10.34	3.45	3.45
2092 D3	Zilkaatsnek	33.88	40.24	7.06	13.18	4.71	0.94
2098 D1	Zilkaatsnek	53.11	15.77	9.96	14.11	5.39	1.66
1977 D4	Krelingspost	43.48	32.61	8.70	10.87	2.17	2.17
Average		46.41	26.47	9.02	12.13	3.93	2.06
Pt/Pd		**1.75**					

Prill Splits in other localities in the Western Bushveld Complex

Crocodile River

5PGE Splits %	
	UG2
Pt	49.7
Pd	21.6
Rh	8.1
Ru	16.6
Ir	3.5
Au	0.5
Pt/Pd	**2.30**

Rustenburg Section

3PGE Splits %		
	MR	**UG2**
Pt	63.7	55
Pd	27.7	34
Rh	4.9	10
Au	3.7	1
Pt/Pd	**2.30**	**1.62**

Marikana

3PGE Splits	
	UG2
Pt	61.8
Pd	27.7
Rh	9.7
Au	0.9
Pt/Pd	**2.23**

Amandelbult

3PGE Splits		
	MR	**UG2**
Pt	61.9	58
Pd	29.5	29
Rh	4.9	12
Au	3.7	1
Pt/Pd	**2.10**	**2.0**

Platinum Map of South Africa (2003), Barker and Associates publishers

Table 9: Prill Splits for the UG2 chromitite layer and UG2 footwall at De Wildt are shown on the left, while the prill splits of the UG2 and MR reefs from other BC localities are given on the right.

7.4. Mineralized UG2 footwall at De Wildt

A mineralized zone below the UG2 chromitite is present in more than 60% of boreholes from the project area (Fig. 40). Chromite is discontinuous over approximately 4.0 m; the zone consists of a chromite-bearing feldspathic pyroxenite or mesonorite mixed with chromitite at millimetre to centimetre scale. In contrast, at Zilkaatsnek (western zone) and Schietfontein farms, the mineralized UG2 footwall is dominantly composed of feldspathic pyroxenite (Table 10), whereas on the Krelingspost Farm, the footwall is composed of a coarse-grained mesonorite.

The mineralized feldspathic pyroxenite footwall layers are brown-grey in colour. The feldspathic pyroxenite is closely mixed at a centimetre scale with chromitite (Fig. 41). It consists of ~5% chromite in the form of disseminations, chromite stringers/blebs and or chromite patches. The feldspathic pyroxenite is commonly medium-grained, with pegmatoidal segregations. In comparison, the mineralized UG2 footwall mesonorite is coarse-grained with rare zones of pegmatite. It is characterized by randomly distributed slivers/stringers of chromite as well as chromite blebs (Fig. 42) and ranges in thickness from 0.29 m to 4.0 m. In borehole SK09 it is approximately 10 m thick.

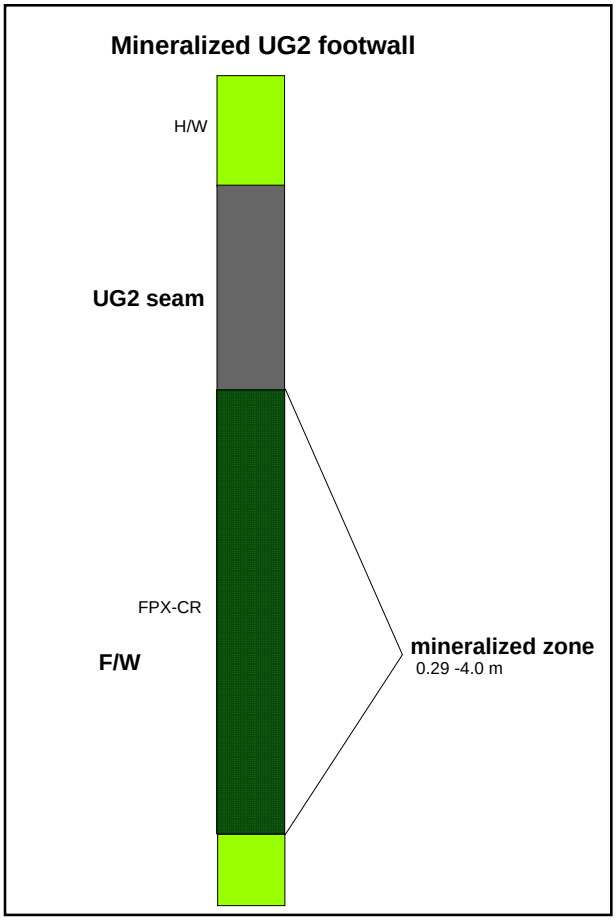


Figure 40: Schematic depiction of the mineralized zone below the UG2 layer. The mineralized footwall units (feldspathic pyroxenite/norite) host disseminated chromite, chromite blebs and chromitite slivers extending up to 4 m below the UG2 chromitite layer.

BHID	Nature of footwall lithology
SK02	Pegmatoidal feldspathic pyroxenite characterized by disseminated chromite and sulphides (pyrrhotite and chalcopyrite)
SK04	Fine to medium grained, pseudoporphyritic feldspathic pyroxenite with disseminated chromite.
SK06	Feldspathic pyroxenite with chromite stringers and chromite inclusions
SK08	Feldspathic pyroxenite which grades into a pegmatoidal norite with minor specs of sulphides
SK09	Feldspathic pyroxenite (with large clinopyroxene phenocrysts in places) and blebs of chromitite, chromite forms in small and large blebs randomly scattered within the feldspathic pyroxenite, discontinuous melanorite layers/patches occur in places.
DWD08	Coarse grained norite with oikocrysts, slivers and blebs of chromite together with some stringers of magnetite sits ~ 13.25 m below the UG2 chromitite layer.
DWD06	Coarse grained to pegmatoidal feldspathic pyroxenite with disseminated chromite and chromite blebs, occurring immediately below the UG2 layer (or UG2 remnant)
DWD09	Immediate footwall is characterized by a medium to coarse grained norite with irregular chromite stringers and blebs.

Table 10: A summary table of the different mineralized UG2 footwall lithologies intersected in various boreholes within the project area.

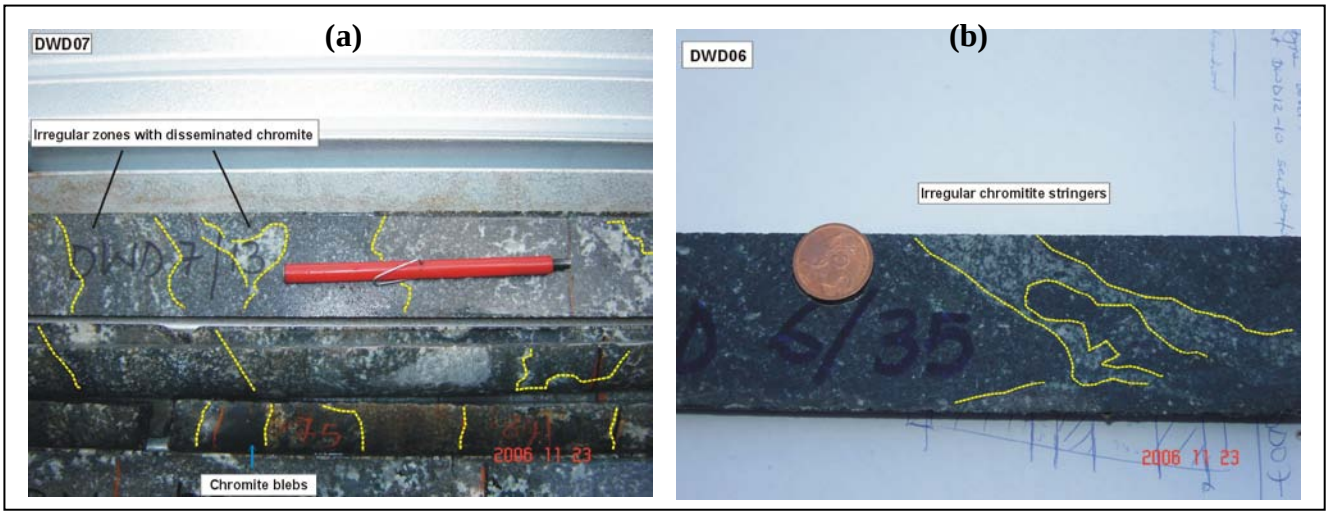


Figure 41: (**a**) UG2 feldspathic pyroxenite footwall characterized by irregular zones with disseminated chromite, intersected in borehole DWD07. (**b**) UG2 feldspathic pyroxenite footwall with irregular and vague chromite stringers, intersected in borehole DWD06.

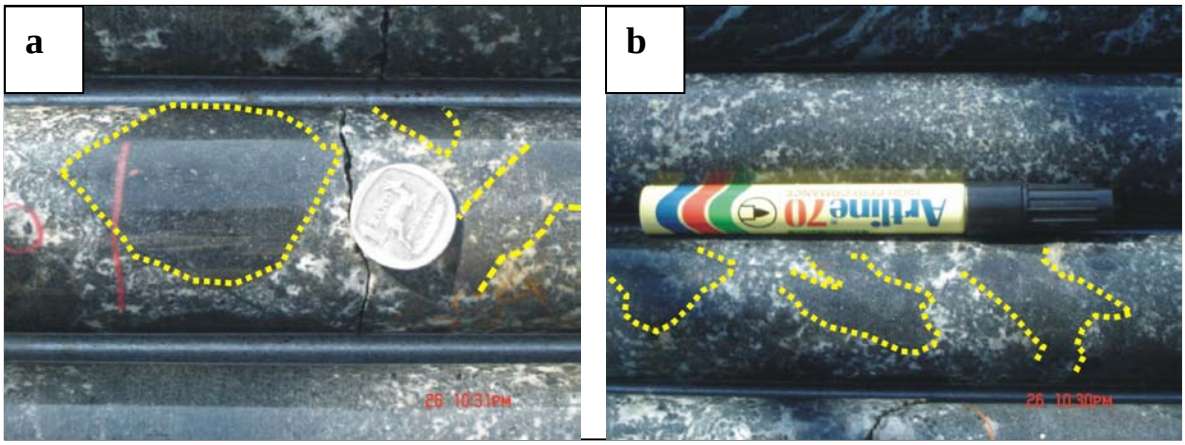


Figure 42: Chromite slivers and chromite blebs in a coarse crystalline-pegmatoidal norite underlying the UG2 chromitite layer in one borehole DWD08 intersection. Chromite patches/blebs and slivers are shown by yellow lines.

7.4.1. UG2 footwall isopach

An isopach map (Fig. 43) of the UG2 footwall isopach was compiled using the thickness of the chromitiferous UG2 footwall (i.e., inclusive of feldspathic pyroxenite and/or mesonorite layers and the lower UG2 chromitite unit where present). In the western and eastern zones of the project area, the thickness of the mineralized UG2 footwall averages 4.0 m. However, several boreholes intersected mineralization extending up to 5.0 m into the UG2 footwall. The central zone is characterised by relatively narrow mineralized footwall layers less than 2.0 m in thickness. Mineralized UG2 footwalls of less than 1.0 m in thickness occur both in the west and central zone.

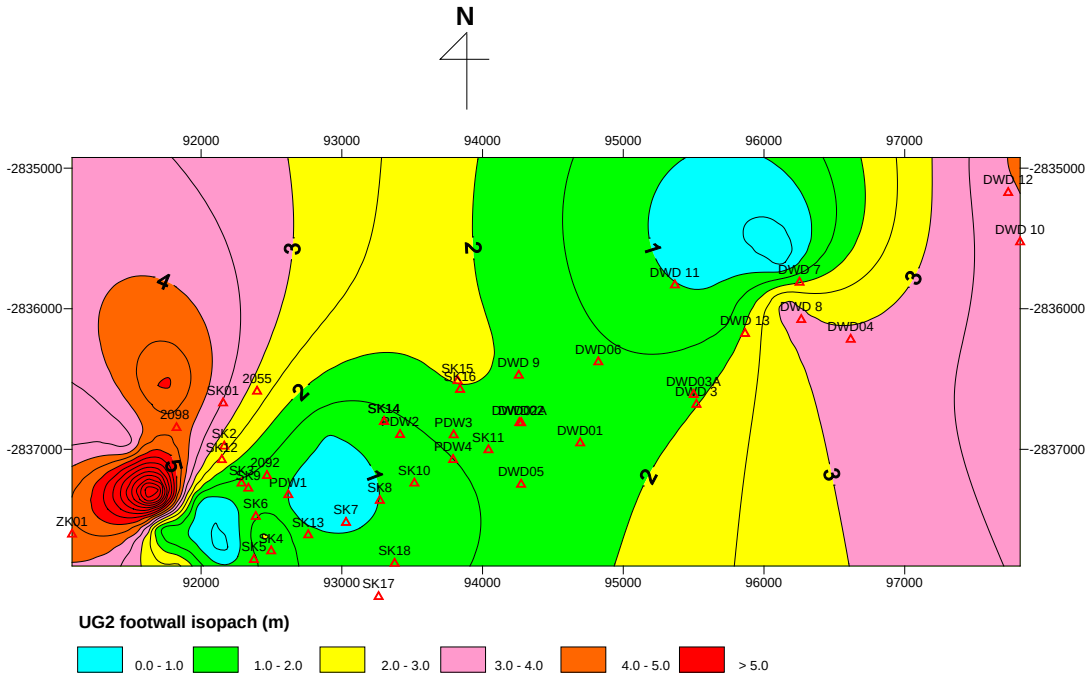


Figure 43: UG2 footwall isopach across the De Wildt project area. The term ‘footwall’ in this case refers to the chromitiferous UG2 footwall units consisting of feldspathic pyroxenite/norite hosting disseminated chromite, chromitite stringers and chromitite blebs.

7.4.2. UG2 footwall isochon

A plot of the PGE grades variation of the mineralized UG2 footwall layers across the prospect is given in Figure 44. The PGE grades are higher in the west and eastern portions of the prospect and range from 2.0-3.0 g/t (5E + Au). Grades exceeding 3.0 g/t (5E + Au) are scattered throughout the western zone at Zilkaatsnek Farm. The mineralized UG2 footwall in the central zone hosts PGE grades less than 2.0 g/t (5E + Au). A clear-cut grade distribution of PGEs along the UG2 footwall could not be established, which could reflect the highly irregular nature of the mineralized units throughout the project area. However, there was a direct correlation between the PGE values and the presence of chromite (Fig. 45).

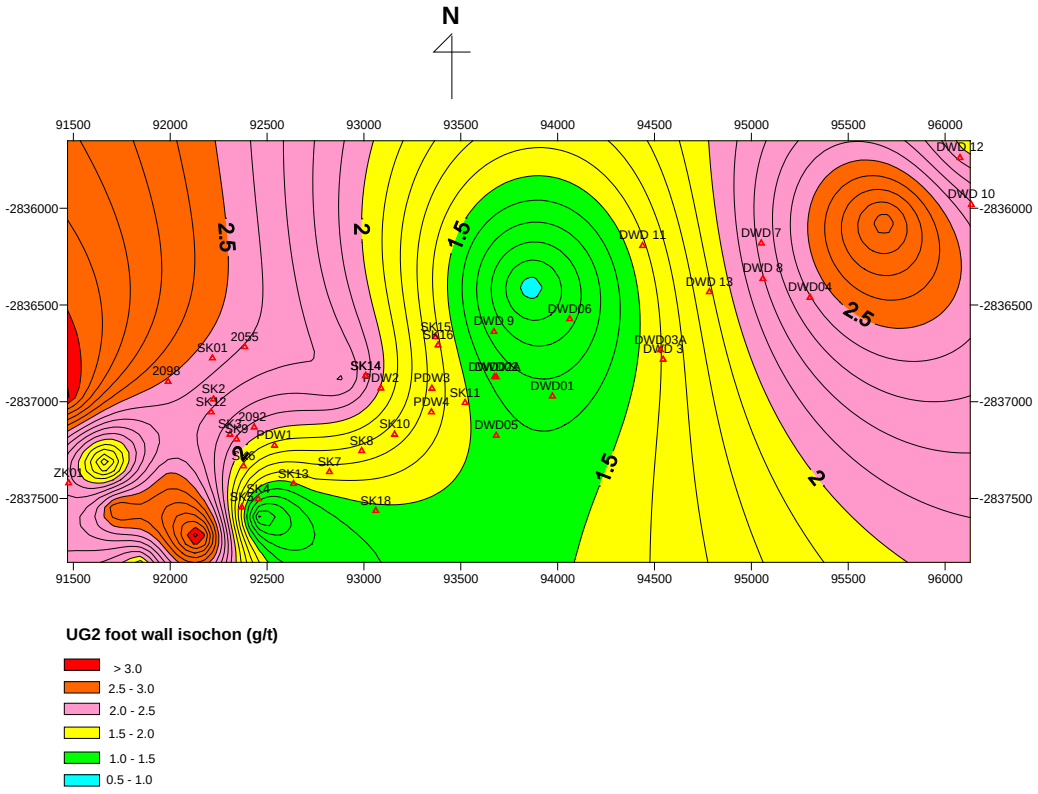


Figure 44: UG2 footwall isochon showing the variation of grades within the mineralized footwall units across the De Wildt project area. The term 'footwall' in this case refers to the chromitiferous UG2 footwall units consisting of feldspathic pyroxenite/norite hosting disseminated chromite, chromitite stringers and chromitite blebs.

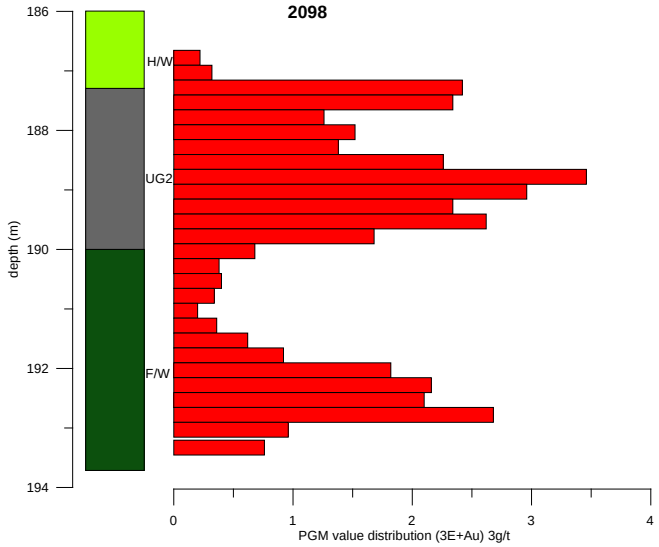


Figure 45: PGE value distribution along the mineralized UG2 footwall unit as represented in borehole 2098. The footwall unit is made up of a feldspathic pyroxenite with disseminated chromite (~30%) and chromite slivers.

The isochon map in Fig. 46 presents centimetre grams per tonne of the 5 PGE's plus Au in the mineralized UG2 footwall. The western zone of the prospect hosts relatively high values with PGE values that range between 400-600 cmg/t. The far western margins of the prospect host PGE values exceeding 600 cmg/t. In the rest of the prospect (central and eastern parts) the mineralized UG2 footwall layers contain PGEs values less than 400 cmg/t.

7.4.3. Combined UG2 and UG2 footwall isopach

The isopach map in Figure 47 presents the combined thickness distribution of UG2 reef and mineralized UG2 footwall across the prospect. The eastern zone of the project area has combined thicknesses ranging between 1.0 m to 3.0 m. Patches/pockets of combined UG2 and UG2 footwall thickness ranging from 3.0 to 5.0 m (and sometimes exceeding 5.0 m) only occur on the western zone. The central zone is characterized by combined thickness of less than 1.0 m and represents a UG2 footwall of insignificant PGE value and/or where the UG2 reef itself is poorly developed**.**

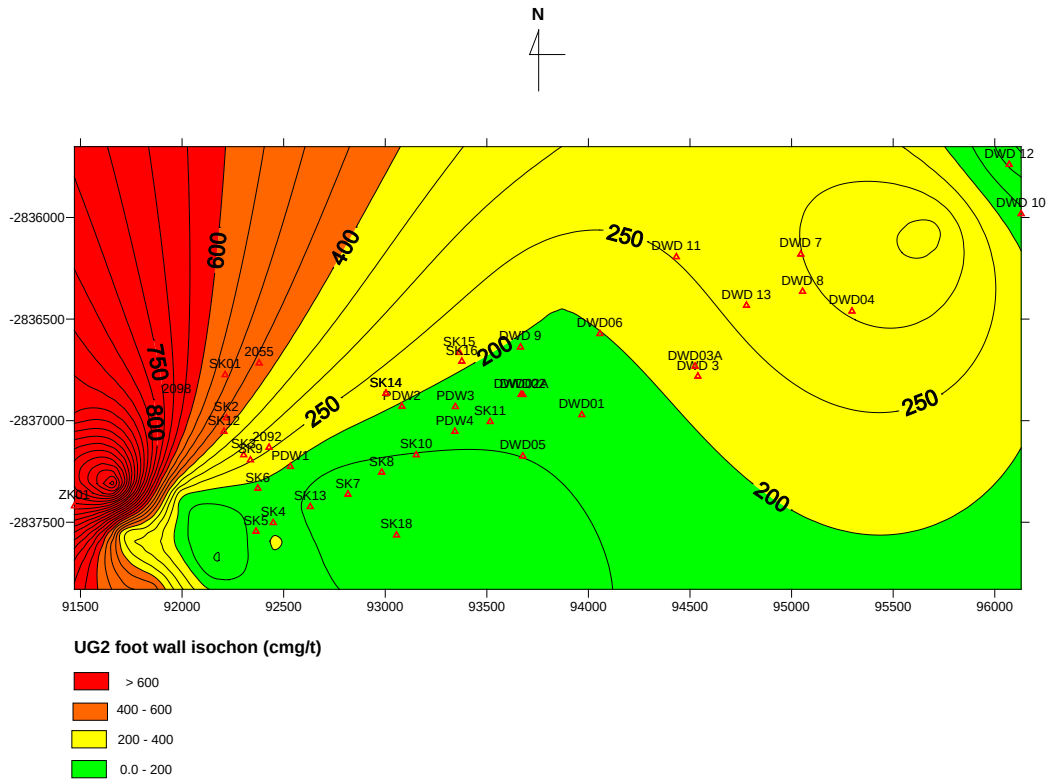


Figure 46: UG2 footwall isochon plot of centimetre grams per tonne (5E+ Au) within the mineralized units across the De Wildt project area.

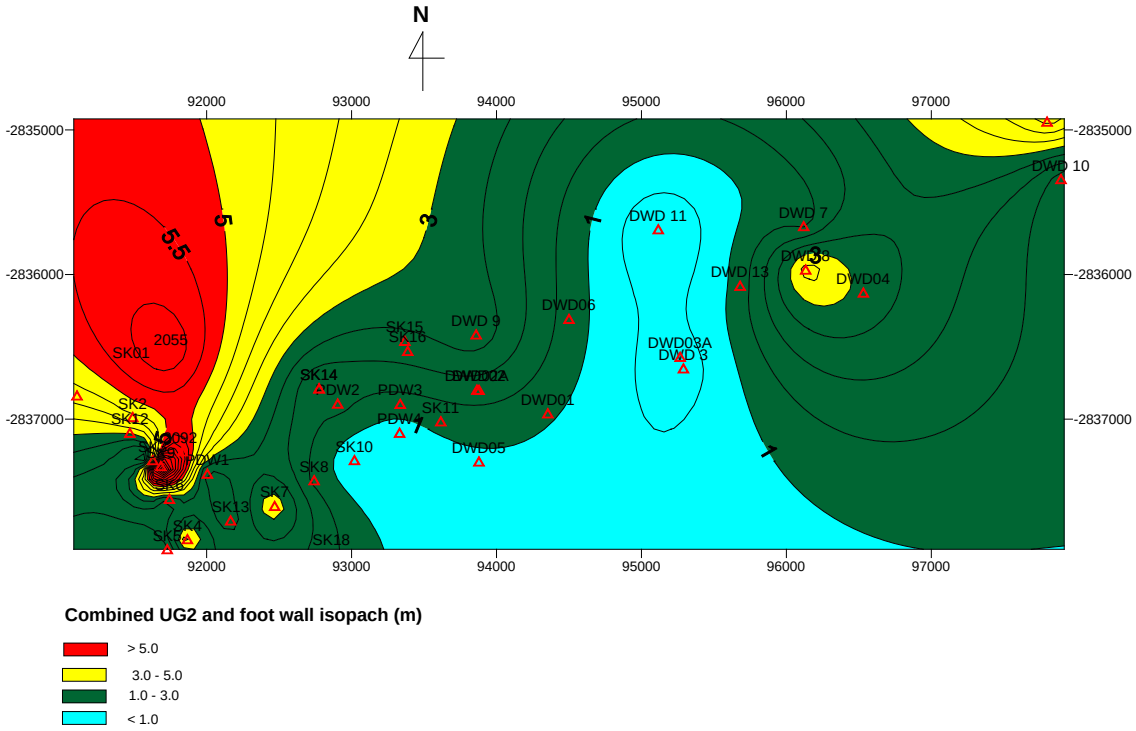


Figure 47: Combined UG2 layer and mineralized footwall isopach. This plot gives total length variation of the mineralized horizon (UG2 seam and footwall) across the De Wildt project area.

CHAPTER 8
DISCUSSION

8.1. Merensky Reef

The Merensky Reef in the De Wildt project area is 11.6 m to 20.5 m in thickness which is greater than intersections at Amandelbult and the Rustenburg area where the reef averages 1.6 m and 1.0 m, respectively (Viljoen, 1994). In addition, the Merensky Reef at De Wildt is medium grained/crystalline but at Amandelbult and Rustenburg area is pegmatoidal (Viljoen, 1994). Furthermore, the PGE grade at De Wildt is sub-economic averaging less than 1.0g/t (3E+Au). The style of the Merensky Reef at De Wildt correlates well with the distal facies of the Merensky Reef that extends from the Western Platinum area to Brits, as documented by Viljoen (1999). He described the distal facies as wide, non-pegmatoidal and low-grade to sub-economic, with few major potholes. A wide and non-pegmatoidal Merensky Reef facies was also reported by Davey (1992) west of De Wildt and east of the Spruitfontein upfold (Fig. 5).

The variable immediate footwall units to the Merensky Reef that were composed of anorthosite or, norite and pyroxenite, could suggest the occurrence of rolling of the Merensky Reef. The irregular bottom contact of the Merensky Reef defined by a chromitite stringer at De Wildt compares favourably with the small-scale undulations at the base of Merensky Reef reported elsewhere in the BC by Van der Merwe and Cawthorn (2005). While there is no definitive model to explain all the features of such structures, Vermaak (1976) attributed these undulations to impact generated dimpling of the floor by boulder-sized or aggregates of chromitite and pyroxenes onto unconsolidated chromitite and underlying anorthosite. However, in boreholes such as PDW02, where the Merensky Reef is situated close to the UG2 layer, it is likely that potholing may have occurred as indicated by attenuated and/or missing stratigraphic layers, with no evidence of faults.

The PGE value distribution within the Merensky Reef at De Wildt, though comparatively lower than in other parts of the BC, is concentrated on the upper portion of the reef and at the bottom, in association with basal chromitite stringers. As such, the Merensky Reef at De Wildt may also be tentatively regarded as ‘top loaded’ and ‘bottom loaded’ with respect to PGE value distribution.

The Bastard Reef (BR) was not intersected in the De Wildt project area. The Bastard Reef to the west of De Wildt was reported by Davey (1992) as noritic in character and about 12 m wide, and could be identified by the presence of an erratic 1-2 mm basal chromitite stringer. However at De Wildt, a predominantly norite sequence that is devoid of any chromitite stringers, made identification of the Bastard Reef impossible; alternatively, it could simply be that this unit was not deposited.

8.2. UG2 Chromitite layer

The two characteristic facies types of the UG2 chromitite layer encountered at De Wildt give some indication of the physical conditions during formation of the chromitite layer. The poikilitic texture observed at De Wildt is common in other parts of the BC (Viljoen et al., 1986, Leeb-Du Toit, 1986) and has been attributed to ortho-pyroxenite crystals forming around and enclosing the pre-existing chromite grains (Leeb-Du Toit, 1986). However, the finely crystalline UG2 chromitite unit that is dominant in the eastern zone of the project area, and which is devoid of any poikilitic texture, indicates rapid cooling of the seam.

Furthermore, the UG2 chromitite layer intersected in boreholes in the De Wildt project area is different from the typical UG2 encountered elsewhere in the western limb of BC in a number of ways. These differences include; (1) the absence of UG2 leader seams/triplets, (2) variation in thickness and the occurrence of a split-UG2 reef facies, (3) the occurrence of a norite in the immediate hangingwall to the UG2 mean seam, (4) the relatively lower PGE content, and (5) the existence of a mineralized UG2 footwall layer**.** Consequently, the interpretation or distinction of the UG2 layer from any other chromitite layer within the Bushveld stratigraphy was ascertained by considering PGE content. This was despite the relatively lower PGE content when compared to other BC localities. In summary:

- **The UG2 layer intersected in all boreholes at De Wildt does not have the usual leader seams or triplets which occur a few centimetres into the immediate overlying UG2 hangingwall pyroxenites** (Viljoen and Schürmann, 1998). The absence of the leader seams is attributed to the coalescence of the leader seams with the main UG2 chromitite seam during formation/emplacement. However, in some intersections where disseminated chromite was present a few centimetres into the UG2 hangingwall, the disseminated chromite is interpreted to be the remnant of poorly developed or disturbed leader seams/triplets. The UG2 is usually overlain by 'leader' chromitite layers whose thickness ranges from 10 to 12 cms and occurs within the immediate hanging-wall feldspathic pyroxenite (Viljoen and Schürmann, 1998).

- **The thickness variations and splitting of the UG2 chromitite layer across the De Wildt project area** (Fig. 48). A localized lateral variation in the development of the UG2 layer from west to the east across the De Wildt prospect was observed. A normal 'A' type facies, consisting of a massive chromitite seam is confined to the western portion at Zilkaatsnek Farm. The UG2 layer separates to form split reef facies towards the east.

  Variations in thickness, lithology and composition within the BC are interpreted with respect to proximity to the main feeder zone located at Union Section (Teigler et al., 1992; Maier and Eales,

1997; Scoon and Teigler (2005). The UG2 and UG1 chromitite layers tend to be thicker in the distal facies, while the Merensky Reef is well developed in the proximal facies but thicker and poorly mineralized in the distal facies (Scoon and Teigler, 2005). Teigler et al. (1992) and Scoon and Teigler (2005) observed that the Upper Critical Zone in the distal facies is thinner and dominated by plagioclase cumulates while in the proximal facies, it is thick, well developed and dominated by pyroxene cumulates. The normal UG2 chromitite (A-type facies) is interpreted to have crystallised and formed far from the main feeder source in the distal facies because of its greater width of up to 1.25 m.

The highly variable UG2 layer at De Wildt that varies in thickness, localized lateral discontinuities, and splitting may be an overprint of syn- and post-Bushveld factors such as faulting, formation of basement highs due to doming, and potholes;

Presence of basement highs – Thinning and/or complete absence of UG2 layer, together with the split-reef facies, is dominantly confined to the eastern zone of the prospect. The eastern zone is considerably disturbed as revealed in aeromagnetic maps that show the zone is crosscut by numerous faults. Also, two quartzite hills that are interpreted to be part of the Transvaal Supergroup, crop out in the eastern zone. It is not known whether these hills are large floor rock bodies or xenoliths rafted away from the Magaliesberg Quartzite Ridge. Regardless, boreholes to the immediate west of these hills intersected only a thin zone of BC mafic rock and these were characterized by a steep layer-dip of up to 60°. The boreholes then intersected the floor rocks (feldspathic quartzite) i.e., the floor rocks were intersected at shallower depth than anticipated (boreholes DWD03, DWD09 and DWD14). This suggests some continuity of the floor rocks at depth to the west and thus the possibility that these rocks form Magaliesberg Quartzite outliers in the BC.

The occurrence of floor upfolds or domes, such as Kookfontein and Spruitfontein in the western BC (Fig. 5, Chapter 2), has been shown to affect the development of the Critical Zone. Uken and Whitey (1997), Scoon (2002) and Gerya et al. (2004) observed thinning and draping of magmatic units above diapers. The Critical Zone is uplifted and attenuated against the flanks of domes such that individual layers or units are significantly thinned and may completely disappear or ‘pinch-out’ (Scoon, 2002). The affected rocks display a strong lineation and foliation. Such basement highs have been explained by Scoon (2002) as the result of diapirism triggered by gravitational loading and heating of floor rocks (Transvaal Supergroup) in response to intrusion by the BC. The variable widths of the UG2 chromitite layer encountered at De Wildt may have also been influenced by formation of these basement structures.

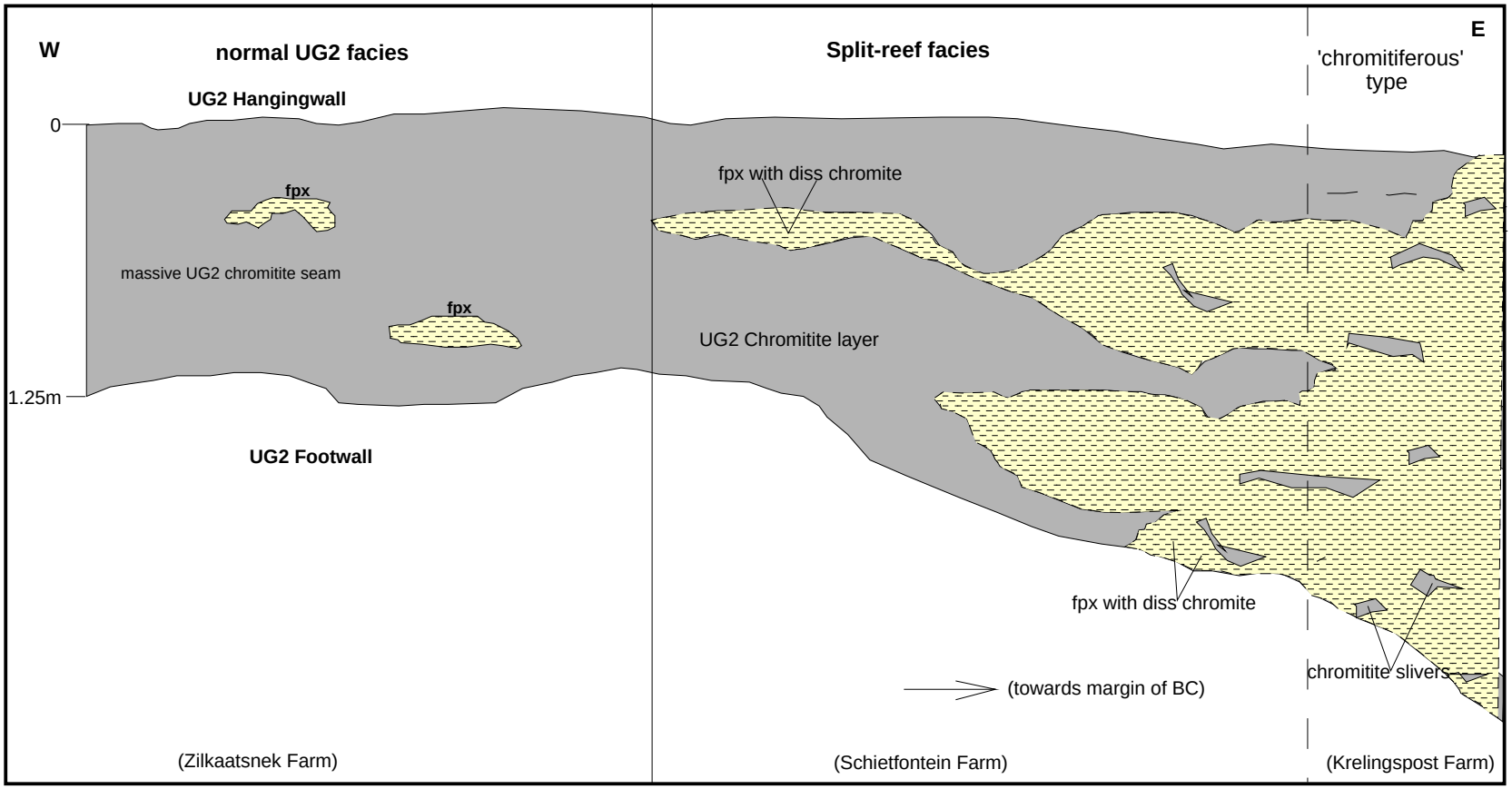


Figure 48: Schematic representation (not to scale) of the UG2 chromitite seam across the De Wildt project area showing the relationship between the UG2 normal reef facies, UG2 split-reef facies and feldspathic pyroxenite (fpx). The normal UG2 facies is confined to the west of the prospect while the split-facies occurs predominantly in the eastern zone on Schietfontein and Krelingspost farms.

Faults and potholes **-** The Schietfontein, Zilkaatsnek and Lindiwe faults are tentatively interpreted as antithetic faults to synthetic faults that form the Brits Graben; the Brits Graben influences the orientation of regional structural lineaments. Fault formation and the associated fracturing are possible modifying factors to the occurrence of normal UG2 reef. While the occurrence of a UG2 seam that is devoid of massive chromitite layer (but consisting of only disseminated chromite hosted within a feldspathic pyroxenite) is puzzling, it may be associated with slumping and faulting of stratigraphic layers. Drillcore from pothole-edge intersections are difficult to interpret and range from pinch-outs of the reef to UG2 reef remnants in the form of chromitite slivers or disseminated chromite in pyroxenite or norite. In contrast, the splitting of the UG2 seam into multi-layers suggests that the formation of the UG2 chromitite was not a single event. Instead, multiple magma injections into the chamber occurred during the crystallization processes to form the UG2 seam at De Wildt.

- **The UG2 layer at De Widlt is predominantly overlain by a norite unit of variable thickness (0.5 – 51 m) instead of the usual UG2 pyroxenite common in other BC localities.** The norite varies from medium to coarse crystalline and is developed in over ninety percent of the boreholes drilled at De Wildt. The absence of the UG2 pyroxenite is interpreted as the result of no deposition or, complete erosion during emplacement of the norite layer. The occurrence of thin and sparse UG2 pyroxenite in some borehole intersections is attributed to partial erosion of the earlier formed cumulate; irregular contacts between the UG2 pyroxenite and the overlying norite support this interpretation. The presence of a norite unit suggests that the Critical Zone rocks at De Wildt crystallized from a highly evolved parental magma. This interpretation concurs with Scoon and Tiegler (1995) who suggested that the Critical Zone in the distal facies of the BC is dominantly characterized by plagioclase cumulates whereas in the proximal facies, pyroxenite cumulates are abundant.

- **The PGE content of the UG2 layer at De Wildt is lower than that from other sites in the western BC.** The grades for the UG2 layer at De Wildt ranged from 1.5 to 3.0 g/t (3PGE + Au) over 1.3 metres, while the mineralized UG2 footwall layer (where developed) averaged 2.0 g/t (3PGE +Au) over 2.35 metres. The lower grades are a result of the greater vertical spread of the primary chromite accumulations and associated PGEs within the relative thick UG2 layer at De Widlt. The PGE values along the UG2 chromitite (A-facies) were preferentially concentrated close to the upper and lower contacts as well in the middle of the massive chromitite layer. The occurrence of a middle PGE peak along the UG2 chromitite layer is a deviation from that encountered in other parts of the BC where the peaks usually occur close to the upper and lower contacts. The three peaked UG2 layer at De Wildt thus contrasts with the ‘top and bottom loaded’

UG2 layer of Maier and Barnes (2008) who suggested that the chromitite seams formed by the injection of chromitite slurries into semi-consolidated footwall cumulates. Instead the observations at De Wildt compare well with Hiemstra (1986) and Cawthorn (2004) who concluded that the UG2 layer is made up of three cyclic units of distinct PGE composition.

However, the prill splits of UG2 chromitite reef intersected at De Wildt are greater than 3:1 for Pt:Pd ratios while the average ratios for the mineralized UG2 footwall is 1.7 (Table 9, Chapter 5). The ratio is higher than in UG2 chromitite layers at other localities in the western BC such as at Amandelbult, Crocodile River and Marikana whose UG2 chromitite Pt:Pd ratio averages 2:1. The relatively high Pt:Pd ratios obtained from the UG2 chromitite layer at De Wildt may imply that;

(a) The leader seams coalesced and became part of the upper chromitite unit; the leader seams have been shown to have higher Pt:Pd ratios similar to those of the UG2 layer at De Wildt (Bleeker pers. Comm., 2007). The UG2 seam at De Wildt was devoid of any leader in addition to being relatively wide. UG2 Leader seams have been shown to bifurcate and coalesce at local scale in other parts of the BC (Viljoen et al., 1986).

(b) The UG2 chromitite layer at De Wildt has been subjected to some degree of fluid activity as evidenced by the presence of replacement magnetite, amphibole, chlorite and epidote within the rocks. Also the UG2 seam at De Wildt is in close proximity to the Transvaal floor rocks. The high fluid activity at De Wildt may have resulted in the remobilization of the highly mobile Pd leaving behind a Pt enriched UG2 chromitite seam. This could account for the relatively lower overall PGE content of the De Wildt UG2 seam and concur with observations of Maier and Bowen (1996) of a Pd depleted UG2 seam at Schietfontein Farm. Hey (1999) demonstrated depletion of Pd at the top of weathered UG2 seam (and its enrichment at the base of the weathered horizon) at Union Section in the northwestern Bushveld Complex, indicating that depletion may be important when interpreting PGE content. Buick et al. (2000) demonstrated that retrogression due to channelled infiltration of fluids from dehydrating country rocks could affect cooling of the RLS mafic rocks.

The presence of replacement magnetite in the form of stringers and lenses within the UG2 chromitite, and the presence of quartz-biotite filled fractures/veins with the UG2 layer at De Wildt suggests that the chromitite was also exposed to late stage magmatic fluids. The very coarse-grained and often pegmatoidal character of the UG2 footwall feldspathic pyroxenite at De Wildt is arguably the result of recrystallization in response to secondary fluid activity. Such textures are common on the UG2 footwall feldspathic pyroxenites in other parts of the BC. For example, Davey (1992) reported an occurrence of a UG2 footwall at Marikana in the western limb of the BC (west of De Wildt prospect)

that consisted of coarse-grained feldspathic pyroxenite and which hosted chromitite stringers averaging ± 1 m in thickness. Regardless, a 4 m wide UG2 footwall pegmatoidal feldspathic pyroxenite hosting lenses and blebs of chromitite may be unique to De Wildt. The formation of the UG2 pegmatoid has been explained in terms of fluidization processes, in which the chromitite may have acted as a barrier to ascending late magmatic fluids (Mathez and May, 2005). Maier and Barnes (2008) suggested that fluidization may have aided downward injection of the chromitite into their footwall. Similarly, in the De Wildt project area, the chromitite lenses and blebs that characterize the mineralized UG2 footwall up to 5 m below the UG2 seam may indicate that the amount of late stage fluid infiltration was higher than usual. As such a greater portion of the basal parts of UG2 seam was physically eroded, resulting in a wide UG2 footwall horizon with chromite lenses and blebs. In concurrence, Penberthy and Merkle (1999) suggested that the unusual elevated PGE content within the UG2 chromitite footwall elsewhere in the BC was caused by the physical erosion of the lowermost part of UG2 by the underlying pegmatoid. The formation of the UG2 pegmatoid has been shown to postdate the formation of UG2 (Hiemstra, 1985).

The occurrence of a UG2 footwall layer consisting of a coarse-grained norite unit hosting blebs and lenses of chromite, as opposed to the usual feldspathic pyroxenite layer, tentatively suggests the presence of a UG2 pothole. The contact between the UG2 and its footwall pyroxenite layer has been shown to be erosional and in UG2 potholes, the footwall units are truncated, transgressed and eroded (Viljoen, 1994, Lomberg et al., 1999). As such, the absence of the usual UG2 footwall pyroxenite layer, coupled with lack of evidence of faults and other structural disturbances, is attributed to potholing of the UG2 chromitite layer.

The Lower Zone and the Lower Critical Zone were not intersected at De Wildt. The fact that the Lower and Lower Critical Zone were not intersected compares well with studies by Kruger (2005) who documented that the Lower and Lower Critical Zones of the BC are only restricted to a belt between Rustenburg and Northam in the western limb of the Bushveld. Similarly, Roberts (1992) noted that the maximum thickness of BC (including the Ruighhoek pyroxenite and now known to constitute the LCZ of the RLS) lies to the west of the De Wildt project area but is absent to the east of the De Wildt project area.

The Merensky Reef-UG2 separation at De Wildt generally ranges between 114 m and 188 m across the project area. However, in some boreholes such as PDW02 and DWD09, the Merensky Reef-UG2 separation is significantly attenuated to less than 30 m. The cause of this is ascribed possibly to Merensky potholes in which the underlying footwall layers were transgressed and eroded. In borehole DWD13, the Merensky Reef pyroxenite overlies a disturbed UG2 chromitite layer. This borehole is interpreted to have intersected a major pothole in which both the Merensky Reef pyroxenite and UG2 chromitite layer have been significantly affected or disturbed.

IRUP bodies/zones were scattered throughout the Merensky Reef-UG2 interval at De Wildt. In borehole DWD12 from Krelingspost Farm, the Merensky Reef together with surrounding norite units was completely replaced by IRUPs. Eales and Cawthorn (1996) attributed the formation of IRUPs to

the passive replacement of existing plagioclase-rich layered rocks by downward magmatic fluid percolation. As such it is likely that the Merensky Reef and other cumulates lying in this interval were subjected to late stage fluids associated with Upper Zone magmas that completely metasomatized and replaced them to the Iron-Rich Pegmatoid. Boreholes collared in the far eastern portion of Krelingspost Farm indicate that the UG2 layer lies close to the Marginal Zone (Figs. 49a-b) which implies thinning and wedging of the Upper Critical Zone towards the east across the project area. On this farm, the UG2 layer may overlie the Marginal Zone rocks (and probably the Transvaal floor rocks as well) as the Critical Zone thins against the floor rocks.

8.3. Metasedimentary xenoliths

Xenoliths of metasedimentary rocks derived from the underlying Transvaal Supergroup occur in the eastern zone of the De Wildt project area but become rare towards the west. The most dominant xenolith rock type is feldspathic quartzite (Fig. 50). The discontinuous quartzite hills on the Krelingspost Farm are interpreted as large floor rock upfolds/highs associated with the main Magaliesberg Mountain Ridge south of the prospect. Hartzer (1995) attributed the occurrence of deformed Transvaal Supergroup country rocks within the BC to various mechanisms including (1) pre-intrusive folding and doming, (2) syn-intrusive xenolith development or doming, and (3) post-intrusive thrusting.

A relatively high percentage of metasedimentary units of variable composition were intersected in the De Wildt project area. The presence of these rocks indicates that the Critical Zone lies in close proximity to the Transvaal Supergroup floor rocks. As such, the xenoliths encountered are interpreted to have rafted-off the Transvaal floor rock and were subsequently incorporated into the magma during the emplacement of the BC. Antonie (2004) noted that zones of increased gamma radiation in the K channel within the De Wildt prospect from radiometric data appeared to delineate basement inliers although this cannot be conclusively established from the limited outcrop and radiometric-dataset available. The De Wildt geology is comparable to the Kliprivier area (Dube, 2006) in the eastern limb of BC in terms of the abundance of floor rock xenoliths within mafic rocks, and the occurrence of wide reefs with diluted PGE grades. The two prospects are situated at the margins of the BC.

The small gravity anomaly to the east of the Brits graben is situated a few kilometres east of the De Wildt prospect and was interpreted by Viljoen (1999) as a feeder zone or magma conduit. This additional point of magma injection may be responsible for the existence of the highly thickened and norite-dominant Upper Critical Zone at De Wildt, and also for the relatively structurally complex stratigraphy prevailing. Other localities in the BC where main feeder zones are interpreted (such as the Amandelbult-Northam areas) are characterized by a relatively complicated stratigraphy (Kruger, 2005). However, Kruger (2005) cautioned interpretation of positive gravity anomalies as representing feeder zones arguing that the anomalies are likely to be enhanced by the inward dip and surface exposure of enormous volumes of dense mafic rocks.

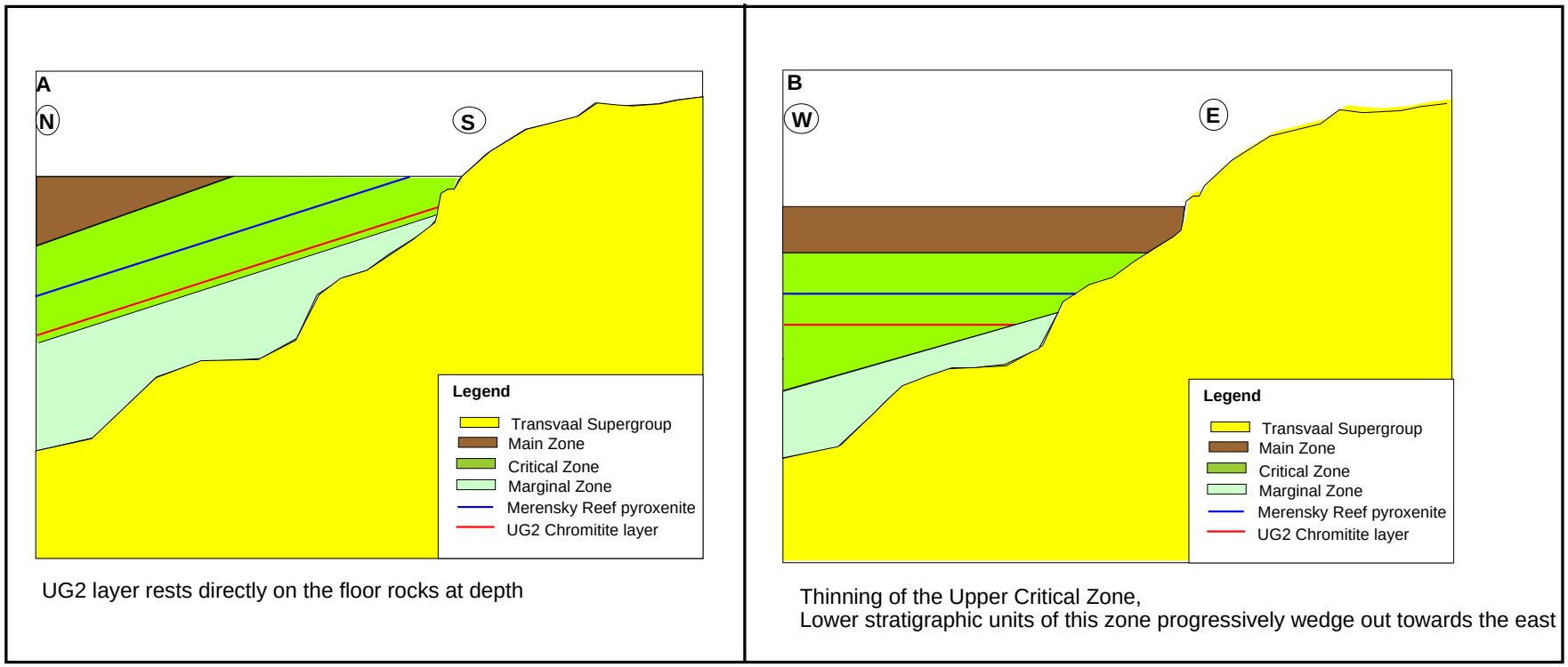


Figure 49: Schematic representation of the stratigraphic succession on the eastern zone of the project area (at Krelingspost Farm and eastward) toward the margin of the BC. In (**A**) the UG2 chromitite layer is interpreted to abut the floor rocks of the Transvaal Supergroup at depth. In (**B)** the wedging out of the Upper Critical Zone occurs i.e. the lower stratigraphic units are cut out against the floor rocks towards the east. This also explains why there was no intersection of the UG1 layer in the eastern portions of the prospect and the absence of UG2 layer out-crop in the vicinity of the quartzite hills.



Figure 50: Potassic quartzite hornfels intersected in borehole at Krelingspost Farm. It is not known whether this unit is connected to the floor or comprises a Transvaal Supergroup outlier.

8.4. Metamorphism

Metasedimentary xenoliths that are interpreted as enclaves of the floor rocks were observed in boreholes throughout the De Wildt project area. The xenoliths are ubiquitously deformed and characterized by micro-structures. Brittle deformation features include micro-fissures/fractures and micro-faults in crosscut to quartz crystals in quartzite. They probably formed during retrograde contact metamorphism associated with cooling of the BC magma or cooling of post-BC dolerite intrusions. Late stage or secondary minerals such as magnetite and chlorite fill these microstructures. Other secondary minerals including biotite occur on the contact of hornfelsed quartzite and dolerite and may be a result of fluid activity (metasomatism) after intrusion of dolerite dykes. The replacement of plagioclase by sericite may indicate interaction of the BC rocks with magmatic fluids associated with dyke intrusion and/or fluids from the dehydration of floor rocks. The occurrence of contact metamorphosed xenoliths within the RLS has been reported elsewhere in the BC (Wallmach et al., 1989; 1995).

Mbonambi (2007) noted the presence of an interchange between quartz and tridymite in microstructures in samples of deformed quartzite xenoliths from drill-core at De Wildt and suggested the interchange indicated prograde metamorphism and subsequently retrograde metamorphism. The presence of feldspathic (potassium-rich) quartzite xenoliths at De Wildt (Fig. 50) may be explained in terms of metasomatism; the interaction of potassium-rich fluids with quartzite xenoliths may have resulted in chemical reactions between quartz (SiO_2) and potassium anions to form a relatively stable assemblage such as the K-feldspar-rich quartzite that is abundant in the prospect.

Overall, the presence of quartz-norite and quartzite xenoliths within the Upper Critical Zone at De Wildt indicates a close spatial relationship of BC mafic units to the Transvaal Supergroup

metasedimentary rocks and the absence of the Lower Zone and Lower Critical Zone, which normally underlie the Upper Critical Zone in a complete succession of the Rustenburg Layered Suite. Hornblende-hornfels facies metamorphism of floor rock xenoliths is characteristic for the De Wildt prospect. The minerals epidote, actinolite and chlorite are characteristic of greenschist facies in the temperature range 300-500°C (Lapidus et al., 1990) and low pressure. The type and extent of metamorphism may have been controlled by the composition of the protolith, i.e., the Pretoria Group of the Transvaal Supergroup.

8.5. Structure and deformation pattern

The NW-trending mineral lineation defined by feldspars within a norite outcrop at Zilkaatsnek Farm is parallel to the regional trend of lineaments such as dykes and faults. The regional trend of the lineaments is likely to have been influenced by the adjacent Brits graben. The interpreted sequence of deformational events at De Wildt is;

1. Formation of NE- and NW-trending scissor faults with west block down.
2. Intrusion of the NE-trending dolerite dykes (Old Dyke) along NE-trending joints and faults (Fig. 14).
3. Intrusion of NW-trending dolerite dykes into pre-existing fracture-fault systems.

The formation of NE- and NW-trending scissor faults may be associated with the formation of drag and/or rollover folds, which would account for the ‘chaotic’ magnetic signature in the central zone giving the impression of a highly disturbed and/or folded zone. Certainly, the Merensky Reef and UG2 layers are intricately disrupted by a series of NE-trending faults at Zilkaatsnek and Schietfontein Farms. In these portions, blocks of mafic rocks have been down-thrown or uplifted (horst and graben) with the implication that the UG2 layer was intersected at confusingly shallow or deeper depths than expected.

Furthermore there is a strong possibility that some distortion or enhancement of magnetic signatures may have occurred as a result of the presence of the highly magnetic IRUP bodies scattered throughout the prospect, as evidenced by their intersections in a number of boreholes. An extensive east-west trending layered sill consisting of meta-quartz dolerites was reported by Roberts (1992) south of the De Wildt project area.

.

CHAPTER 8

CONCLUSIONS

Airborne magnetic and drill core data revealed that the three farms making up the De Wildt project area are highly disturbed by faults, potholes, intruded by dyke swarms and modified by the presence of floor rock up-folds and xenoliths. A full stratigraphic succession of the Rustenburg Layered Suite of the Bushveld Complex is not developed at De Wildt; the Lower Zone (LZ) and Lower Critical Zone (LCZ) are not developed. As such the Upper Critical Zone was developed in close proximity to the floor rocks.

The Merensky Reef in the De Wildt project area, while exhibiting its regional character (non-pegmatoidal, wide-type of the distal facies) has undergone further thickening up to about 20 m. Thinning or wedging-out of the Upper Critical Zone stratigraphic succession towards the east, was observed in the vicinity of basement highs/upfolds. Both the Merensky Reef and UG2 layers were generally correlated along strike within the farm portions. However, the UG2 layer exhibited an extra-ordinary lateral variation from west to east.

On Zilkaatsnek Farm, the UG2 layer was massive and well packaged while at Schietfontein and Krelingspost farms, it became split and multi-layered, and in some cases only consisted of disseminated chromite and chromite lenses within a feldspathic pyroxenite. The thickness variations of the UG2 layer and its localized lack of lateral continuity is attributed to; (1) the presence of large potholes, (2) the presence of basement/floor-rock up folds and xenoliths and (3) post-Bushveld faulting. While the splitting of the UG2 seam may not be fully understood, it does suggest that multiple magma injections took place during the crystallization processes to form the chromitites. The relatively high Pt:Pd ratios of the UG2 chromitite at De Wildt indicates that the UG2 layer has been exposed to late stage magmatic and/or meteoric fluids with the subsequent remobilization of Pd.

The NW trend of dykes at De Wildt is a regional feature and their emplacement is interpreted to have been determined/controlled by the pre-existing structural lineaments (fractures and faults) associated with formation of the Brits graben. Fault formation at De Wildt is interpreted as antithetic to that associated with the formation of the Brits graben. Dyke-related metamorphism of the BC mafic rocks at De Wildt is insignificant. Instead, contact metamorphism of Transvaal Supergroup sedimentary xenoliths is intense.

REFERENCES

Acocks, J.P.H., 1988. Veld types of South Africa. Memoirs of the Botanical Survey of South Africa 57: 1-146.

Antoine, L., 2004. Memorandum to Nkwe Platinum (Pty) Limited (07 January 2004): Technical note on the results of the airborne geological survey by Fugro Services, De Wildt project, western Bushveld. Internal company report to Nkwe Platinum (Pty) Limited (unpublished).

Ashwal, L.D, Webb, S.J., Knoper, M.W., 2005. Magmatic stratigraphy in the Bushveld Northern Lobe: continuous geophysical and mineralogical data from the 2950 m Bellevue drillcore. South African Journal of Geology 8(2), 199-232.

Boudreau, A.E., 1992. Volatile fluid overpressure in layered intrusions and the formation of potholes. Australian Journal of Earth Sciences 39, 277– 287.

Bristow, D.G., Cawthorn, R.G., Harmer, J., Lee, C.A., Tegner, C., Viljoen, M.J., Walraven, F., Wilson, J.R., 1993. Symposium on layering in igneous complexes. Field excursion to the Bushveld Complex, 11th-17th September, 1993, 60p.

Buick, I.S., Gibson, R.L., Cartwright, I., Maas, R., Wallmach, T., Uken, R., 2000. Fluid flow in metacarbonates associated with emplacement of the Bushveld Complex, South Africa. Journal of Geochemical Exploration 60-70, 391-395.

Burger, A.J., Coertze, F.J., 1973-1974. Age determinations - April 1972 to March 1974. Annals of the Geological Survey of South Africa 10, 135-141.

Butcher, A.R., Merkle, R.K.W., 1991. Unsual textures and structures associated with a magnetite layer in the Bushveld Complex: a contribution to the adcumulate debate. Mineralogical Magazine 55, 465-477.

Butcher, P. J., Merkle, M., 1991. Structure and rock sequences of the Critical Zone of the eastern Bushveld Complex. Special Paper, Mineralogical Society of America 1, 93-107.

Button, A., 1986. The Transvaal sub-basin of the Transvaal Sequence. In: Anhaeusser, C.R., Maske, S., (Eds.), Mineral deposits of Southern Africa, Volume I. Geological Society of South Africa, Johannesburg, pp. 811–817.

Carr, H.W., Kruger, F.J., Groves, D.I., Cawthorn, R.G. 1999. The petrogenesis of Merensky Reef potholes at the western platinum mine, Bushveld Complex: Sr-isotopic evidence for synmagmatic deformation. Mineralium Deposita 34, 335-347.

Campbell, I.H., 1986. A fluid dynamic model for the potholes of the Merensky Reef. Economic Geology 81, 1118–1125.

Cawthorn, R.G., Webb, S.J., 2001. Connectivity between the western and eastern limbs of the Bushveld Complex. Tectonophysics 330, 195-209.

Cawthorn, R.G. 2004 Origin of variation of Pt/Pd values in the UG2 chromitite layer, Bushveld Complex. Geoscience Africa, University of the Witwatersrand, July 2004, pp. 110-113.

Cawthorn, R.G., 2005. Pressure fluctuations and the formation of PGE-rich Merensky and chromitite reefs. Mineralium Deposita 40, 231-235.

Cawthorn, R.G., Eales, H.V., Walraven, F., Uken, R., Watkeys M.K., 2006. The Bushveld Complex. In: Johnson, M.R., Anhaeusser, C.R., Thomas, R.J., (Eds.), The Geology of South Africa. Geological Society of South Africa. Johannesburg/Council for Geoscience, Pretoria, pp. 261-281.

Chief Directorate: Survey and Mapping, 1996. 2527DB 1:50 000 geological map sheet Brits. South Africa (Fifth Edition, 1996), Republic of South Africa.

Clarke, B., Uken, R., Reinhardt, J., 2008. Structural and compositional constraints on the emplacement of the Bushveld Complex, South Africa. Lithos 11, 21-36.

Clarke, B.M., Uken, R., Watkeys, M.K., Reinhardt., 2005. Folding of the Rustenburg layered suite adjacent to the Steelpoort pericline: implications for syn-Bushveld tectonism in the eastern Bushveld Complex. South Africa Journal of Geology 108, 397-412.

Cousins, C.A., 1959a. The Bushveld Igneous Complex, The geology of South Africa's Platinum resources. Platinum Metals Review 3, 94-99.

Cousins, C.A., Feringa, G., 1964. The chromite deposits of the western belt of the Bushveld Complex. In: Haughton S.H., (Ed.) The geology of some ore deposits in southern Africa. Special Publications of the Geological Society of South Africa 2, 183-202.

Dankert, B.T., Hein, K.A.A., 2010. Evaluating the structural character and tectonic history of the Witwatersrand Basin. Precambrian Research 177, 1-22.

Davey S.R., 1992. Lateral variations within the Upper Critical Zone of the Bushveld Complex on the farm Rooikoppies 297 JQ, Marikana, South Africa. South African Journal of Geology 95, 141-149.

Davison, G.E., Chunnett, G.K., 1999. Seismic exploration for Merensky Reef: The way ahead. South African Journal of Geology 102, 261-267.

De Klerk, W.J., 1995. Textures exhibited by feldspars in the Giant Mottled Anorthosite (GMA) of the Bastard unit in the Upper Critical Zone, Western Bushveld Complex. Mineralogy and Petrology 54, 25-34.

Eales, H.V., 2001. A first Introduction to the geology of the Bushveld Igneous Complex and those aspects of South African geology that relate to it. The Council of Geosciences 1, pp. 7.

Eales, H.V., Cawthorn, R.G., 1996. The Bushveld Complex. In: Cawthorn, R.G. (Ed.) Layered Intrusions. Developments in Petrology 15, 103-145 and 181-229.

Eriksson, P.G., Altermann, W., Hartzer, F.J., 2007. The Transvaal Supergroup and its Precursors. In: Johnson, M.R., Anhaeusser, C.R., Thomas, R.J., (Eds.), The Geology of South Africa. Geological Society of South Africa, Johannesburg/Council for Geoscience, Pretoria, pp. 237-260.

Eriksson, P.G., Hattingh, P.J., Altermann, W., 1995. An overview of the geology of the Transvaal Sequence and Bushveld Complex, South Africa. Mineralium Deposita 30, 98-111.

Eriksson, P.G., Schweitzer, J.K., Bosch, P.J.A., Schreiber, U.M., Van Deventer, J.L., Hatton, C.J., 1993. The Transvaal Sequence: an Overview. Journal of African Earth Sciences 16, 25-51.

Farquhar, J., 1986. The Western Platinum Mine. In: C.R., Maske, S., (Eds.), Mineral Deposits of Southern Africa, Volume II. Geological Society of South Africa. Johannesburg, pp. 1135-1142.

Frimmel, H.E., Minter, W.E.L., 2002. Recent Developments Concerning the Geological History and Genesis of the Witwatersrand Gold Deposits, South Africa. In: R. Goldfarb and R.L. Nielsen (Eds.), Global Exploration 2002 - Integrated Methods for Discovery. Special Publication. Society of Economic Geologists, Littleton, pp. 17-45.

Gerya, T.V., Uken, R., Reinhardt, J., Watkeys, M.K., Maresch, W.V., Clarke, B.M.., 2004. Cold diapirs triggered by intrusion of the Bushveld Complex: Insight from two dimensional numerical modelling. In: Whitey, D.L., Teyssier, C., and Siddoway, C.S., (Eds.) Gneiss domes in orogeny: Boulder, Colorado, Geological Society of America Special Paper 380, 117-127.

Hall, A.L., 1932. The Bushveld Igneous Complex of Central Transvaal. Memoir 28, Union of South Africa Geological Survey, Government Printer, Pretoria, 1932.

Hammond, H., 1998. Structural Interpretation of Aeromagnetic data; a rudimentary guide. Unpublished technical memo to North Limited, Australia, pp. 1-46.

Harmer R.E., Sharpe M.R., 1985. Field relations and strontium isotope systematics of the marginal rocks of the Eastern Bushveld Complex. Economic Geology 80: 813–837.

Harmer, R.E., 1985. Rb-Sr isotopic study of units of the Penaars River Alkaline Complex, north of Pretoria, South Africa. Transactions of the Geological Society of South Africa 88, 215-223.

Hartzer, F.J., 1995. Transvaal Supergroup inliers: geology, tectonic development and relationship with Bushveld Complex, South Africa. Journal African Earth Sciences 21, 521-547.

Hatton, C.J., Schweitzer, J.K., 1995. Evidence for synchronous extrusive and intrusive Bushveld magmatism. Journal of African Earth Sciences 21, 579-594.

Hatton, C.J., Von Gruenewaldt, G., 1985. The geological setting and petrogenesis of the Bushveld chromitite layers. Research. Report., Institute of Geological Research on the Bushveld Complex, University of Pretoria 57, 1-48.

Hey, P.V., 1999. The effects of weathering on the UG2 Chromitite reef of the Bushveld Complex, with special reference to platinum group minerals. South African Journal of Geology 102, 251-260.

Hiemstra, S.A., 1985. The distribution of some platinum-group elements in the UG2 Chromitite layer of the Bushveld Complex. Economic Geology 80, 944-957.

Judeel, G. du T., Hartmann, A.W., 2008. Ground support at Crocodile River Mine located in the Brits graben of the western limb of the Bushveld Complex. Abstracts, 6th International Symposium on Ground Support in mining and Civil Engineering Construction, Capetown 30 March – 3 April 2008, pp. 525-544.

Kinnaird, J.A., Kruger, F.J., Nex, P.A.M., Cawthorn, R.G., 2002. Chromite formation – a key to understanding processes of platinum enrichment. Transactions of the Institute of Mining and Metallurgy 111, B23-B35.

Kinloch, E.D., Peyerl, W., 1990. Platinum Group minerals in various rock types of the Merensky Reef: Genetic implications. Economic Geology 85, 537-555.

Kruger, F.J., 2005. Filling the Bushveld Complex magma chamber: lateral expansion, roof and floor interaction, magmatic unconformities, and the formation of giant chromitite, PGE and Ti-V-magnetite deposits. Mineralium Deposita 40, 451-472.

Lapidus, D.F., 1990. Collins dictionary of geology. Harper Collins publishers, UK, pp. 265.

Leeb-Du Toit, A., 1986. The Impala Platinum Mines. In: Anhaeusser, C.R., Maske, S., (Eds.), Minerals Deposits of Southern Africa, Volume II. Geological Society of South Africa. Johannesburg, pp. 1091-1106.

Lipin, B.R., 1993. Pressure increases, the formation of chromite seams, and the development of the Ultramafic series in the Stillwater Complex, Montana. Journal of Petrology 34, 955-976.

Lomberg, K., Rupprecht, S., Cunningham, G., 2006. Crocodile River Mine, South Africa. Independent Technical Report prepared for RSG Global on behalf of Barplats Investment Limited, 122p.

Lomberg, K.G., 1991. Motivation to relinquish the options to the mineral rights to portions of Zilkaatsnek 439 JQ, Geological Memorandum No. 188, Platinum and Bushveld Exploration Mineral Resource Division-Rotund Project, 22 October 1991.

Lomberg, K.G., Martin, E.S., Patterson, M.A., Venter, J.E., 1999. The morphology of potholes in the UG2 Chromitite layer and Merensky Reef (pothole reef facies) at Union Section, Rustenburg Platinum Mines. South African Journal of Geology102, 209-220.

Lurie, J., 1986. Mineralization of the Pilanesberg Alkaline Complex. In: Anhaeusser, C.R., Maske, S., (Eds.), Mineral Deposits of Southern Africa, Volume II. Geological Society of South Africa, Johannesburg, pp. 2215-2228.

Maier, W., Barnes, S.J., 2008. Platinum-group elements in the UG1 and UG2 chromitites and the Bastard reef, at Impala platinum mine, western Bushveld Complex, South Africa: Evidence for late magmatic cumulate instability and reef constitution. South African Journal of Geology 111, 159-176.

Maier, W.D., 2005. Platinum-group element (PGE) deposits and occurrences: mineralization styles, genetic concepts, and exploration criteria. Invited presidential review, Journal of Earth Sciences 41, 165-191.

Maier, W.D., Eales, H.V., 1997. Correlation within the UG2-Merensky Reef interval of the Western Bushveld Complex, based on geochemical, mineralogical and petrological data. Geological Survey South Africa Bulletin, 120, 56.

Maier, W.D., Bowen, M.P., 1996. The UG2-Merensky Reef interval of the Bushveld Complex, northwest of Pretoria. Mineralium Deposita 31, 386-393.

Martin, D. McB., Clendenin, C.W., Krapež, B., McNaughton, N.J., 1998. Tectonic and geochronological constraints on late Archaean and Palaeoproterozoic stratigraphic correlation within and between the Kaapvaal and Pilbara Cratons. Journal of the Geological Society 155, 311-322.

Mathez, E.A., Mey, J.l., 2005. Character of the UG2 chromitite and host rocks and petrogenesis of its pegmatoidal footwall, northeastern Bushveld Complex. Economic Geology, 100, 1617-1630.

Mbonambi, H.M., 2006. Relative Chronology of Intrusive, Structural and Metamorphic Events through Petrographic and Microstructural Investigation of Diamond Drill Core, De Wildt area, Brits. Unpublished B.Sc. (Hon) research draft, University of the Witwatersrand Johannesburg.

Mitchell, A.A., Manthree, R., 2002. The Giant Mottled Anorthosite: a transitional sequence at the top of the Upper Critical Zone of the Bushveld Complex. South African Journal of Geology 105, 15-24.

Moen, F.H.G., 1989. A petrological study of Bushveld-type rocks from boreholes on the Moloto geophysical anomaly, northeast of Pretoria. South African Journal of Geology 92, 84-94.

Moen, R.T., 1989. The geochemistry of pyroxenites at 12#, Impala platinum mine. Technical report.

Naldrett, A.J., Wilson, A., Kinnaird, J., Chunnett, G., 2009. PGE Tenor and Metal Ratios within and below the Merensky Reef, Bushveld Complex: Implications for its Genesis. Journal of Petrology 50, 625-659.

Pattison, D.R.M., Tracy, R.J., 1991. Phase equilibria and thermobarometry of calcareous, ultramafic and mafic rocks, and iron formations. In Kerrick, D.M., (Ed.) Contact metamorphism. Reviews in Mineralogy 26, 105-206. (Mineralogical Society of America.)

Penberthy, C.J., Merkle, R.K.W., 1999. Lateral variations in the platinum-group element content and mineralogy of the UG2 Chromitite layer, Bushveld Complex. South African Journal of Geology 102, 240-250.

Roberts, K., 1992. An investigation of the floor and marginal rock-layered rock relationships of the Bushveld Complex, northwest of Pretoria. Unpublished Master of Science thesis, Geological Survey (Pretoria), 131p. ISBN: 0621144177.

Rozendaal, A., Toros, M., Anderson, J.R., 1986. The Rooiberg tin-deposits, West-central Transvaal. In: Anhaeusser, C.R., Maske, S., (Eds.), Mineral Deposits of Southern Africa, Volume II. Geological Society of South Africa, Johannesburg, 1307-1328.

SACS (South Africa Committee for Stratigraphy), 1980. Stratigraphy of South Africa. Part 1: (Kent, L.E, Compiler), Lithostratigraphy of the Republic of South Africa, South West Africa/Namibia, and the Republics of Bophuthatswana, Transkei and Venda. Geological Survey of South Africa Handbook 8, 690p.

Schiffries, C.M., Rye, D.M., 1990. Stable isotope systems of the Bushveld Complex: Constraints on hydrothermal processes. American Journal of Science 290, 209-245.

Schürmann LW, Grabe PJ, Steenkamp CJ (1998) Chromium. In: Wilson M.G.C., Anhaeusser, C.R. (Eds.) Mineral Resources of South Africa, 6th Edition. Council Geoscience, Handbook, Volume 16, pp 90–105.

Scoon, R.G., Teigler, B., 1995. A new LG-6 chromitite reserve at Eerste Geluk in the boundary between the central and southern sectors of the eastern Bushveld Complex. Economic Geology 90, 969-982.

Scoon, R.N., 2002. A new occurrence of Merensky Reef on the flanks of the Zaaikloof Dome, northeastern Bushveld Complex: Relationship between diapirism and magma replenishment. Economic Geology 97, 1037-1049.

Scoon, R.N., Mitchell, A.A., 1994. Discordant iron-rich ultramafic pegmatites in the Bushveld Complex and their relationship to iron-rich intercumulus and residual liquids. Journal of Petrology 35, 881-917.

Sharpe, M. R., Chadwick, B., 1982. Structures in Transvaal sequence rocks within and adjacent to the eastern Bushveld Complex. Transactions of the Geological Society of South Africa 85, 29–41.

Stevens, G., Gibson, R.L., Droop, G.T.R., 1997. Mid-crutal granulite facies metamorphism in the Central Kaapvaal craton. The Bushveld Complex connection. Precambrian Research 82, 113-132.

Tankard, A.J., Jackson, M.P.A., Eriksson, K.A., Hobday, D.K., Hunter, D.R., Minter, W.E.L., 1982. Crustal Evolution of Southern Africa, 3.8 Billion Years of Earth History. Published by Springer-Verlag (New York, N.Y.), pp.6 and 174.

Tiegler, B., Eales, H.V., Scoon, R.N., 1992. The cumulate succession in the Critical Zone of the Rustenburg Layered Suite at Brits, western Bushveld Complex. South African Journal of Geology 95, 17-28.

Uken, R., 1998. The Geology and Structure of the Bushveld Complex metamorphic aureole in the Olifants River area. Doctor of Philosophy thesis, University of Natal Durban, South Africa, 277p.

Uken, R., Watkeys, M.K., 1997. Diapirism initiated by the Bushveld Complex, South Africa. Geology 25, 723-726.

Van der Merwe, J., Cawthorn, R.G., 2005. Structures at the base of the Upper Group 2 chromitite layer, Bushveld Complex, South Africa, on Karee Mine (Lonmin Platinum). Lithos 83, 214-228.

Van der Merwe, M.J., 2008. The geology and structure of the Rustenburg Layered Suite in Potgietersrus/Mokopane area of the Bushveld Complex, South Africa. Mineralium Deposita 43, 405-420.

Vermaak, CF., 1976. The Merensky Reef- thoughts on its environment and genesis. Economic Geology 71, 1270-1298.

Vermaak, C.F., 1995. The Platinum Group Metals; a global perspective. Published by MINTEK (South Africa), ISBN-10: 0869999265, 247p.

Vermaak, C.F., Hendricks, L.P., 1976. A review of the mineralogy of the Merensky Reef, with specific reference to new data on the precious metal mineralogy. Economic Geology 77, 1244-1269.

Vermaak, C.F., Van Der Merwe, M.J., 2000. The platinum mines and deposits of the Bushveld Complex, South Africa. Council for Mineral Technology, Randburg, South Africa, 118 pp.

Vermaak, C.F., Von Greunewaldt, G., 1986. Introduction to the Bushveld. In: Anhaeusser, C.R., Maske, S., (Eds.), Minerals Deposits of Southern Africa, Volume II. Geological Society of South Africa, Johannesburg, pp. 1021-1029.

Viljoen, M.J., 1994. A review of regional variations in facies and grade distribution of the Merensky Reef, Western Bushveld Complex with some mining implications. Journal of the South African Institute of Mining and Metallurgy 3, 183-194.

Viljoen, M.J., 1999. The nature and origin of the Merensky Reef of the western Bushveld Complex based on geological facies and geophysical data. South African Journal of Geology 102, 221-239.

Viljoen, M.J., Hieber, R., 1986. The Rustenburg Section of Rustenburg Platinum Mines Limited with reference to the Merensky Reef. In: Anhaeusser, C.R., Maske, S., (Eds.), Mineral deposits of Southern Africa, Volume II. Geological Society of South Africa, Johannesburg, pp. 1107-1134.

Viljoen, M.J., Schürmann, L.W., 1998. Platinum Group Metals. In: Wilson, M.G.C., Anhaeusser, C.R., (Eds.) Mineral Resources of South Africa, 6th edition. Handbook Council for Geosciences 16, pp. 532-568.

Viljoen, M.J., Theron, J., Underwood, B., Walters, B.M., Weaver, J., Peyerl, W., 1986. The Amandelbult Section of Rustenburg Platinum Mines Limited, with reference to the Merensky Reef. In: Anhaeusser, C.R., Maske, S., (Eds.), Minerals Deposits of Southern Africa, Volume II. Geological Society of South Africa, Johannesburg, pp. 1041-1060.

Wallmach, T., Hatton, C.J., Droop, G.T.R., 1989. Extreme facies of contact metamorphism developed in calc-silicate xenoliths in eastern Bushveld Complex. Canadian Mineralogist 27, 509-523.

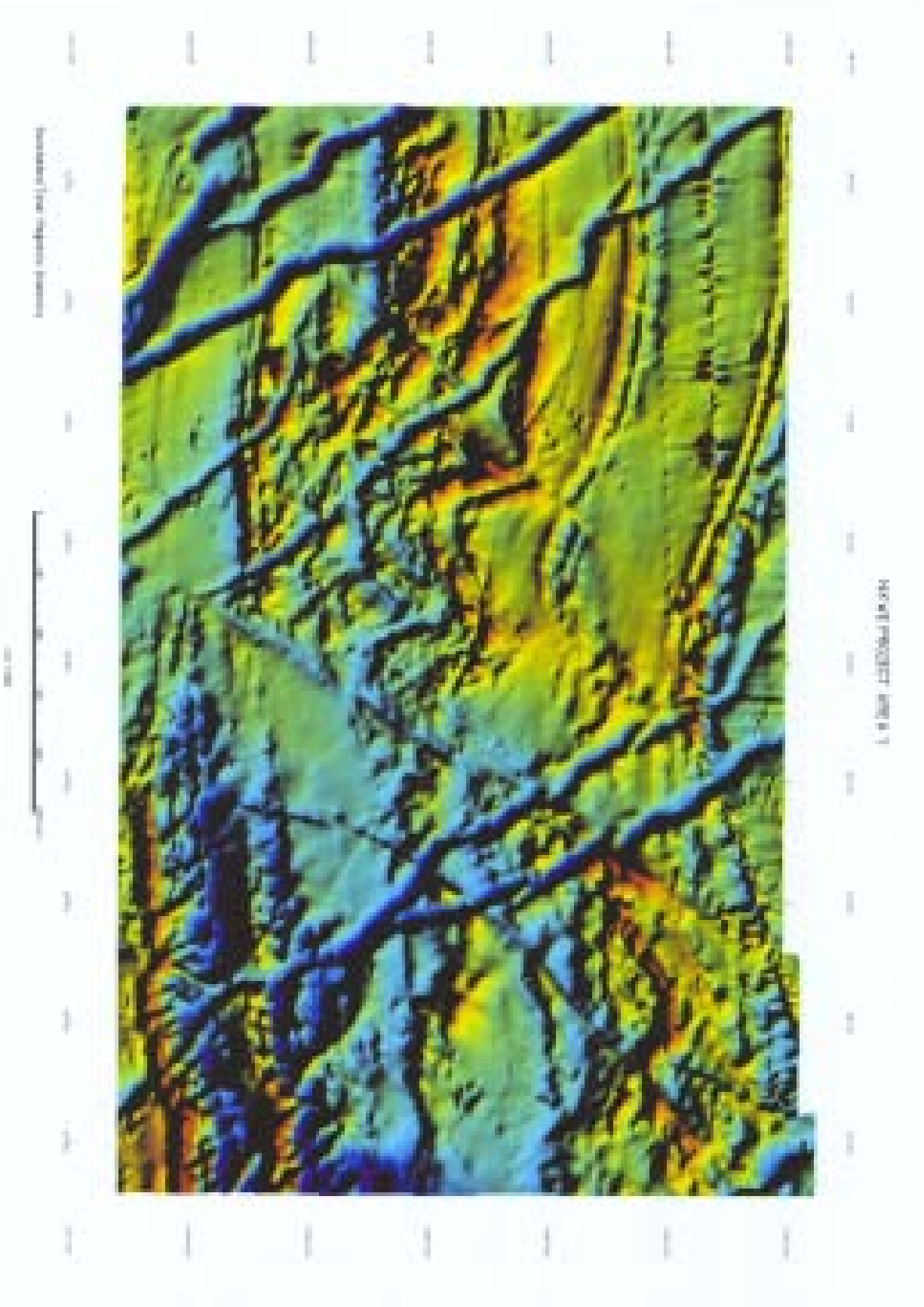
Wallmach, T., Hatton, C.J., De Waal, S.A., Gibson, R.L., 1995. Retrogressive hydration of calc-silicate xenoliths in the eastern Bushveld Complex: evidence for late magmatic fluid movement. Journal of African Earth Sciences 21, 633-646.

Walraven, F., 1997. Geochronology of the Rooiberg Group, Transvaal Supergroup, South Africa. Information Circular, 316. Economic Geology Research Unit, University of the Witwatersrand, 21 p.

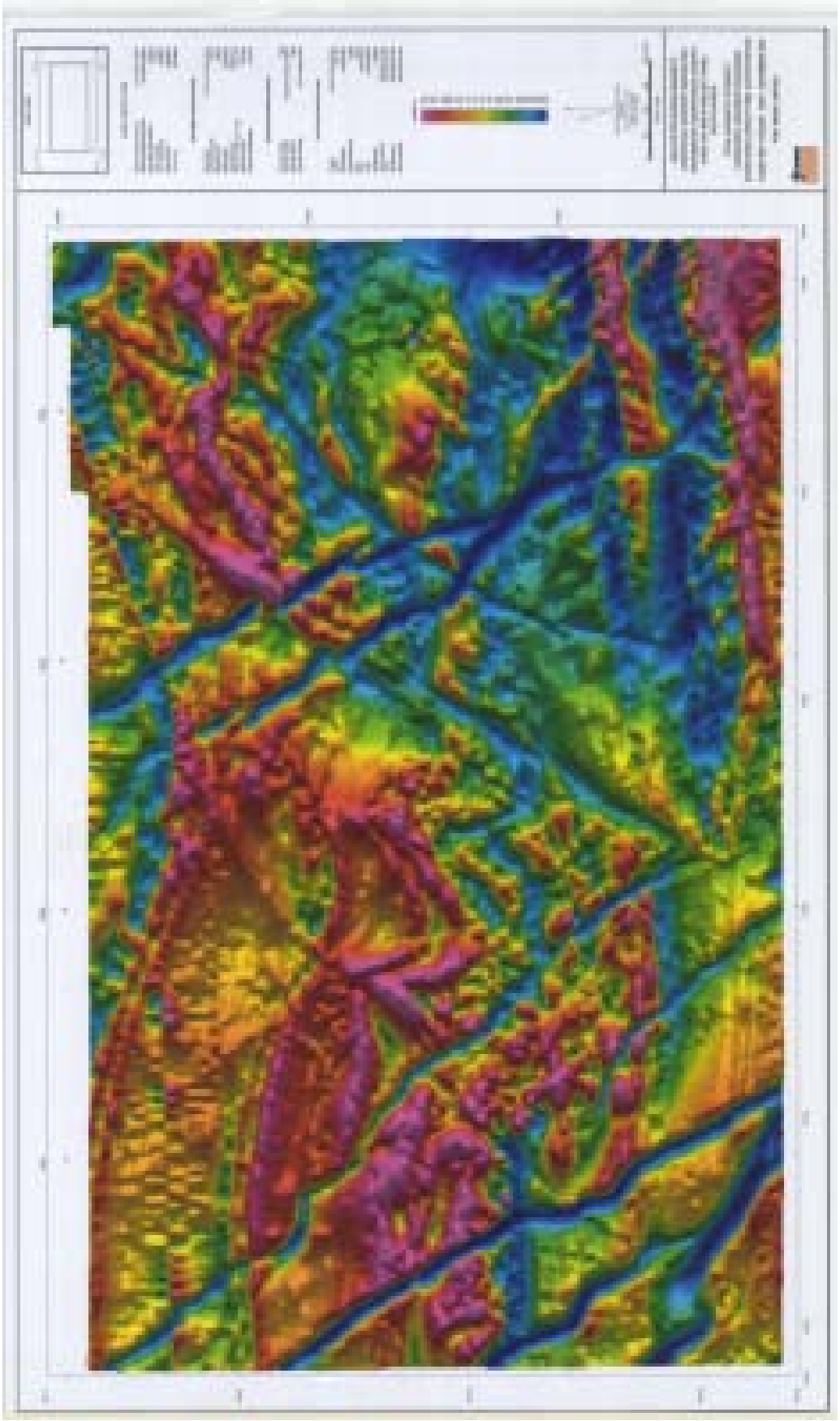
Walraven, F., Armstrong, R.A., Kruger, F.J., 1990. A chronostratigraphic framework for the north–central Kaapvaal Craton. Tectonophysics, 171, 23-48.

Wilhelm, H.J., Zhang, H., Chen, F.L., Elsenbroek, J.H., Lombard, M., de Bruin, D., 1997. Geochemical exploration for platinum-group elements in the Bushveld Complex, South Africa. Mineralium Deposita 32, 349-361.

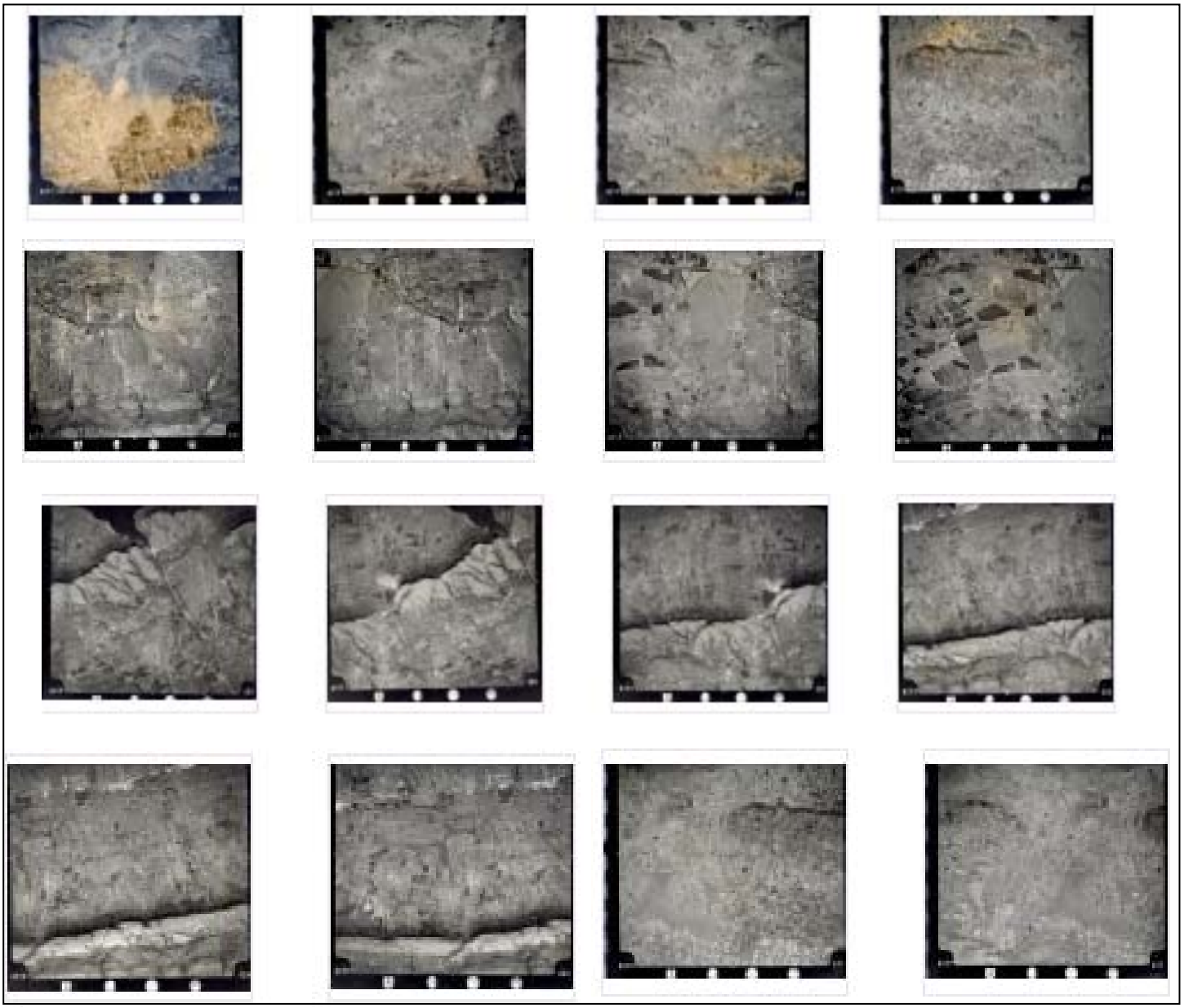
APPENDIX



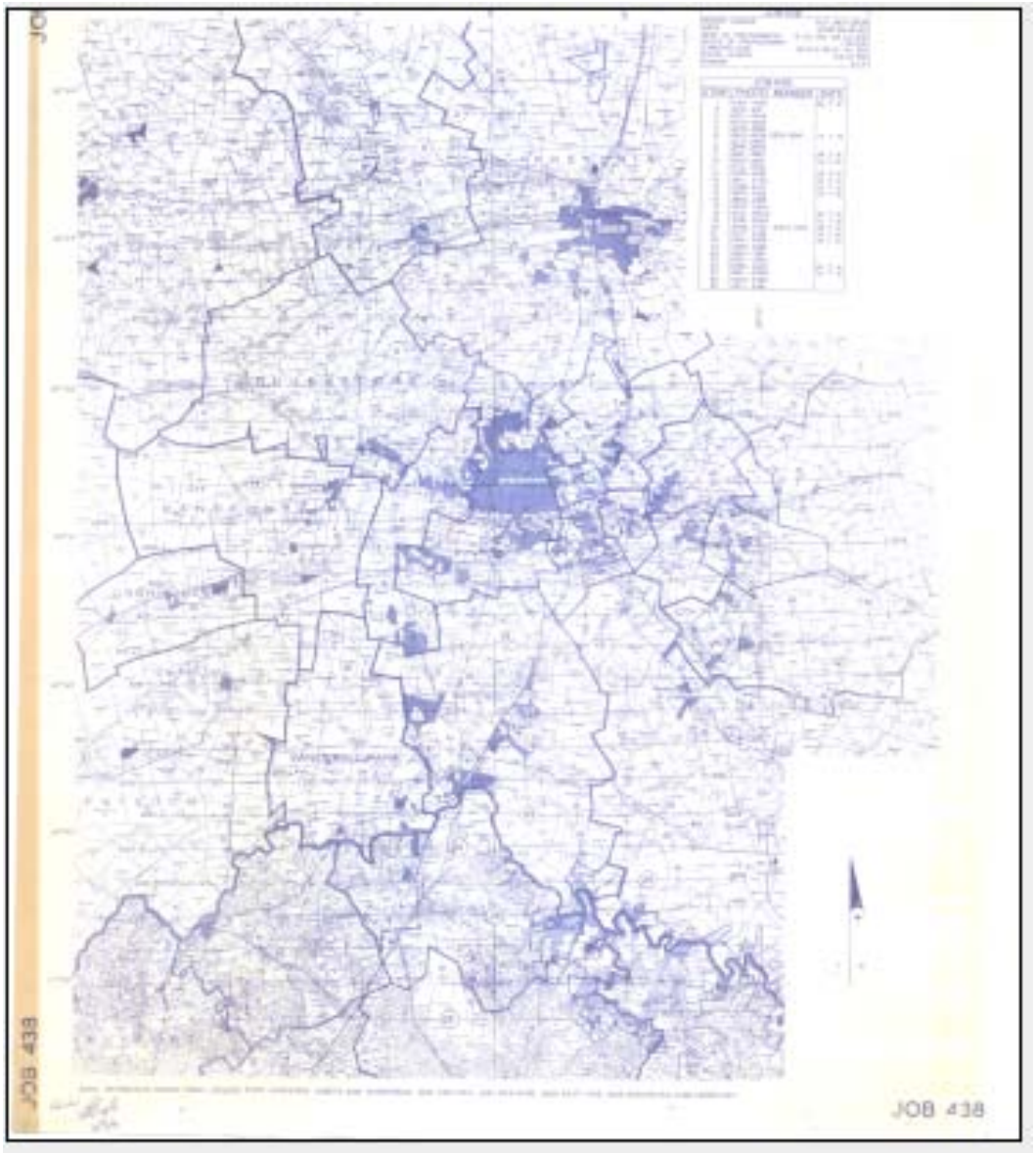
1.0. 1st vertical magnetic derivative map of the De Widlt project area.



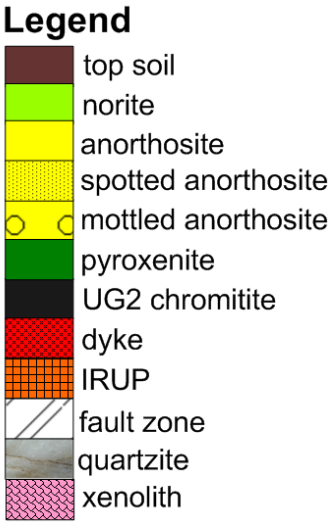
2.0. Total magnetic intensity map of the De Widlt project area.



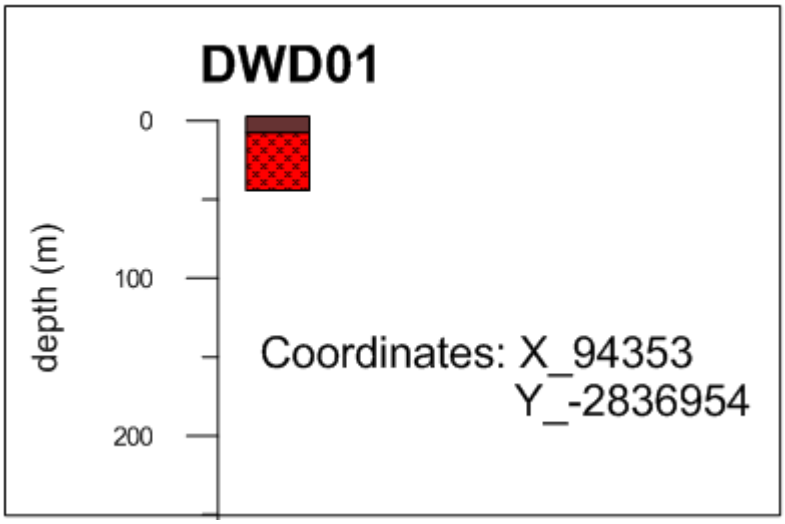
3.0. Ungeoreferenced raster images over the De Wildt project area and surrounding areas.



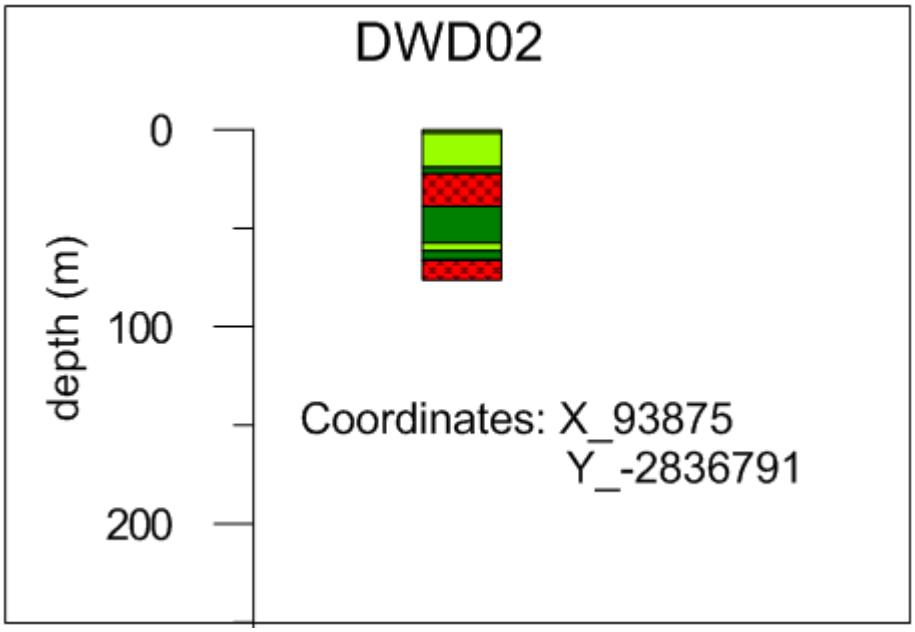
4.0. Flight plan over the De Widlt project area



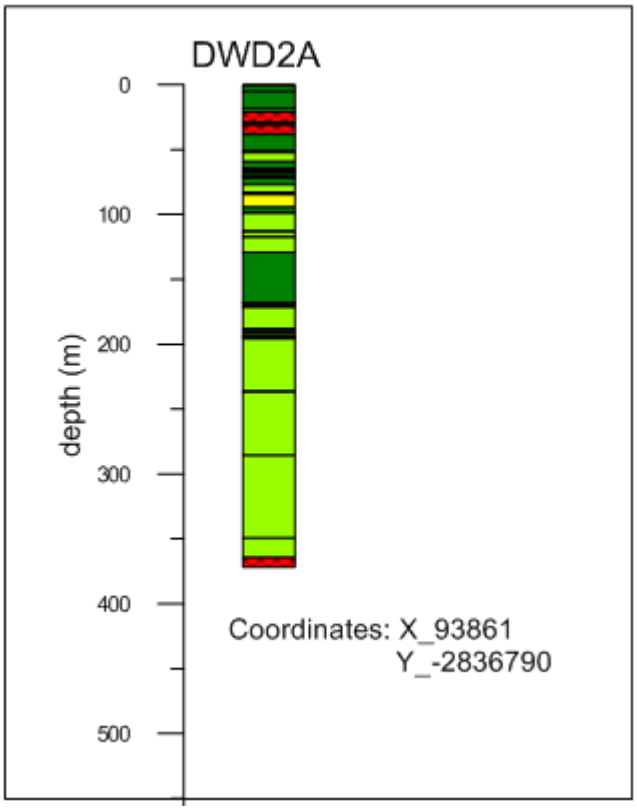
5.1. Stratigraphic legend used in all boreholes



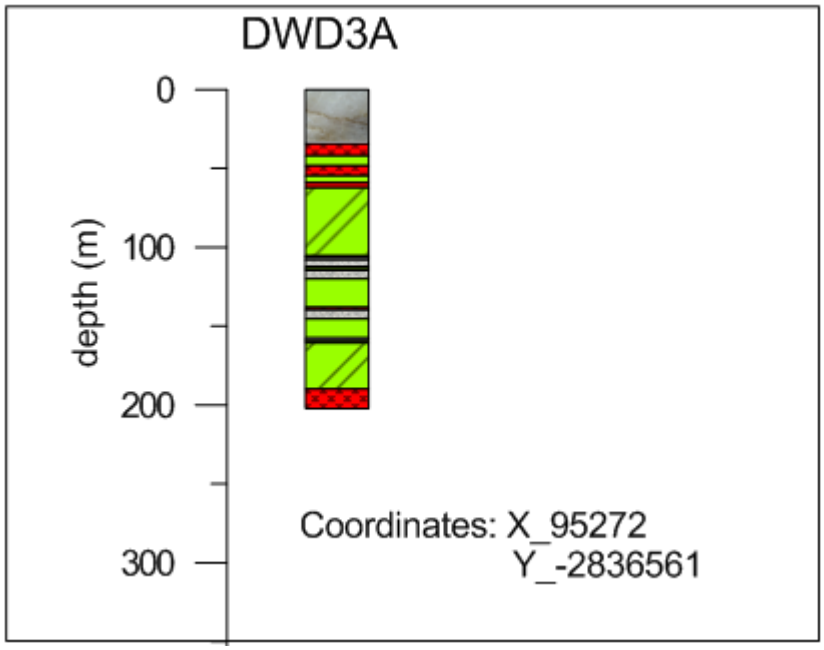
5.2. Stratigraphic log for borehole DWD01



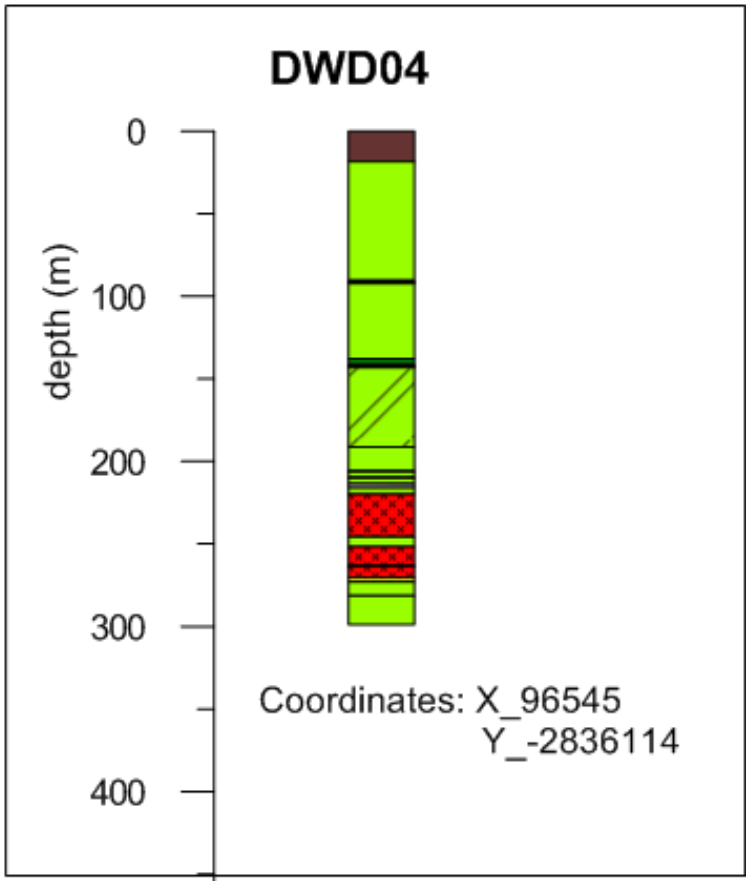
5.3. Stratigraphic log for borehole DWD02



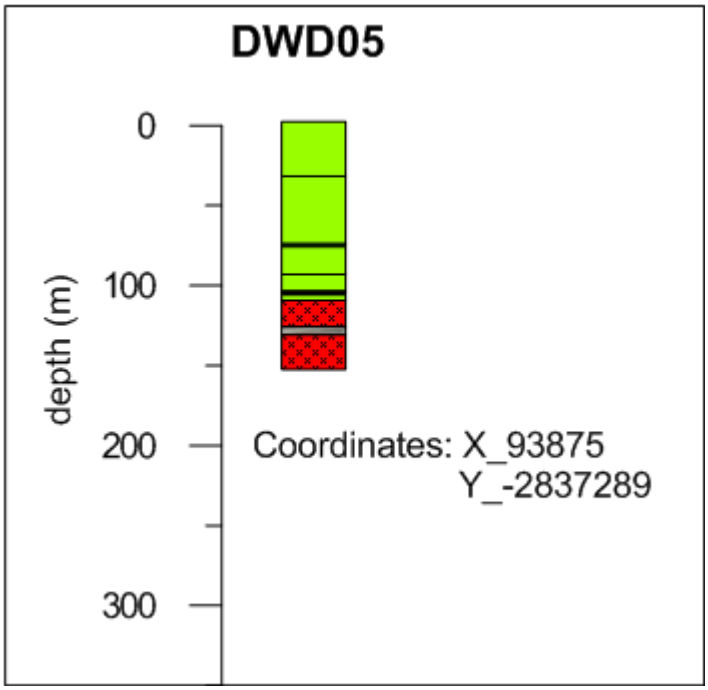
5.4. Stratigraphic log for borehole DWD2A



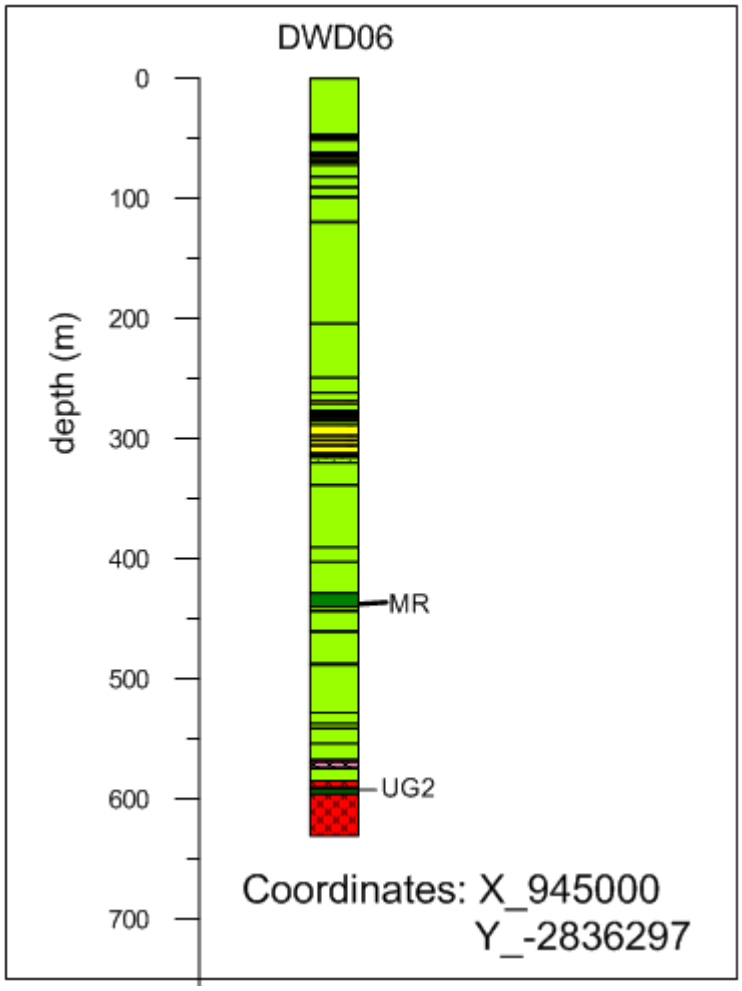
5.5. Stratigraphic log for borehole DWD3A



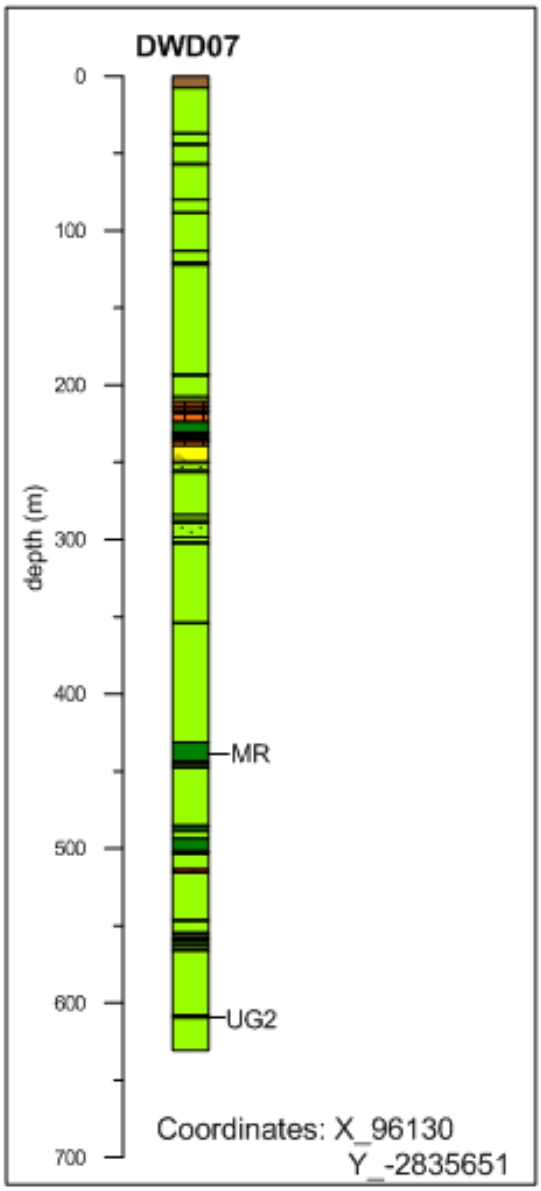
5.6. Stratigraphic log for borehole DWD04



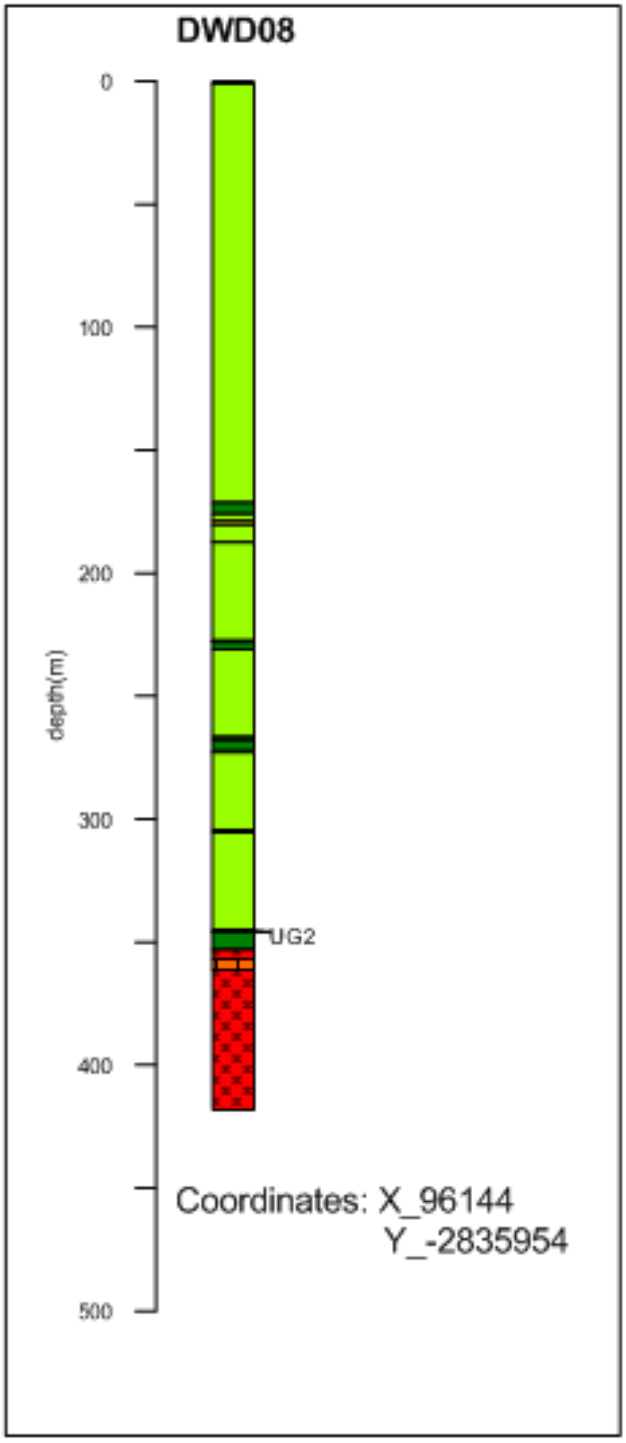
5.7. Stratigraphic log for DWD05



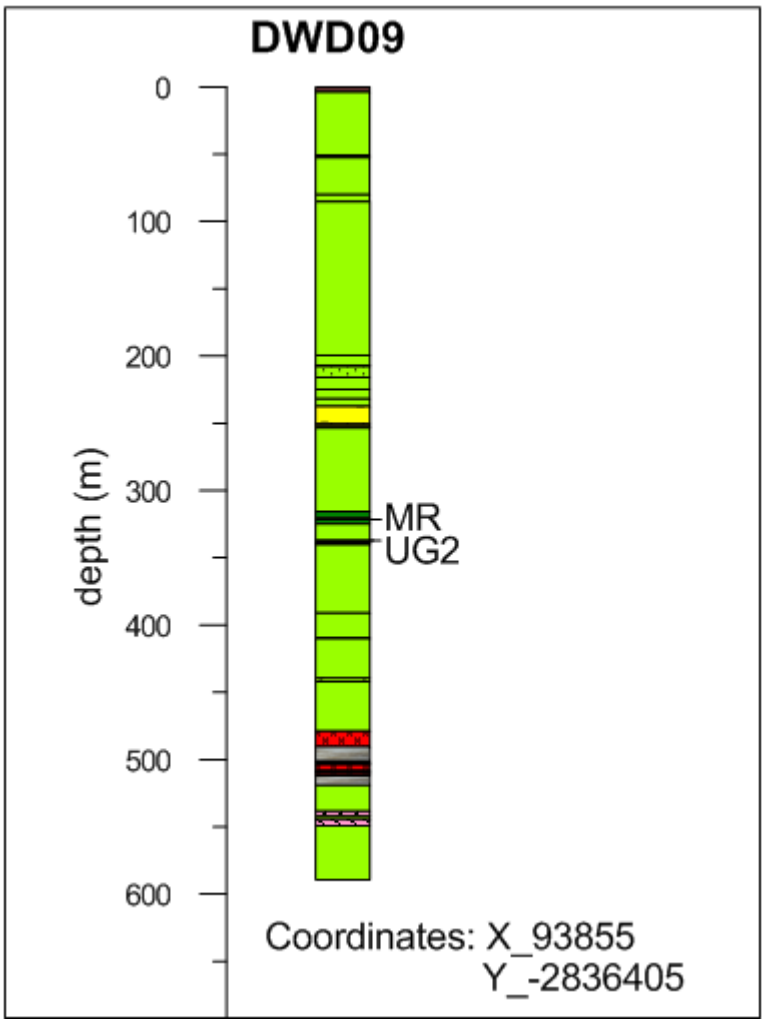
5.8. Stratigraphic log for borehole DWD06



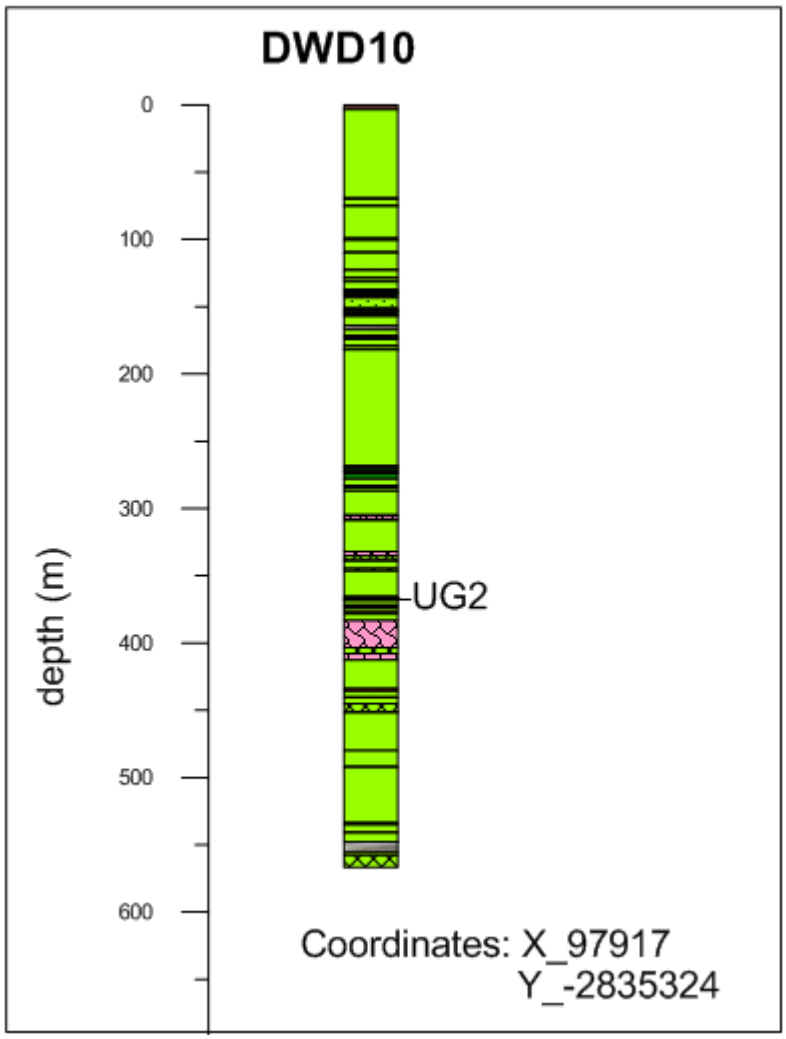
5.9. Stratigraphic log for DWD07



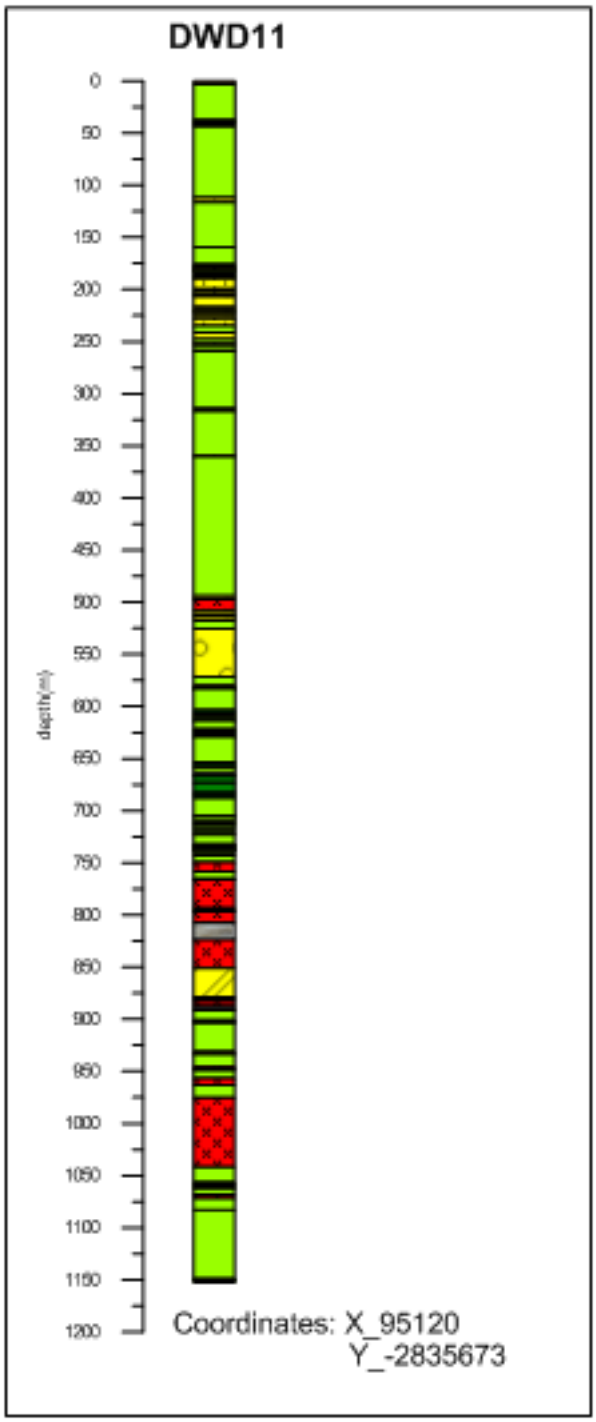
5.10. Stratigraphic log for borehole DWD08



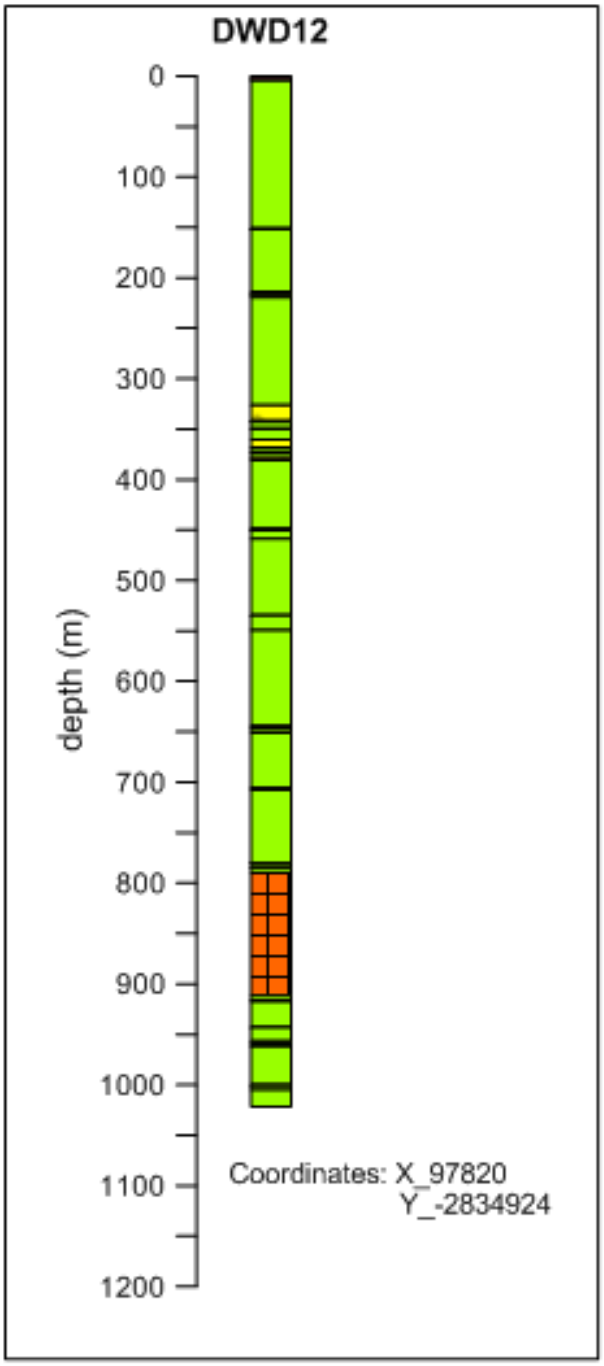
5.11. Stratigraphic log for borehole DWD09



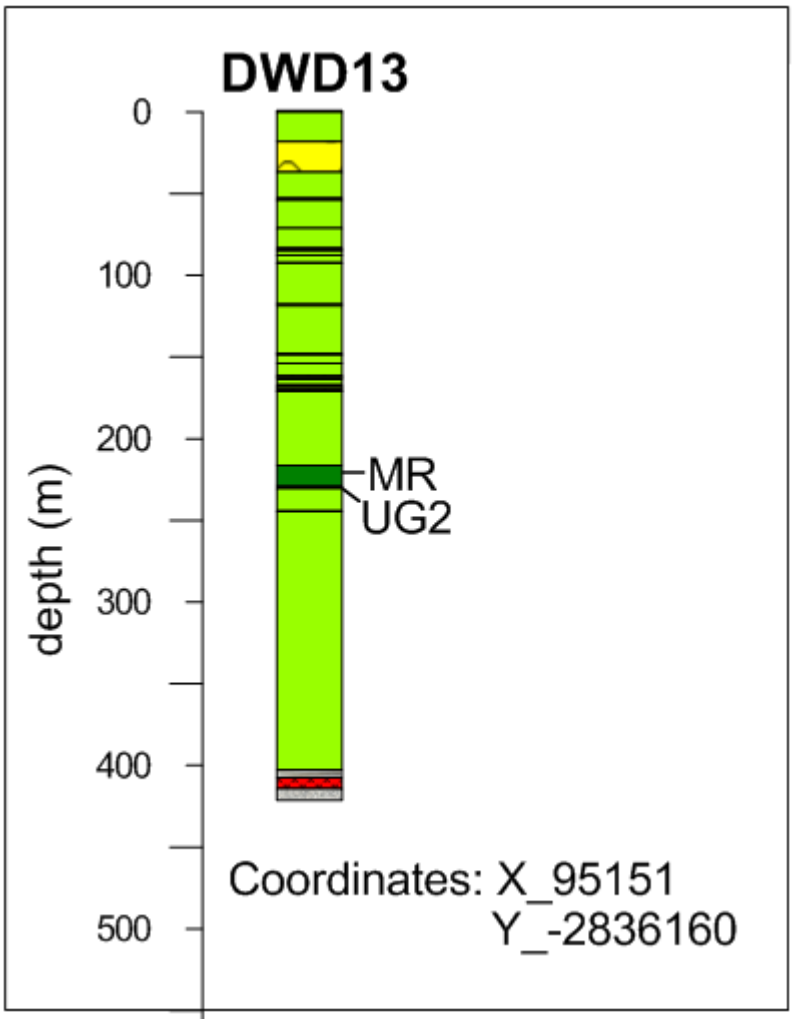
5.12. Stratigraphic log for borehole DWD10



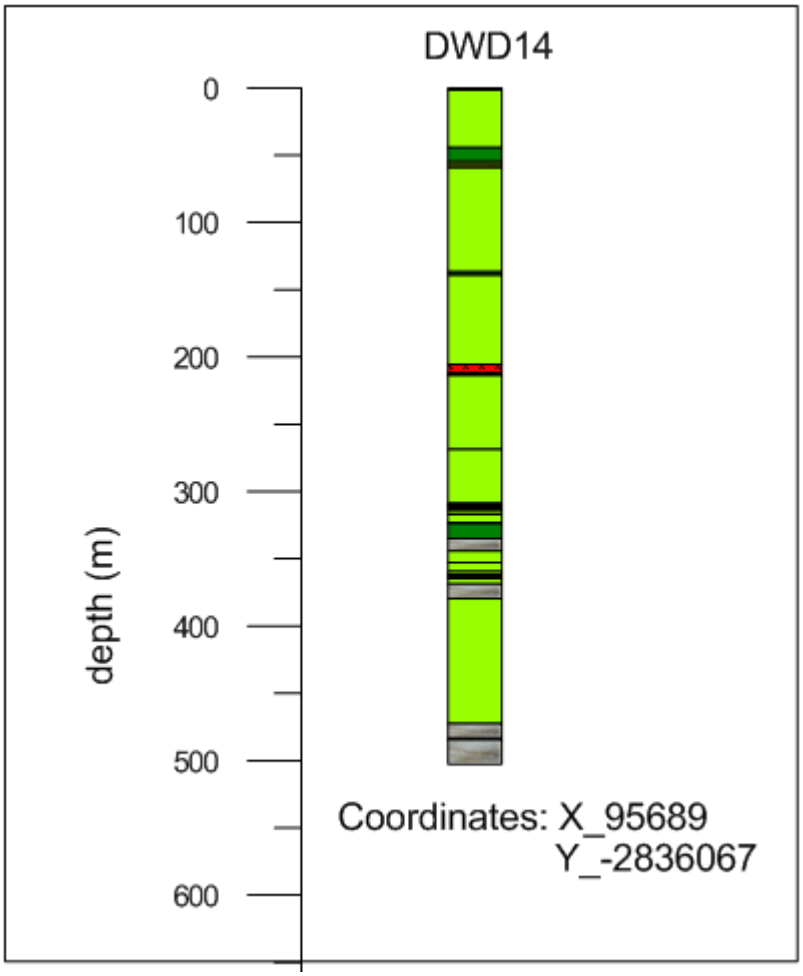
5.13. Stratigraphic log for borehole DWD11



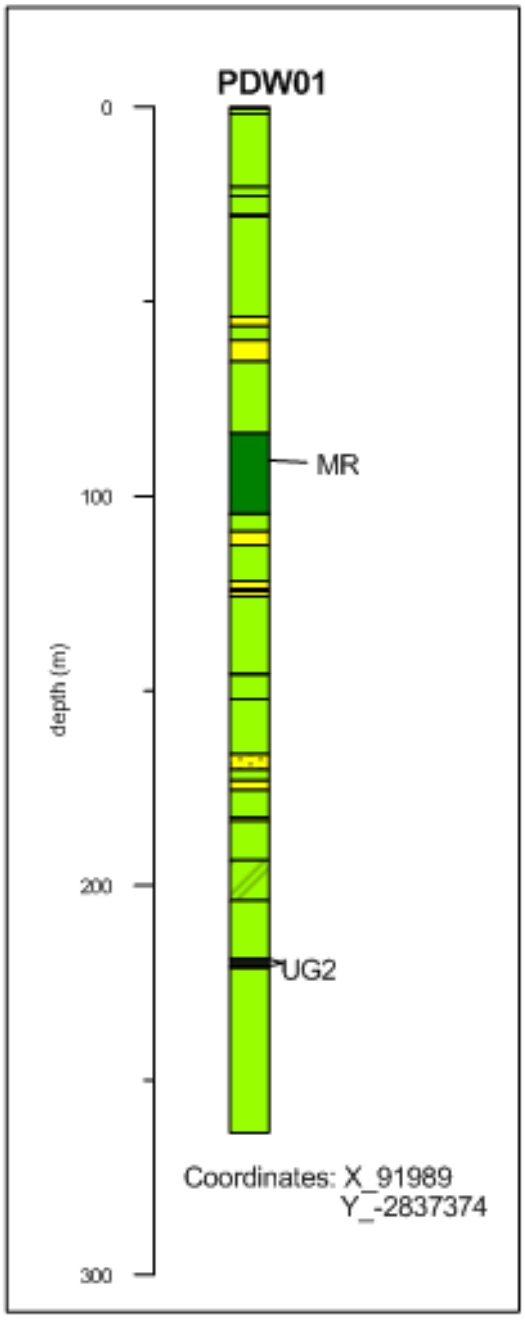
5.14. Stratigraphic log for borehole DWD12



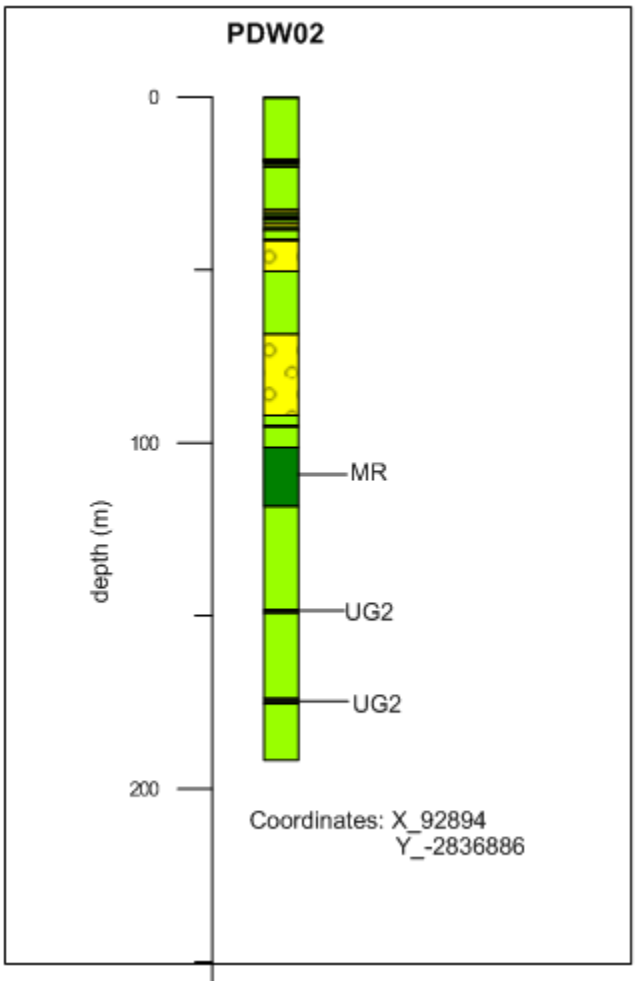
5.15. Stratigraphic log for borehole DWD13



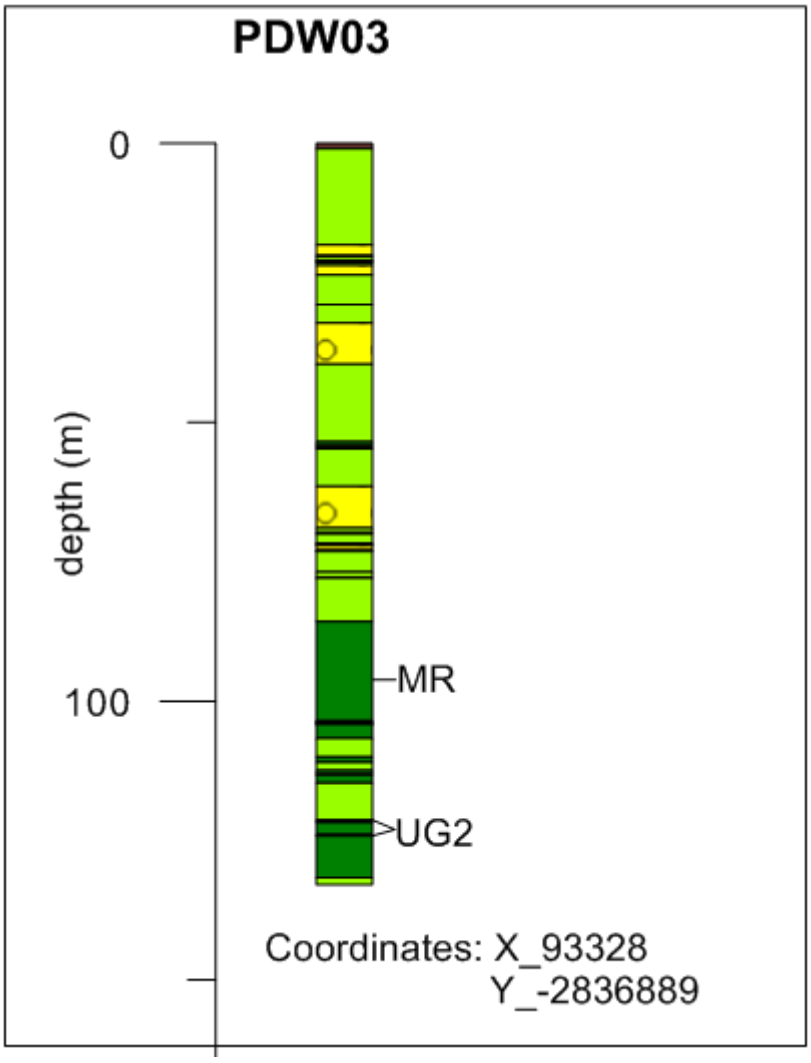
5.16. Stratigraphic log for borehole DWD14.



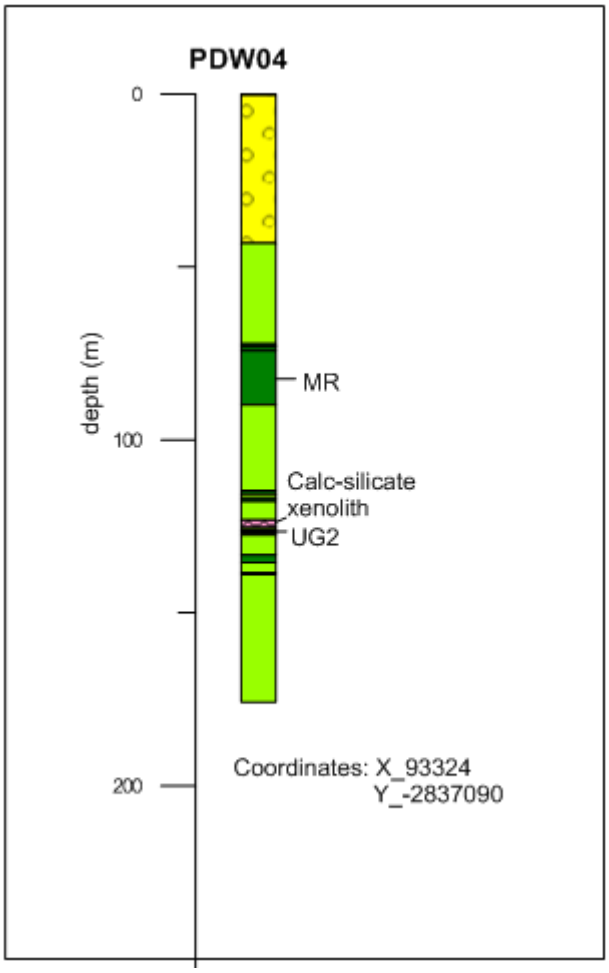
5.17. Stratigraphic log for borehole PDW01



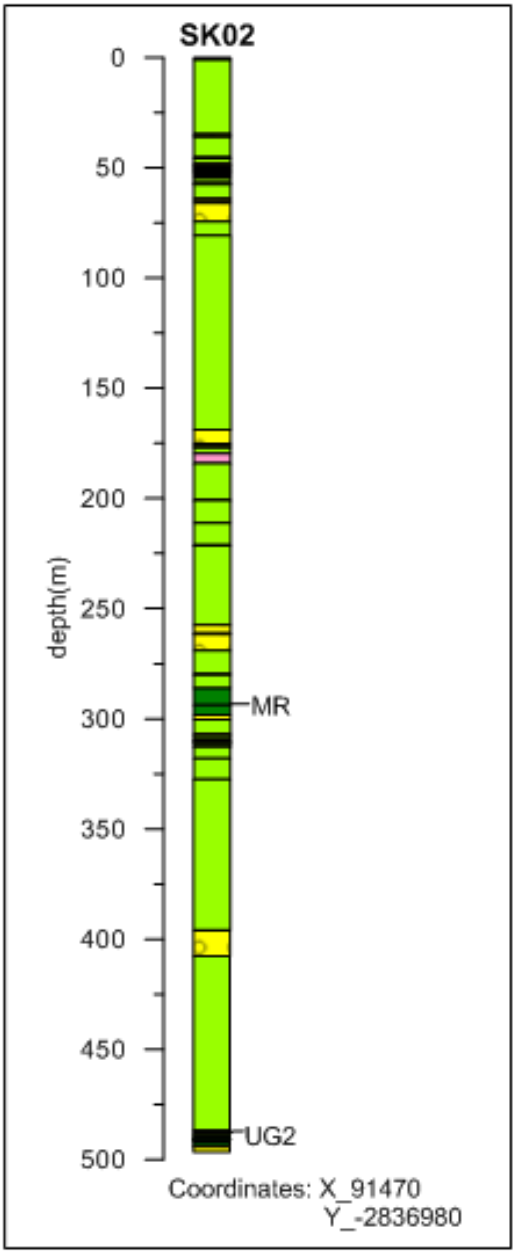
5.18. Stratigraphic log for borehole PDW02



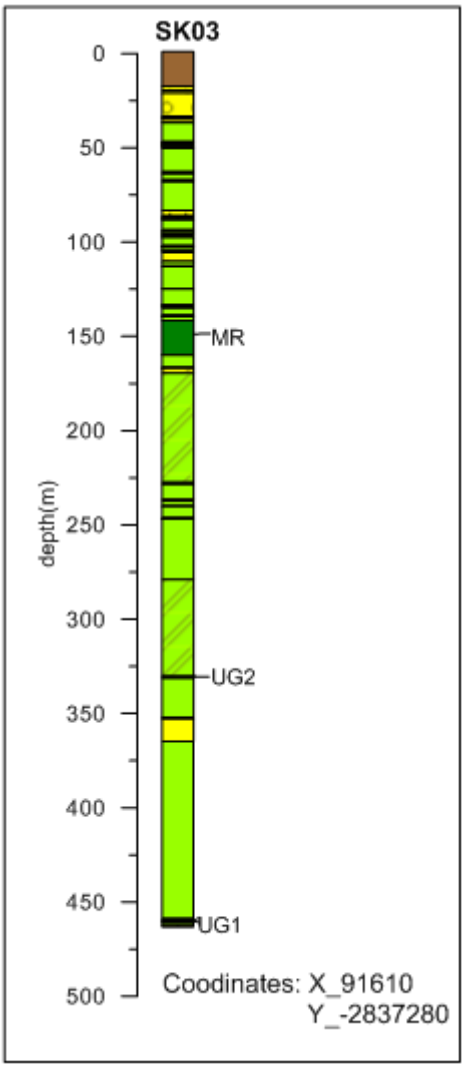
5.19. Stratigraphic log for borehole PDW03.



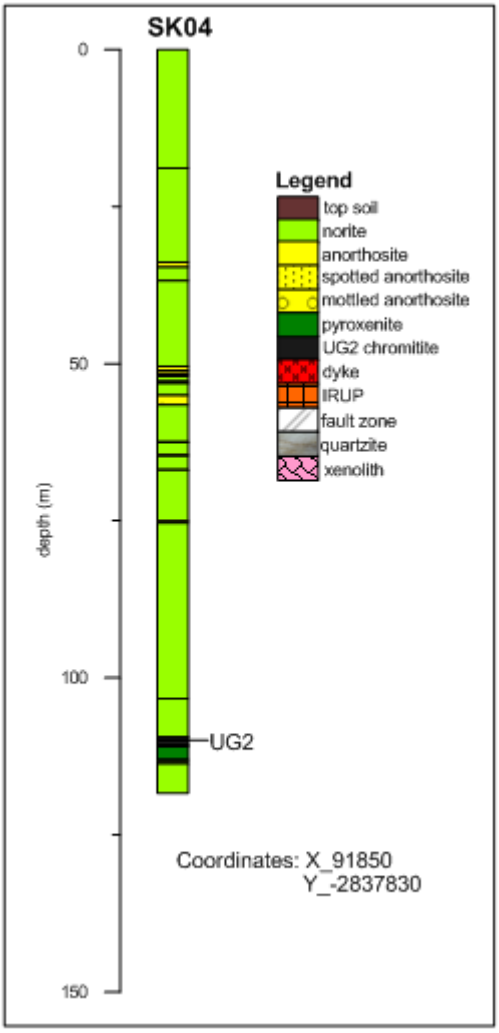
5.20. Stratigraphic log for borehole PDW04



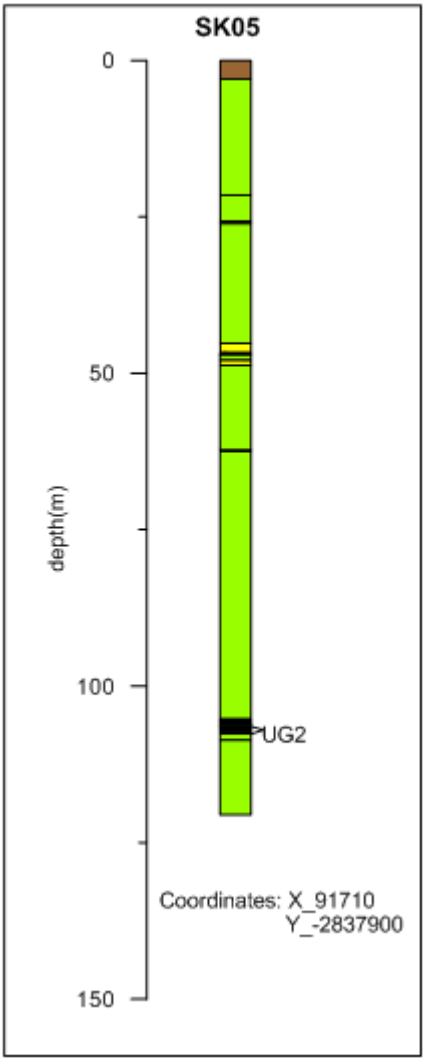
5.21. Stratigraphic log for borehole SK02



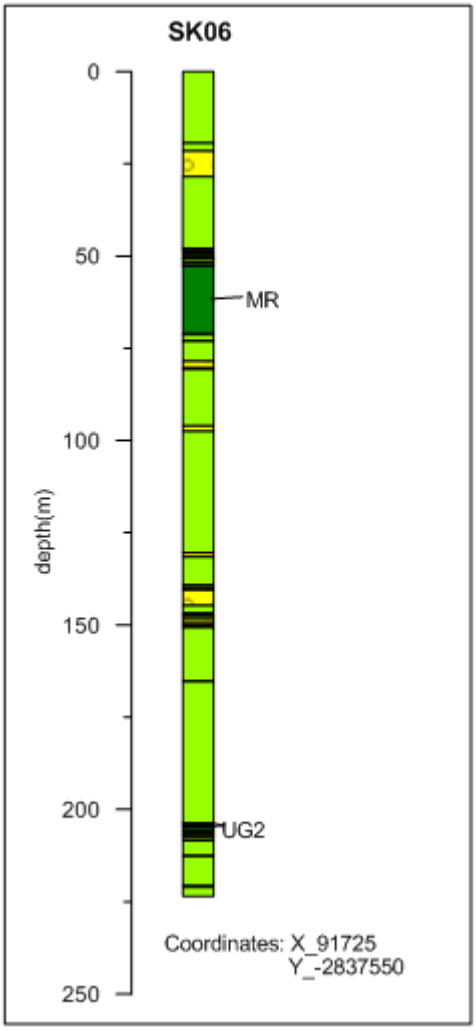
5.22. Stratigraphic log for borehole SK03



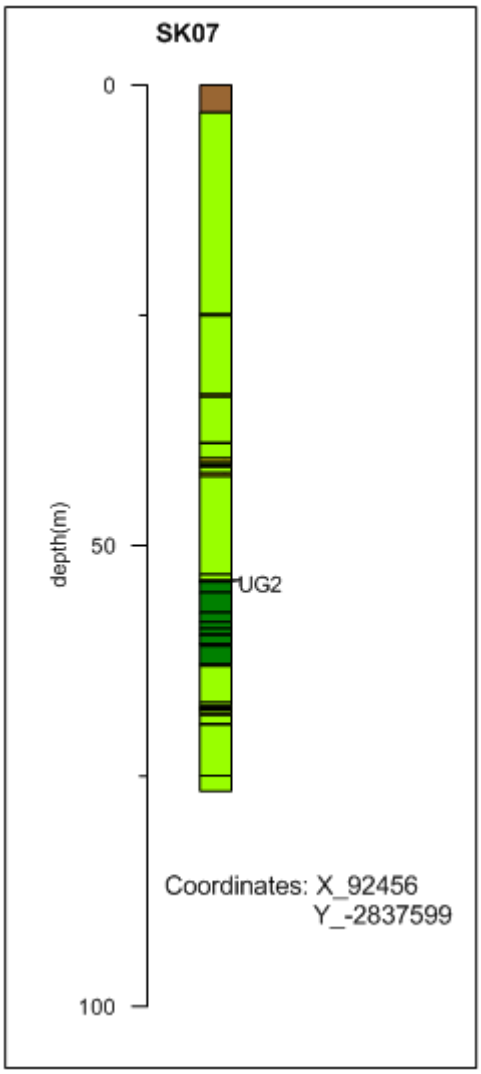
5.23. Stratigraphic log for borehole SK04.



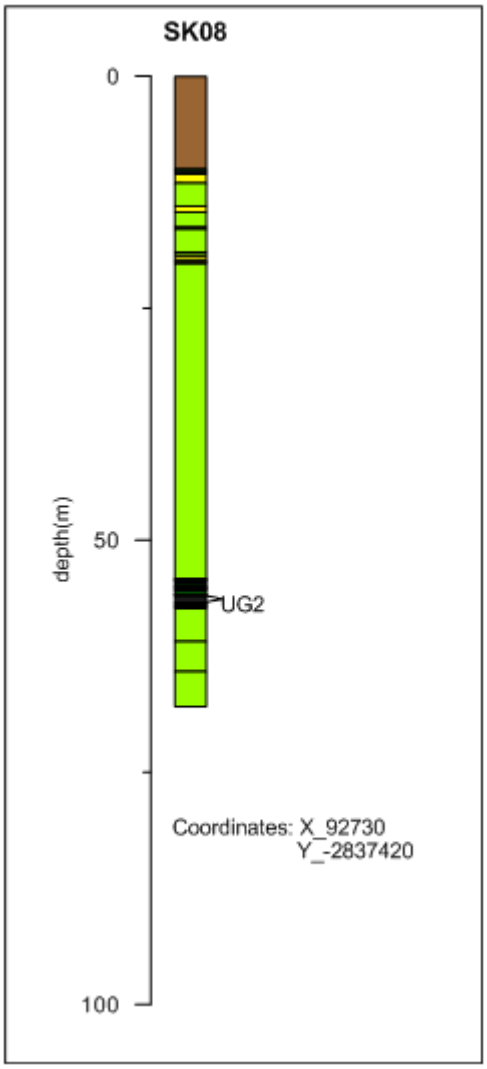
5.24. Stratigraphic log for borehole SK05.



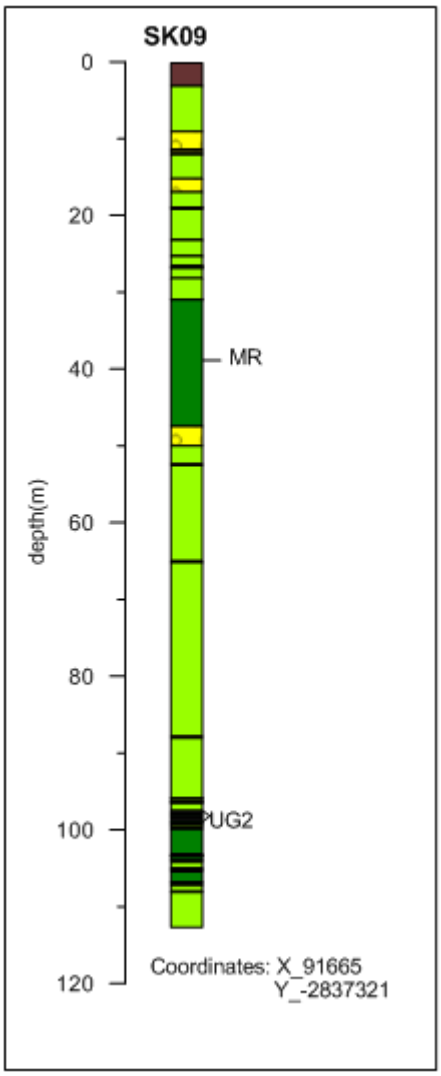
5.25. Stratigraphic log for borehole SK06.



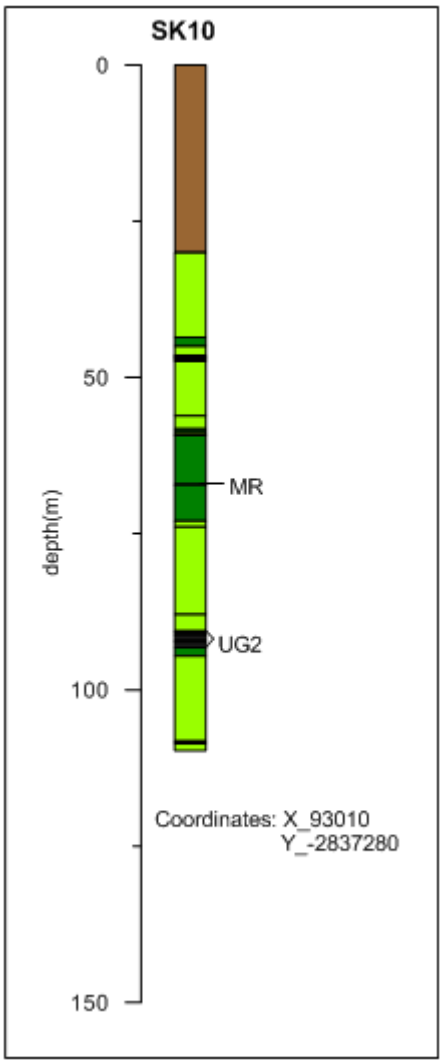
5.26. Stratigraphic log for borehole SK07.



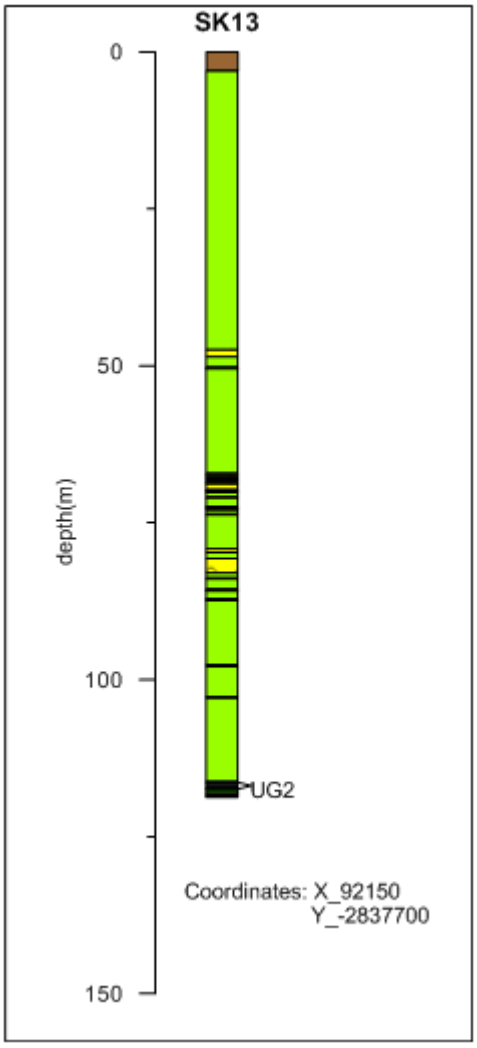
5.27. Stratigraphic log for borehole SK08.



5.28. Stratigraphic log for borehole SK09.



5.29. Stratigraphic log for borehole SK10.



5.30. Stratigraphic log for borehole SK13.

UG2 chromitite grades									Footwall				
				sampled interval						sampled interval			
BH ID	X COLL	Y COLLAR	Z COLLAR	From	To	Thickness	5E+Au	cmg/t	From	To	Thickness	5E + Au	cmg/t
SK01	91460	-2836630	1208										
SK2	91470	-2836980	1214	486.85	488.10	1.25	6.24	780.35	488.10	491.32	3.22	3.12	1004.64
SK3	91610	-2837280	1218	331.22	331.94	0.72	4.65	334.57					
SK4	91850	-2837830	1228	109.53	110.64	1.11	6.72	746.26	110.64	113.31	2.67	1.85	493.95
SK5	91710	-2837900	1229	106.48	107.57	1.09	3.15	343.31					
SK6	91725	-2837550	1223	203.91	204.26	0.69	3.32	229.02	204.26	206.00	1.09	2.75	299.75
SK7	92456	-2837599	1232	53.77	55.07	1.30	2.60	337.85	55.07	57.27	2.20	0.97	213.4
SK8	92730	-2837420	1228	55.63	57.35	0.72	3.21	230.84	57.35	58.01	0.66	1.57	103.62
SK9	91665	-2837321	1225	95.72	97.41	1.69	2.60	439.20	97.41	107.84	10.43	1.48	1543.64
SK10	93010	-2837280	1222	90.62	91.26	0.64	2.54	162.71					
SK13	92150	-2837700	1218	116.40	117.76	1.36	2.64	359.20	117.76	118.05	0.29	3.21	93.09
SK14	92764	-2836781	1218	224.17	225.57	1.40	3.35	469.00					
DWD 2A	95295	-2836642	1233	194.80	195.05	0.25	0.37	9.36					
DWD 7	96130	-2835651	1232	607.93	609.03	1.10	1.24	135.95	608.43	608.63	0.20	1.90	37.9514
DWD 9	93855	-2836405	1218	337.12	337.84	0.72	1.79	128.54	337.84	340.00	2.16	0.94	202.241
DWD 8	96144	-2835954	1238	345.21	345.81	0.60	1.60	95.88	359.06	362.27	3.21		
DWD 10	97917	-2835324	1249	367.07	368.19	1.12							
DWD 11	95120	-2835673	1221										
DWD 12	97820	-2834924	1242	999.90	1000.61	0.71	1.32		1000.61	1004.77	4.16		
DWD 13	95689	-2836067	1234						230.41	231.66	1.25	2.97	371.399
PDW1	91989	-2837374	1222	218.97	220.66	1.00	2.17	217.22					
				219.72	220.47	0.75	2.52	189.1326					
PDW2	92894	-2836886	1220	147.93	148.68	0.75	2.23	167.60					
				219.47	220.47	1.00	2.31	230.954					
PDW3	93328	-2836889	1220	121.30	121.75	0.45	2.08	93.82					
				121.75	124.29	2.54	2.31	586.62316					
PDW4	93324	-2837090	1222	125.98	126.73	0.75	0.89	66.48					
2098	91083	-2836830	1216	189.69	190.82	1.13	4.38	495.15	190.82	193.94	3.12		
2055	91736	-2836535	1213	298.71	300.02	1.31	3.18	416.71	493.60	498.77	5.17		
2092	91816	-2837219	1221	186.94	188.24	1.30	3.72	483.26	188.29	193.46	5.17		
DWD01	94353	-2836954	1232										
DWD02	93875	-2836791	1225										
DWD 3	95295	-2836642	1233										
DWD03A	95272	-2836561	1232										
DWD04	96545	-2836114	1249										
DWD05	93875	-2837289	1233										
DWD06	94500	-2836297	1216										
SK11	93610	-2837010	1228										
SK12	91450	-2837090	1228										
SK14	92764	-2836781	1218										
SK15	93360	-2836450	1222										
SK16	93380	-2836520	1225										
SK18	92850	-2837930	1238										
ZK01	90237	-2837694	1209										

6.0. UG2 chromitite and UG2 footwall grades at De Wildt project.

ANALYTICAL SCIENCE TEST REPORT **Project No: 60580401** **INT2401 Login Date 2005/11/28 10:59:44**

AUTHORISED BY **Date Authorized 2005/12/07 22:25:32**

TRACE ICP SECTION Tumo Molatuli Lab Technician **Customer: Ms BUSI RICHARD** **Checked by**

Clement Thanjekwayo

empty **T0042** **Tumo Molatuli**

The results relate only to the items tested Accredited ASD-MET-OES-SP005;ASD-MET-AAS-SP001;ASD-MET-C16/26;ASD-MET-C06/37;ASD-MET-SPT006;ASD-MET-SPT007;ASD-MET-SPT008;ASD-MET-FA002

Sample Name	Description	Rep		Pt ppm	Pd ppm	Rh ppm	Ru ppm	Ir ppm	Au ppm			
INT2401/1	R59448 PDWI: ID3	1		1.7	0.4	0.31	0.52	<0.10	<0.10			
INT2401/2	R59449 PDWI: ID4	1		0.88	0.15	0.18	0.48	0.12	<0.10			
INT2401/2	R59449 PDWI: ID4	2		0.91	0.15	0.18	0.46	0.14	<0.10			
INT2401/3	R59450 PDWI: ID5	1		1.21	0.17	0.24	0.62	<0.10	<0.10			
INT2401/4	R59451 PDWI: ID6	1		2.25	0.33	0.39	0.86	0.15	<0.10			
INT2401/4	R59451 PDWI: ID6	2		2.28	0.34	0.38	0.85	0.11	<0.10			
INT2401/5	R59452 PDWI: ID7	1		1.4	0.28	0.27	0.61	<0.10	<0.10			
INT2401/5	R59452 PDWI: ID7	2		1.27	0.25	0.25	0.56	<0.10	<0.10			
INT2401/6	R59453 PDWI: ID8	1		1.22	0.63	0.28	0.54	<0.10	<0.10			
INT2401/6	R59453 PDWI: ID8	2		1.04	0.59	0.23	0.47	<0.10	<0.10			
INT2401/7	R59454 PDWI: ID9	1		1.36	1.05	0.32	0.7	<0.10	<0.10			
INT2401/8	R59440 2092: DID	1		2.06	2.11	0.38	0.77	<0.10	<0.10			
INT2401/8	R59440 2092: DID	2		2.13	2	0.4	0.82	<0.10	<0.10			
REF: sarm65		1		2.39	1.24	0.52	0.89	0.16	<0.10			
ACC.VALUE		1		2.64	1.28	0.52	0.85	0.18	<0.10			
				0								

Method Numbers
ASD/MET/TRR001

COMMENTS
Samples analyzed as received.

INT2401/1/3/7 Insufficient sample for duplicate analysis.

7.0. Prill split results for boreholes PDW01 and 2092.